nature geoscience

SUPPLEMENTARY INFORMATION

https://doi.org/10.1038/s41561-018-0089-5

In the format provided by the authors and unedited.

Chilean megathrust earthquake recurrence linked to frictional contrast at depth

M. Moreno[1,2*], S. Li[1,3], D. Melnick[4,5], J. R. Bedford[1], J. C. Baez[6], M. Motagh[1,7], S. Metzger[1], S. Vajedian[7], C. Sippl[1], B.D. Gutknecht[8], E. Contreras-Reyes[9], Z. Deng[1], A. Tassara[5,10] and O. Oncken[1]

[1]GFZ Helmholtz Centre Potsdam, German Research Centre for Geosciences, Telegrafenberg, Potsdam, Germany. [2]Departamento de Geofísica, Facultad de Ciencias Físicas y Matemáticas, Universidad de Concepción, Concepción, Chile. [3]Department of Earth and Environmental Sciences, University of Iowa, Iowa City, IA, USA. [4]Instituto de Ciencias de la Tierra, TAQUACH, Universidad Austral de Chile, Valdivia, Chile. [5]Millennium Nucleus The Seismic Cycle Along Subduction Zones, Valdivia, Concepción, Chile. [6]Centro Sismológico National, Universidad de Chile, Facultad de Ciencias Físicas y Matemáticas, Santiago, Chile. [7]Institute of Photogrammetry and GeoInformation, Leibniz Universität Hannover, Hannover, Germany. [8]Institut für Planetare Geodäsie, Technische Universität Dresden, Dresden, Germany. [9]Departamento de Geofísica, Facultad de Ciencias Físicas y Matemáticas, Universidad de Chile, Santiago, Chile. [10]Departamento de Ciencias de la Tierra, Facultad de Ciencias Químicas, Universidad de Concepción, Concepción, Chile.
*e-mail: marcos@gfz-potsdam.de

Suplementary information to "Chilean megathrust earthquake recurrence linked to frictional contrast at depth"

Moreno, M., Li, S., Melnick, D., Bedford, J.R., Baez, J.C., Motagh, M., Metzger, S., Vajedian, S., Sippl, C., Gutknecht, B., Contreras-Reyes, E., Deng, Z., Tassara, A., and Oncken, O.

This supporting information provides all the Supplementary Figures (S1-S15).

Figure S1.Series of figures showing the GPS time-series (left column) for east, north and vertical component and the model residuals (right column). The model accounts for a linear, interseismic rate, antenna offsets (yellow squares), earthquake offsets (pink stars) and seasonal oscillations. The bottom left subfigure shows the location of the analysed GPS station (yellow circle), earthquake locations and magnitudes accounted for in the time-series modelling (stars) and background seismicity (cyan dots). The bottom right figure illustrates the G-matrix used in the inversion, with the parameters for all components on the x-axis and the G-value for each data point on the y-axis.

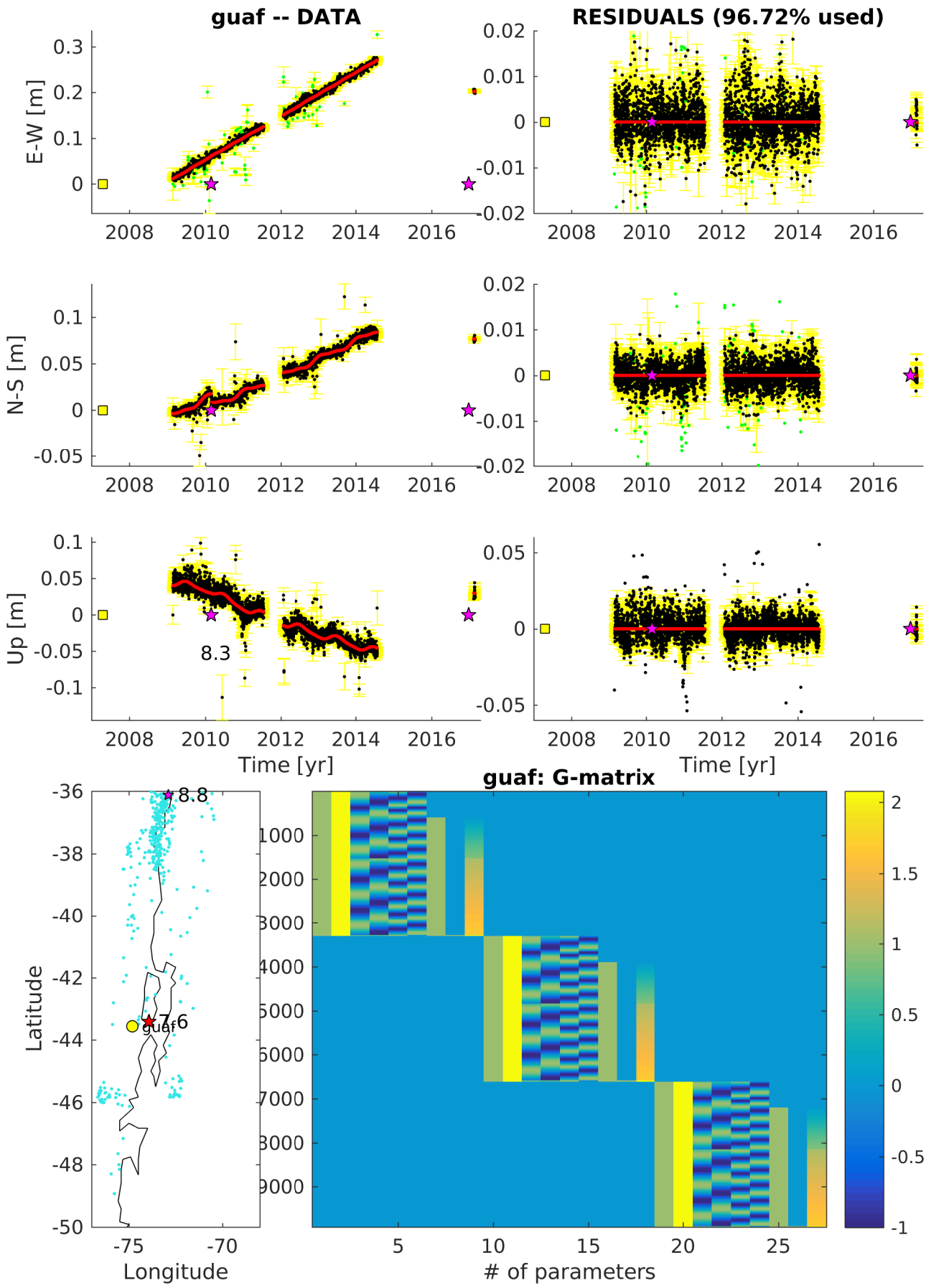
guaf -- DATA
RESIDUALS (96.72% used)
E-W [m]
N-S [m]
Up [m]
8.3
Time [yr]
guaf: G-matrix
8.8
7.6
guaf
Latitude
Longitude
# of parameters

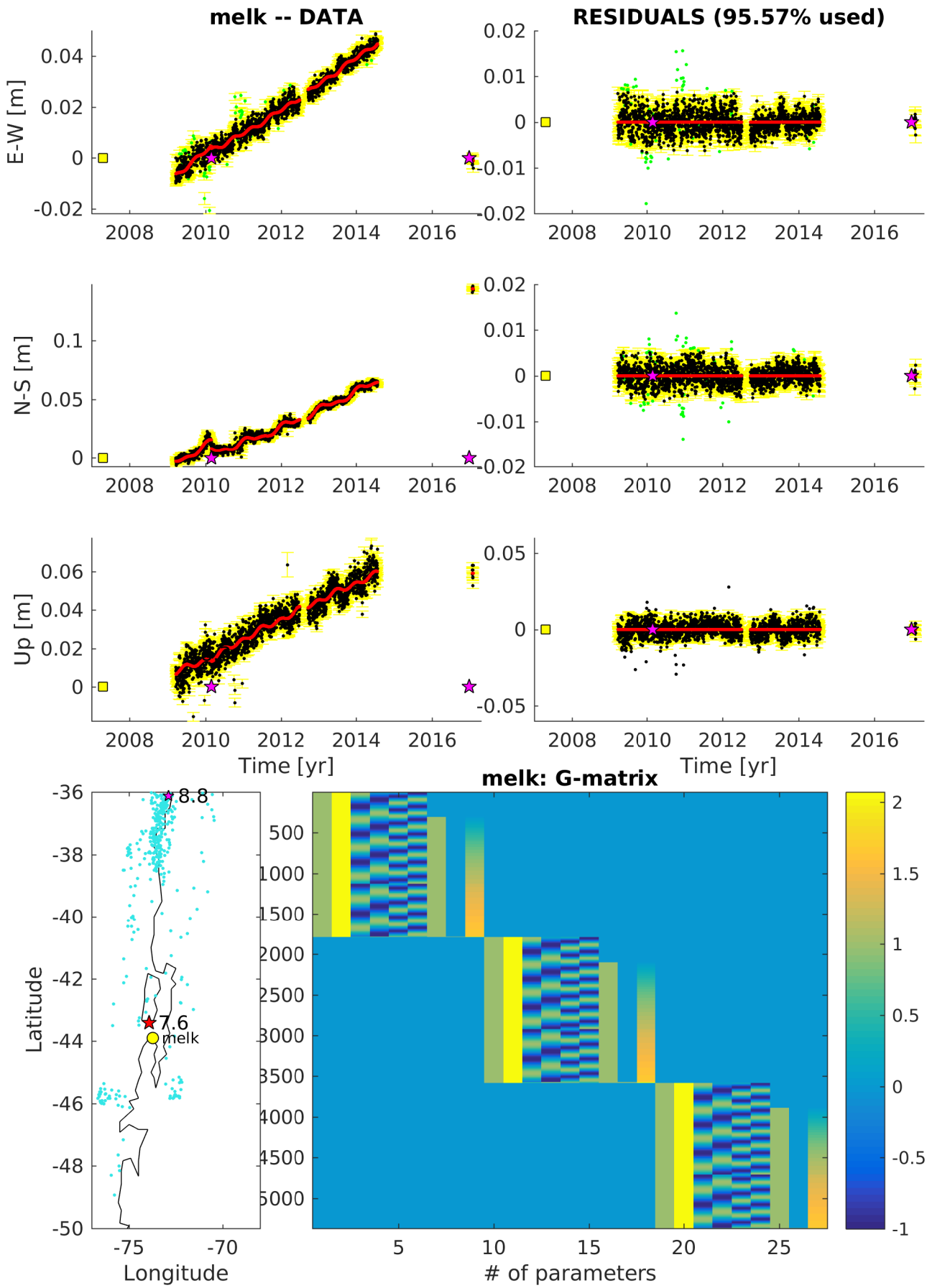
melk -- DATA
RESIDUALS (95.57% used)
E-W [m]
N-S [m]
Up [m]
Time [yr]
melk: G-matrix
8.8
7.6
melk
Latitude
Longitude
# of parameters

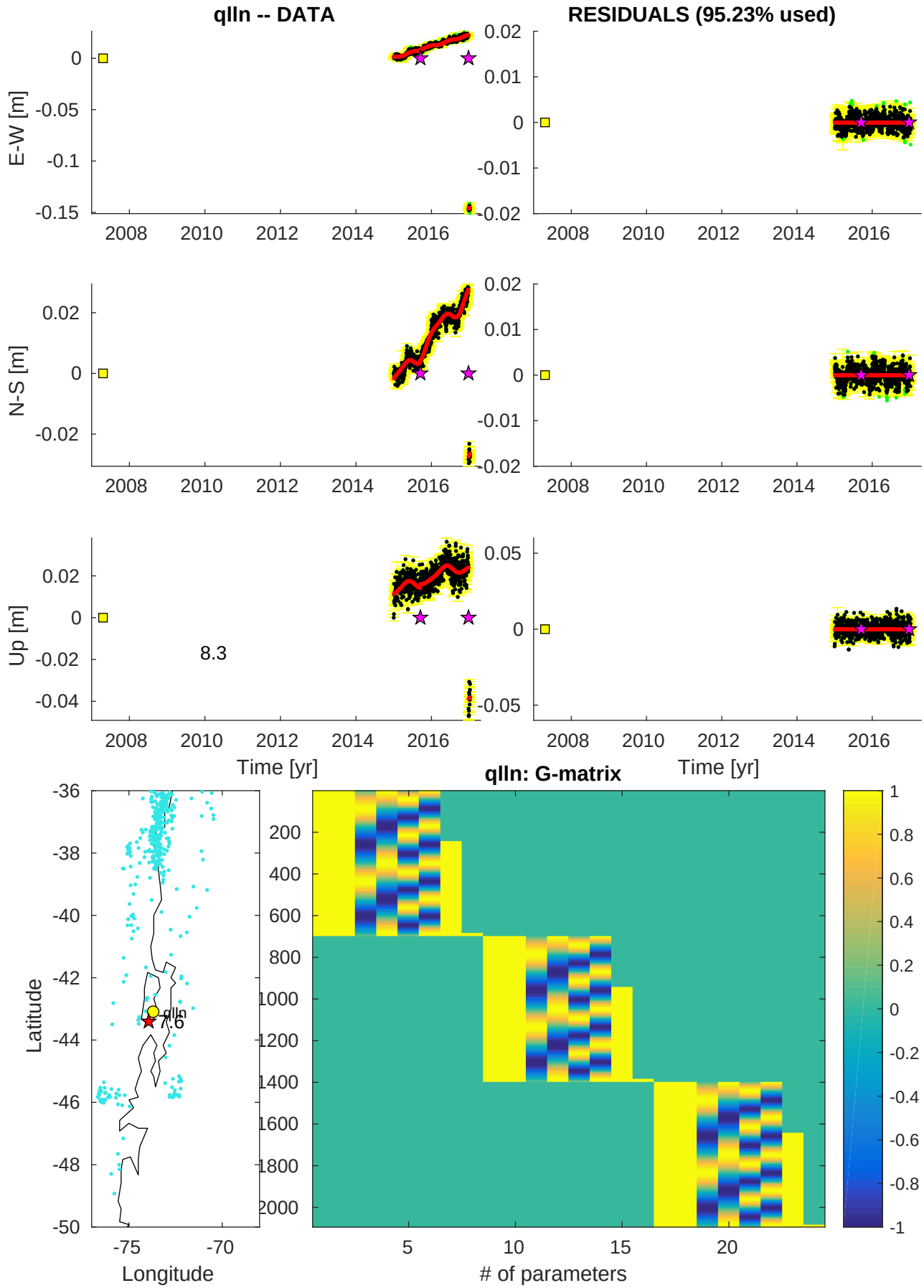
qlln -- DATA
RESIDUALS (95.23% used)
E-W [m]
N-S [m]
Up [m]
8.3
Time [yr]
Time [yr]
qlln: G-matrix
Latitude
Longitude
qlln
7.6
# of parameters

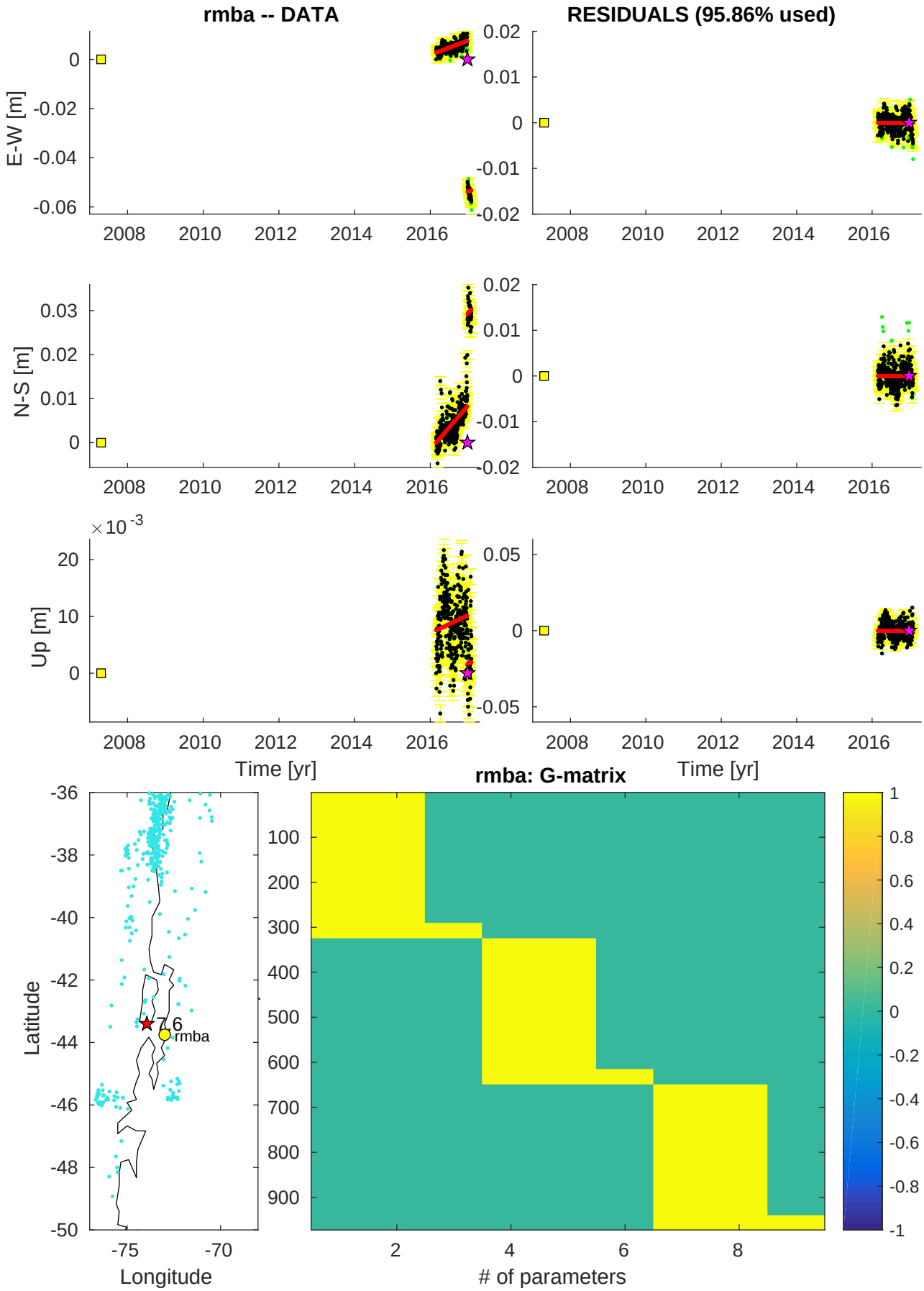
rmba -- DATA
RESIDUALS (95.86% used)
E-W [m]
N-S [m]
Up [m]
×10 -3
Time [yr]
rmba: G-matrix
Latitude
Longitude
rmba
# of parameters

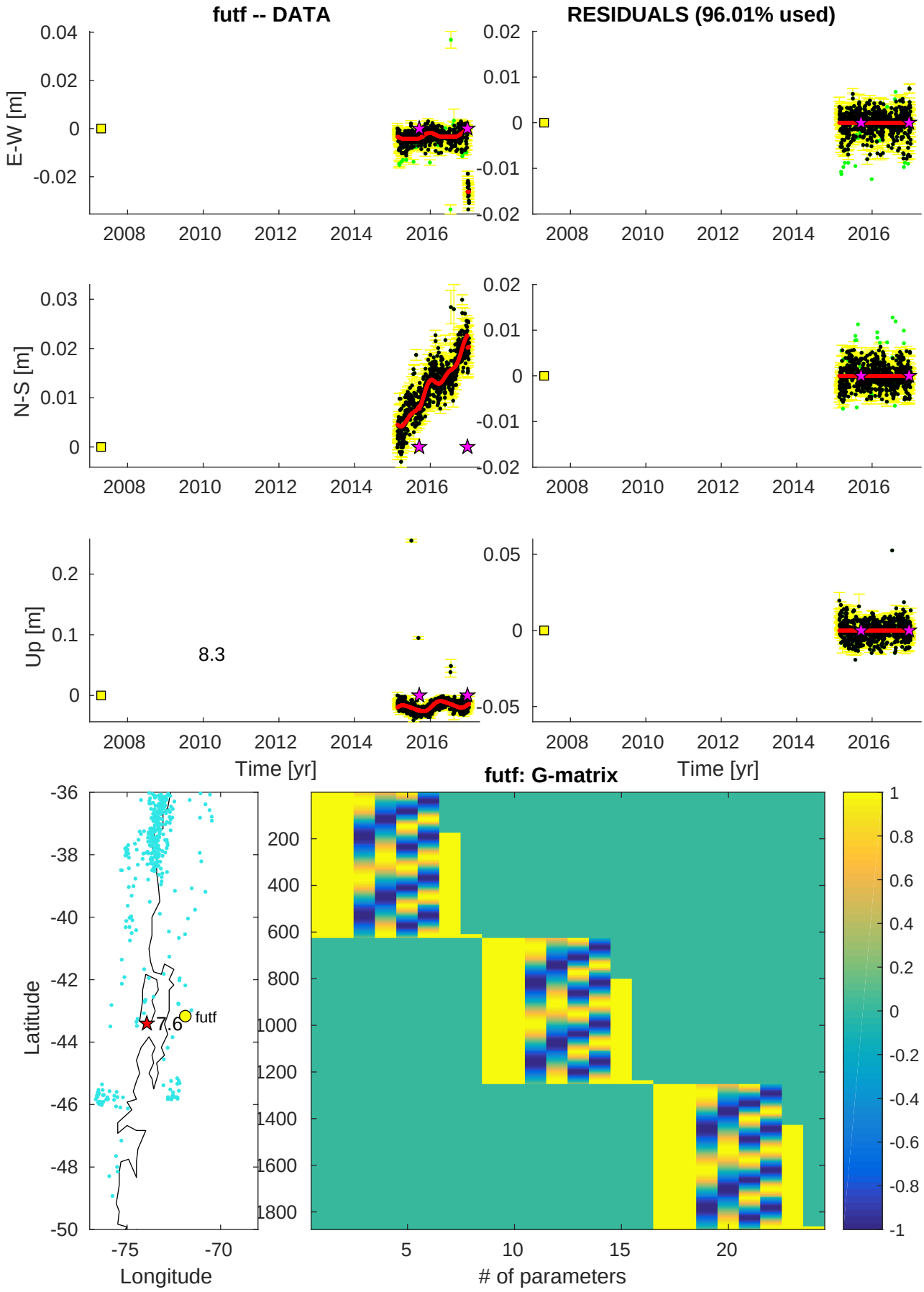
futf -- DATA
RESIDUALS (96.01% used)
E-W [m]
N-S [m]
Up [m]
8.3
Time [yr]
Time [yr]
futf: G-matrix
Latitude
Longitude
7.6
futf
# of parameters

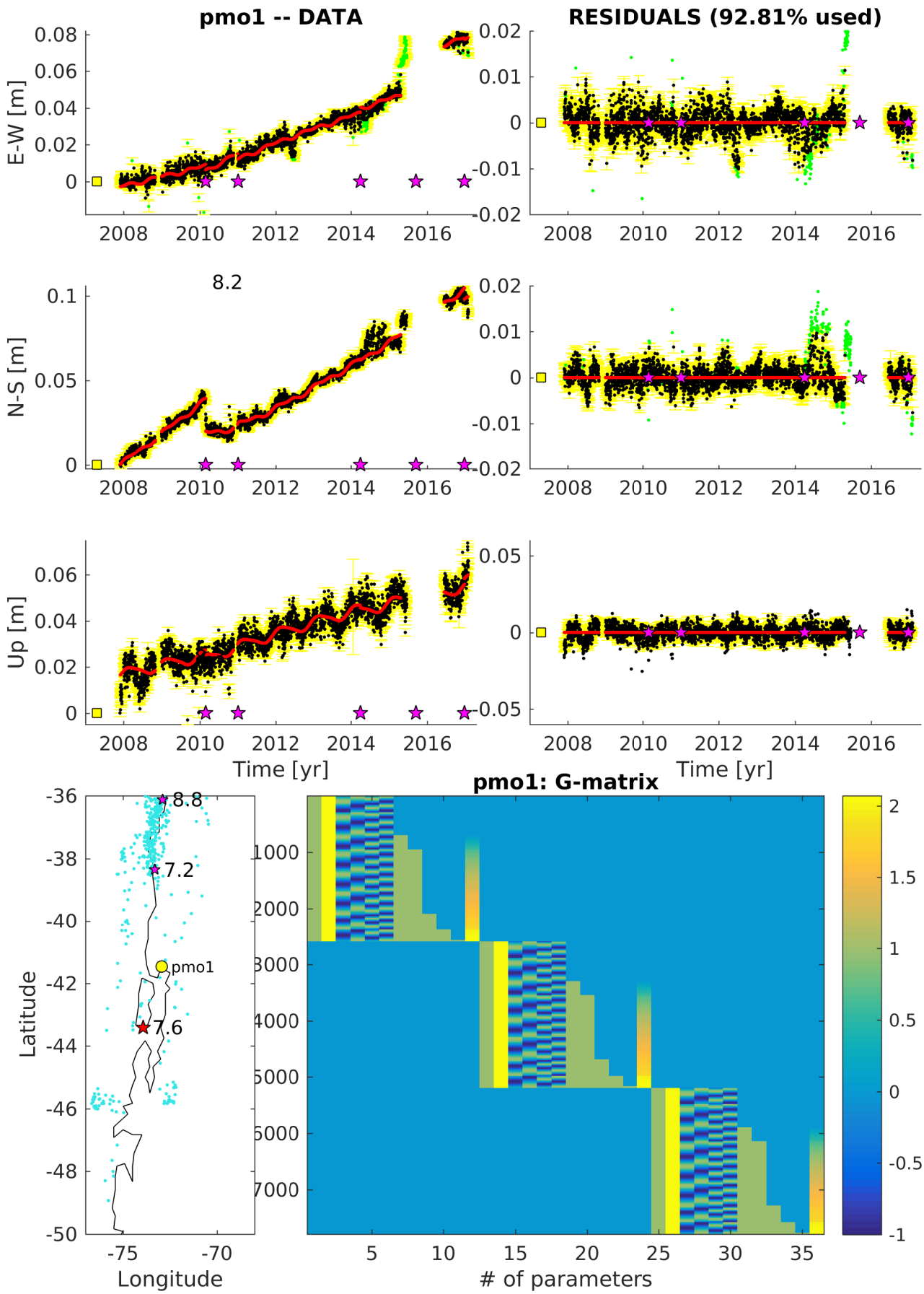
pmo1 -- DATA
RESIDUALS (92.81% used)
E-W [m]
N-S [m]
Up [m]
8.2
Time [yr]
pmo1: G-matrix
Latitude
Longitude
pmo1
8.8
7.2
7.6
# of parameters

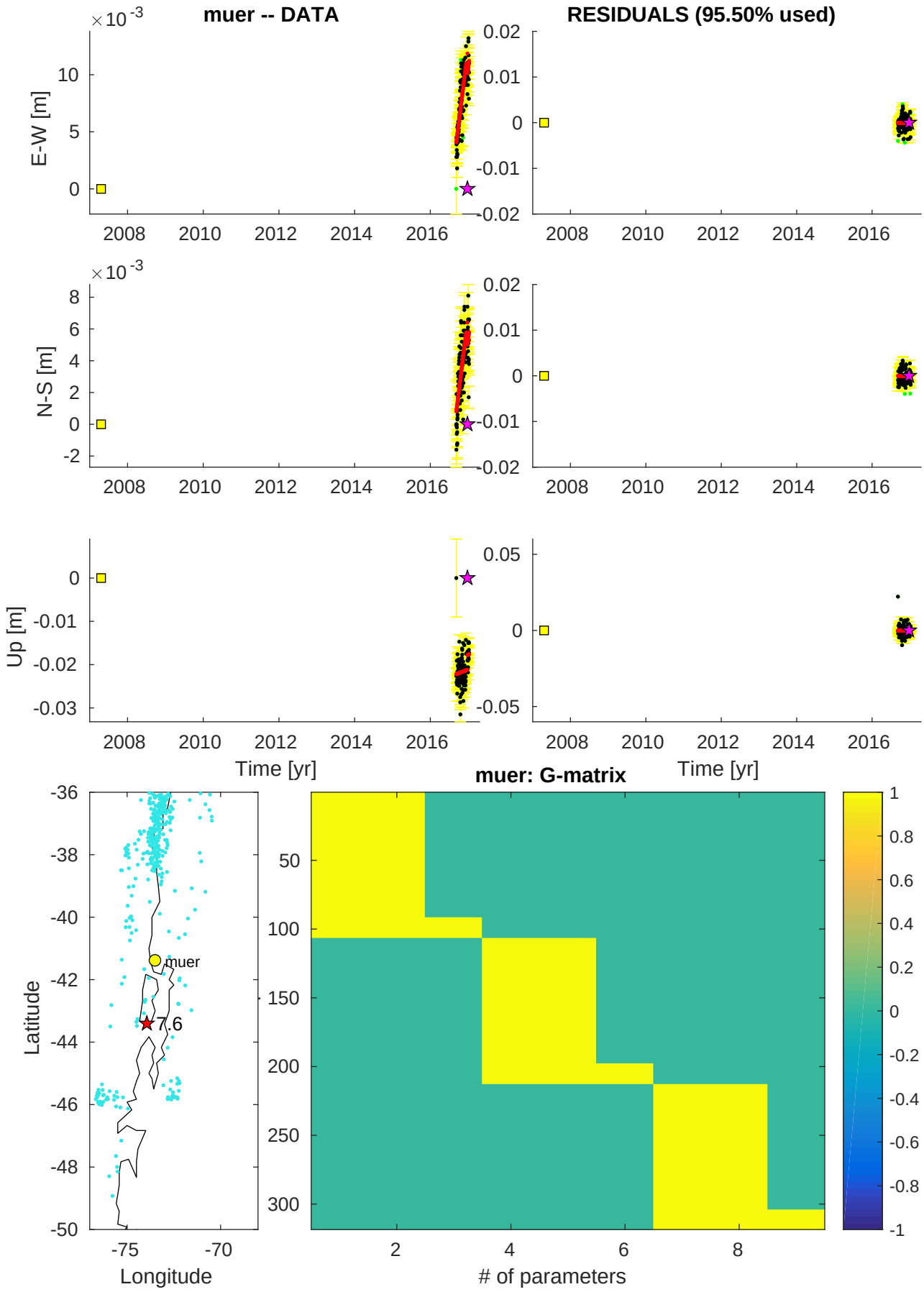
muer -- DATA
RESIDUALS (95.50% used)
E-W [m]
N-S [m]
Up [m]
Time [yr]
muer: G-matrix
muer
7.6
Latitude
Longitude
# of parameters

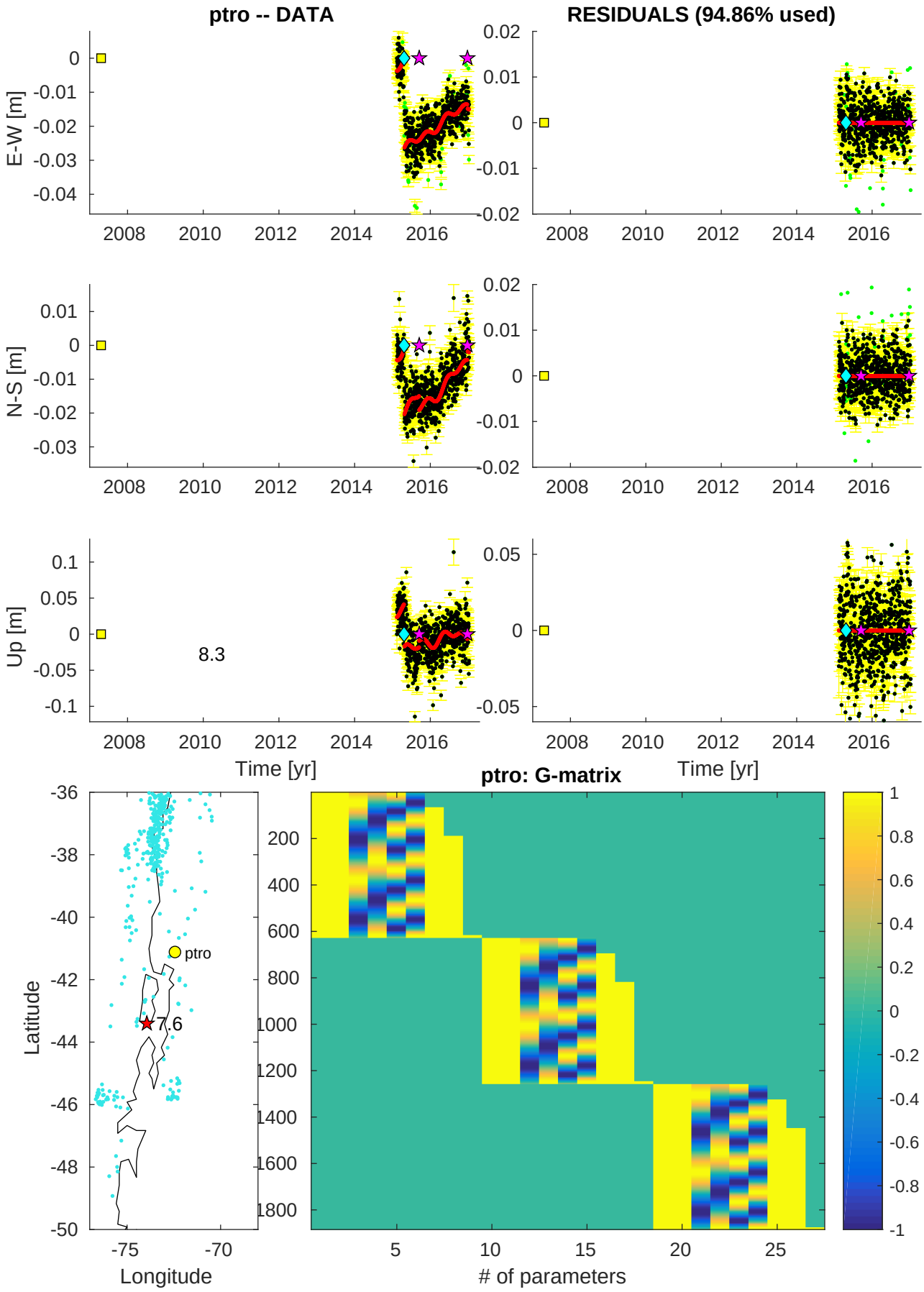
ptro -- DATA
RESIDUALS (94.86% used)
E-W [m]
N-S [m]
Up [m]
8.3
Time [yr]
Time [yr]
ptro: G-matrix
ptro
7.6
Latitude
Longitude
# of parameters

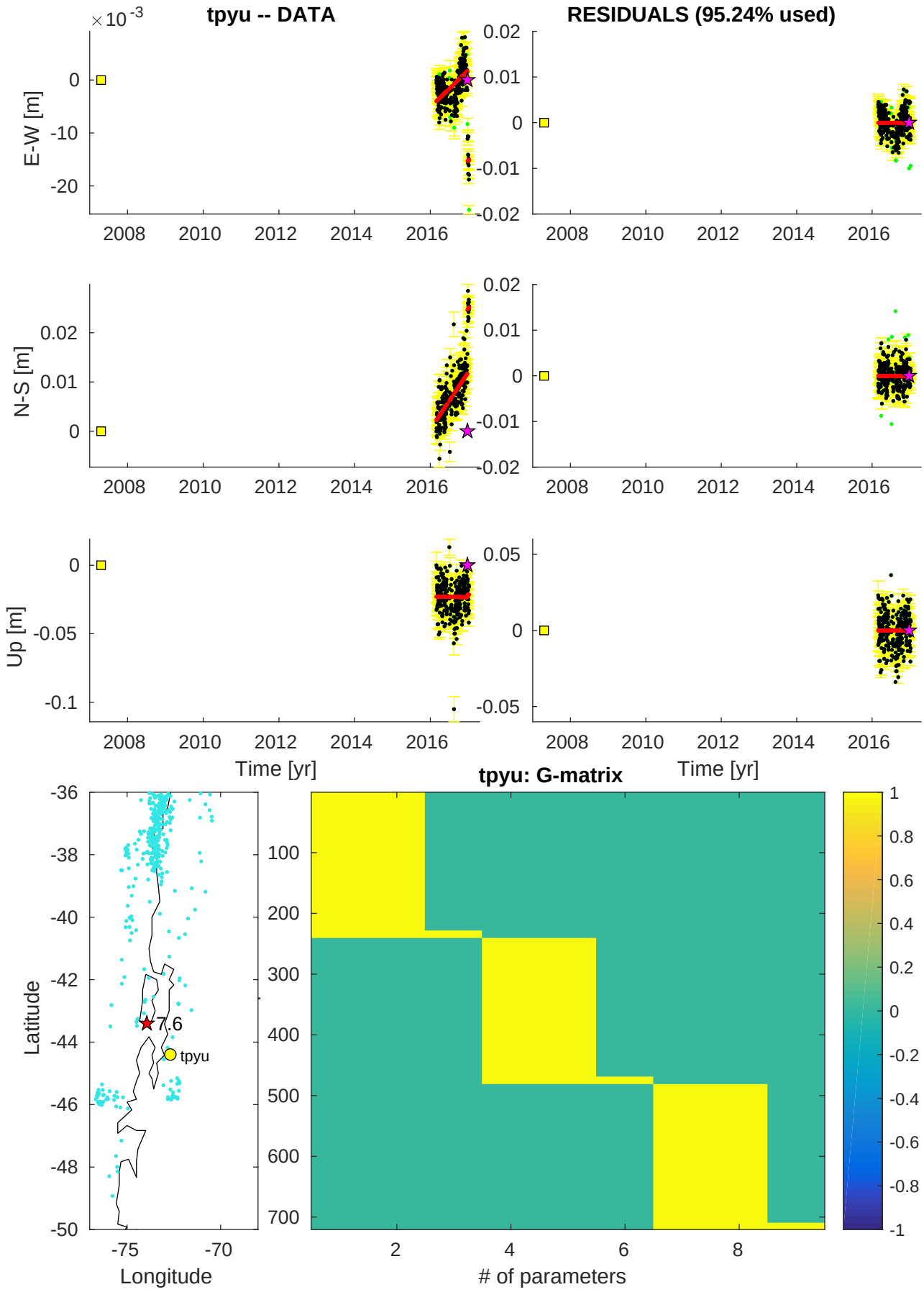
tpyu -- DATA
RESIDUALS (95.24% used)
E-W [m]
N-S [m]
Up [m]
Time [yr]
tpyu: G-matrix
Latitude
Longitude
7.6
tpyu
# of parameters

Figure S2. Series of figures showing the geocoded, wrapped interferograms from an ascending Sentinel-1 , a descending Sentinel-1 , and a descending ALOS SAR image pair. L indicates the line-of-sight, H the flight direction (heading).

-42.4
-42.6
-42.8
-43
-43.2
-43.4
-43.6
-43.8
-44
-44.2
-44.4

L
H

-2.7 cm 2.7

-74.5 -74 -73.5 -73 -72.5 -72 -71.5

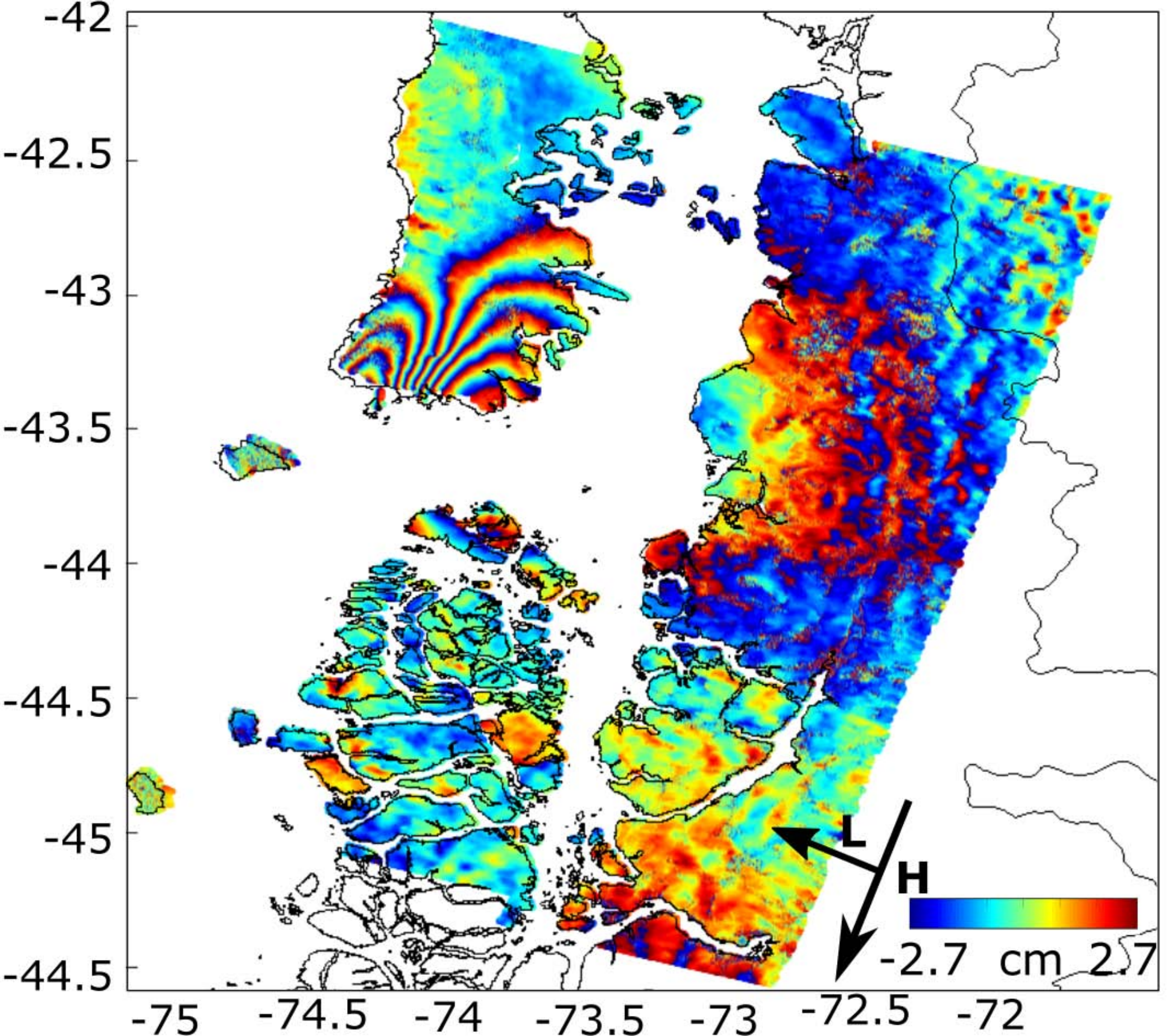
-42
-42.5
-43
-43.5
-44
-44.5
-45
-44.5
-75
-74.5
-74
-73.5
-73
-72.5
-72
L
H
-2.7 cm 2.7

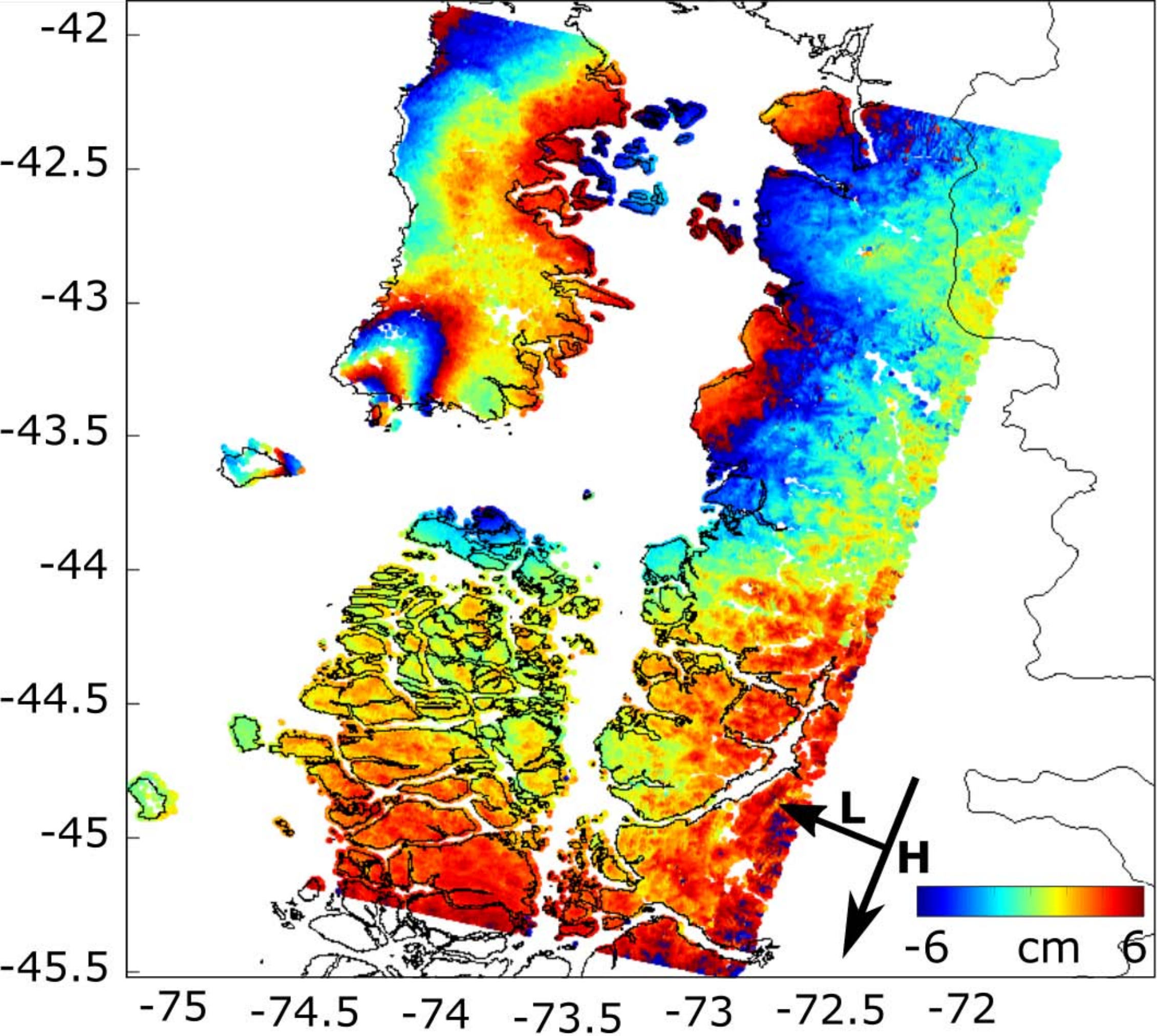
-42
-42.5
-43
-43.5
-44
-44.5
-45
-45.5
-75
-74.5
-74
-73.5
-73
-72.5
-72
L
H
-6
cm
6

Figure S3. Unwrapped inteferograms formed from: a) Sentinel-1 ascending; b) Sentinel-1 descending and; c) ALOS SAR image pair, including the slip model presented here. The line-of-sight (LOS) is perpendicular to the flight direction.

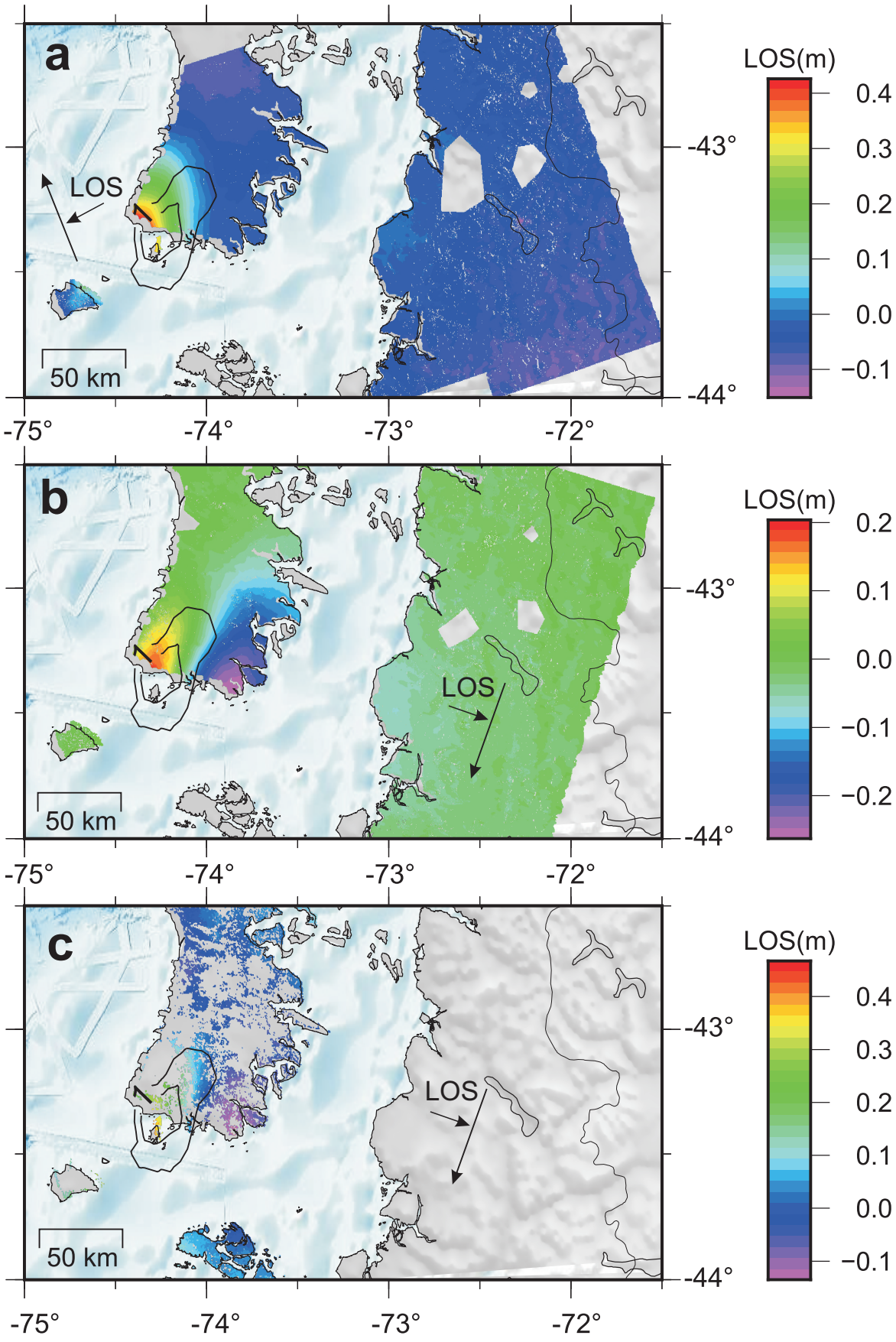
a
LOS
50 km
-43°
-44°
-75°
-74°
-73°
-72°
LOS(m)
0.4
0.3
0.2
0.1
0.0
−0.1
b
LOS
50 km
-43°
-44°
-75°
-74°
-73°
-72°
LOS(m)
0.2
0.1
0.0
−0.1
−0.2
c
LOS
50 km
-43°
-44°
-75°
-74°
-73°
-72°
LOS(m)
0.4
0.3
0.2
0.1
0.0
−0.1

Figure S4. Subsampled LOS displacement data (see also Fig. S2 and S3) used in the joint inversion.

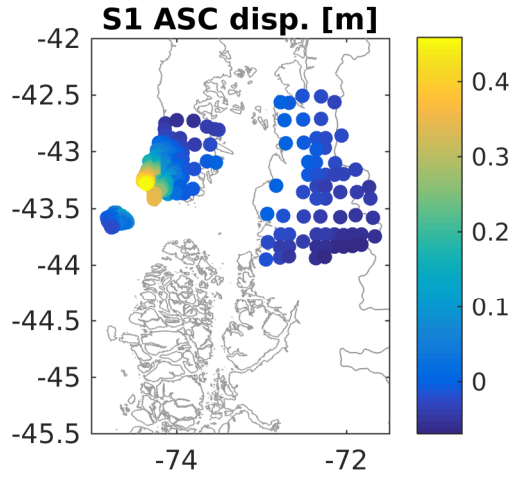
S1 ASC disp. [m]
-42
-42.5
-43
-43.5
-44
-44.5
-45
-45.5
-74
-72
0.4
0.3
0.2
0.1
0

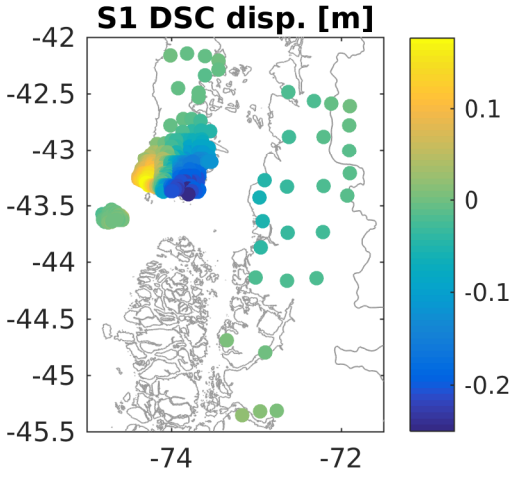
S1 DSC disp. [m]
-42
-42.5
-43
-43.5
-44
-44.5
-45
-45.5
-74
-72
0.1
0
-0.1
-0.2

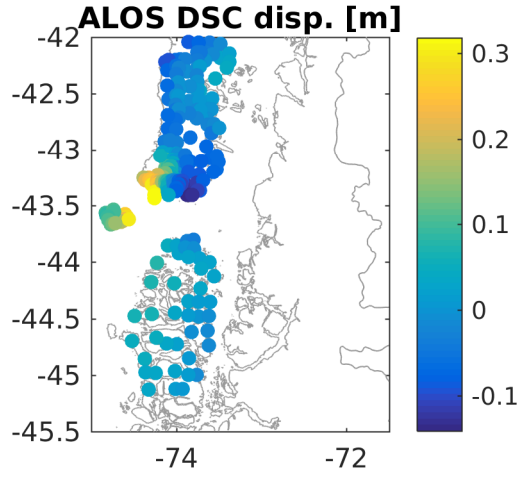
ALOS DSC disp. [m]
-42
-42.5
-43
-43.5
-44
-44.5
-45
-45.5
-74
-72
0.3
0.2
0.1
0
-0.1

Figure S5. Series of figures showing the trade-off curve and checkerboards test. The trade-off curve was estimated between the RMS error (y-axis) and the weight of the Tikhonov damping (x-axis). The chosen damping parameter is shown by a red circle. The input data used in the checkerboard tests are shown in the figures. Three sizes of synthetic slip patch were tested. Top left panels show the recovered slip model using the same damping parameters as used in the inversion of the real data. Top right panels show the misfit to the synthetic Sentinel Ascending data. Bottom left panels show the misfit to the synthetic Sentinel Descending data as well as the vertical GPS model predictions (magenta) compared to the synthetic vertical displacements (black). Bottom right shows the misfit to the synthetic ALOS Descending data as well as the horizontal GPS model predictions (magenta) compared to the synthetic horizontal displacements (black).

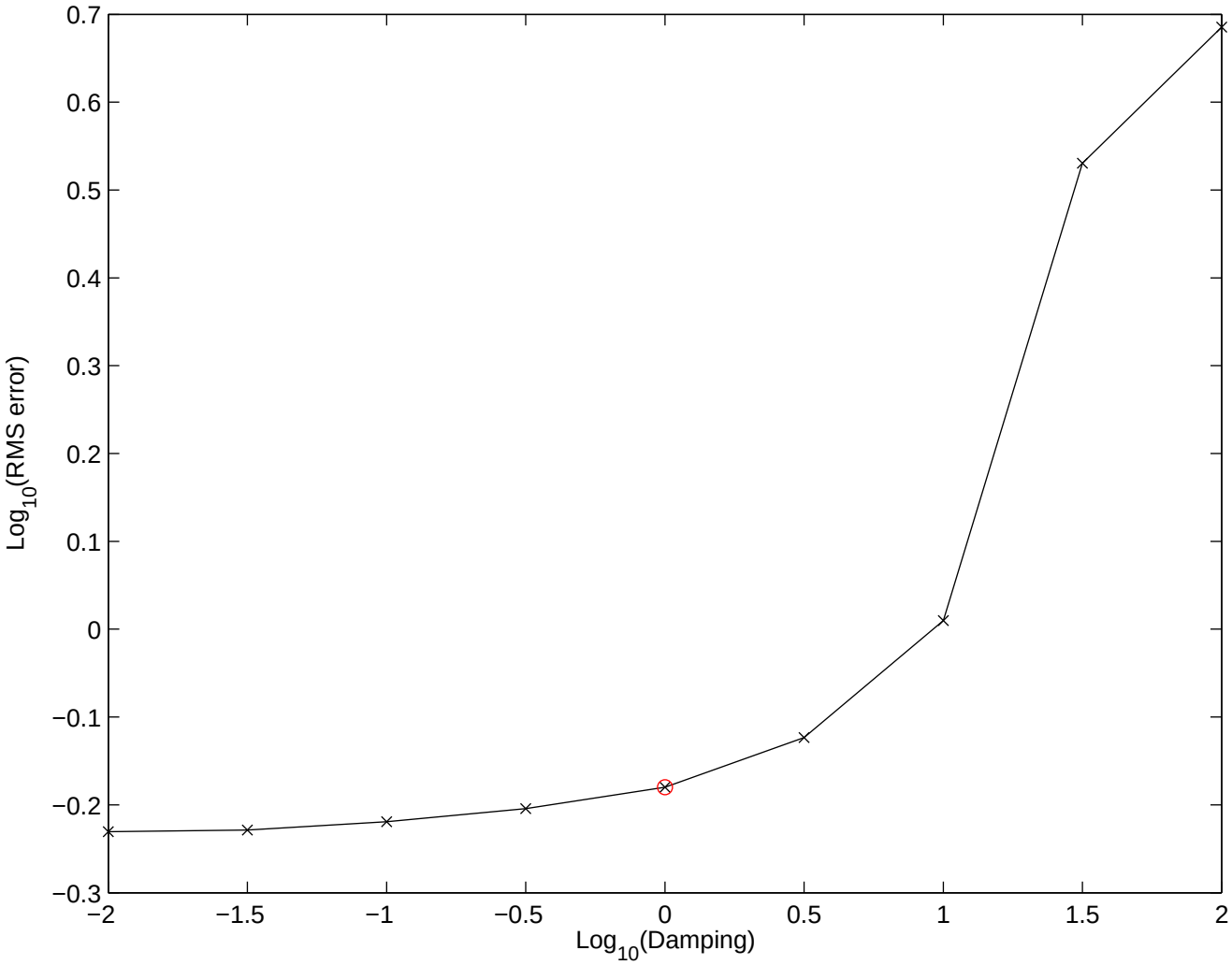
0.7
0.6
0.5
0.4
0.3
0.2
0.1
0
−0.1
−0.2
−0.3
−2
−1.5
−1
−0.5
0
0.5
1
1.5
2
Log10(RMS error)
Log10(Damping)

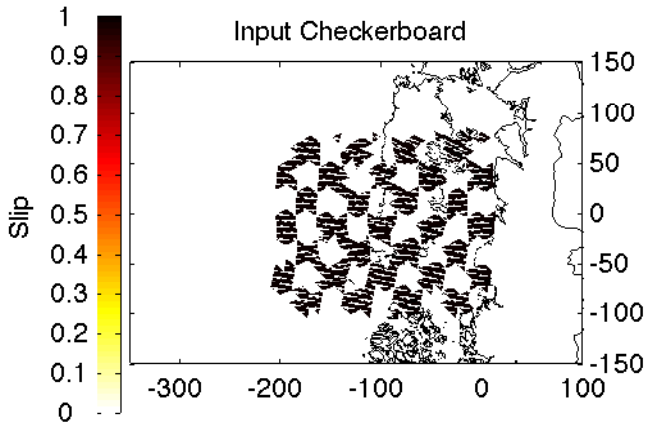
Input Checkerboard
Slip
1
0.9
0.8
0.7
0.6
0.5
0.4
0.3
0.2
0.1
0
150
100
50
0
-50
-100
-150
-300
-200
-100
0
100

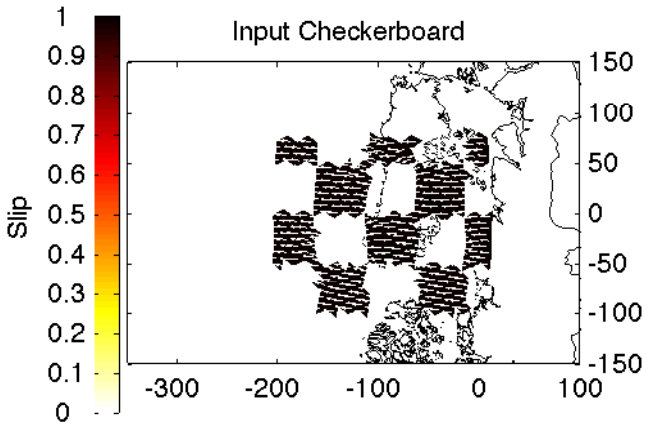
Input Checkerboard
Slip
1
0.9
0.8
0.7
0.6
0.5
0.4
0.3
0.2
0.1
0
150
100
50
0
-50
-100
-150
-300
-200
-100
0
100

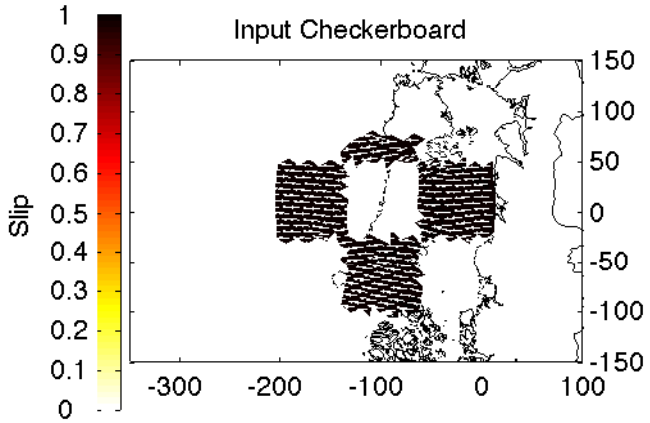
Input Checkerboard
Slip
1
0.9
0.8
0.7
0.6
0.5
0.4
0.3
0.2
0.1
0
150
100
50
0
-50
-100
-150
-300
-200
-100
0
100

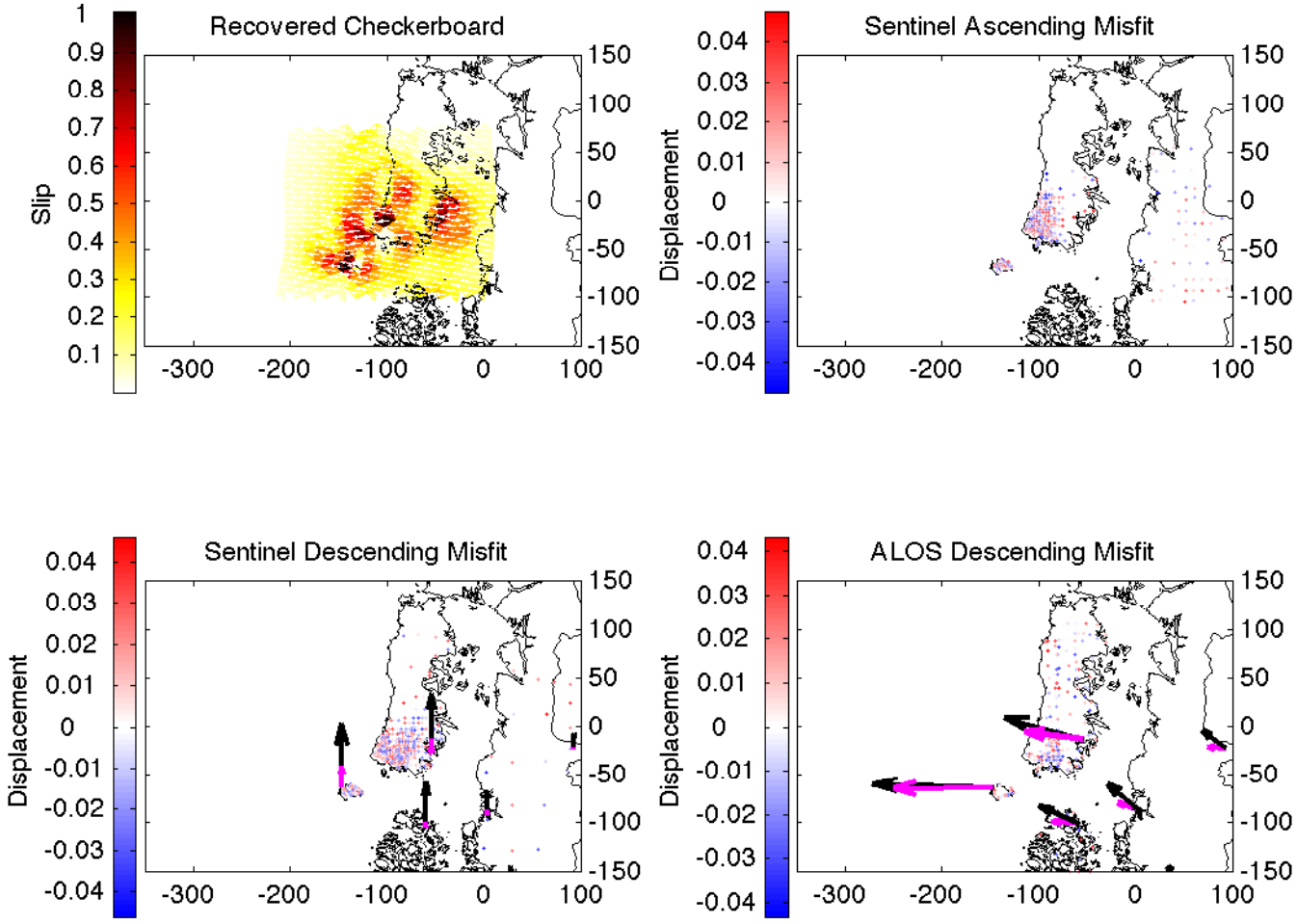
Recovered Checkerboard
Slip
1
0.9
0.8
0.7
0.6
0.5
0.4
0.3
0.2
0.1
-300
-200
-100
0
100
150
100
50
0
-50
-100
-150
Sentinel Ascending Misfit
Displacement
0.04
0.03
0.02
0.01
0
-0.01
-0.02
-0.03
-0.04
Sentinel Descending Misfit
ALOS Descending Misfit

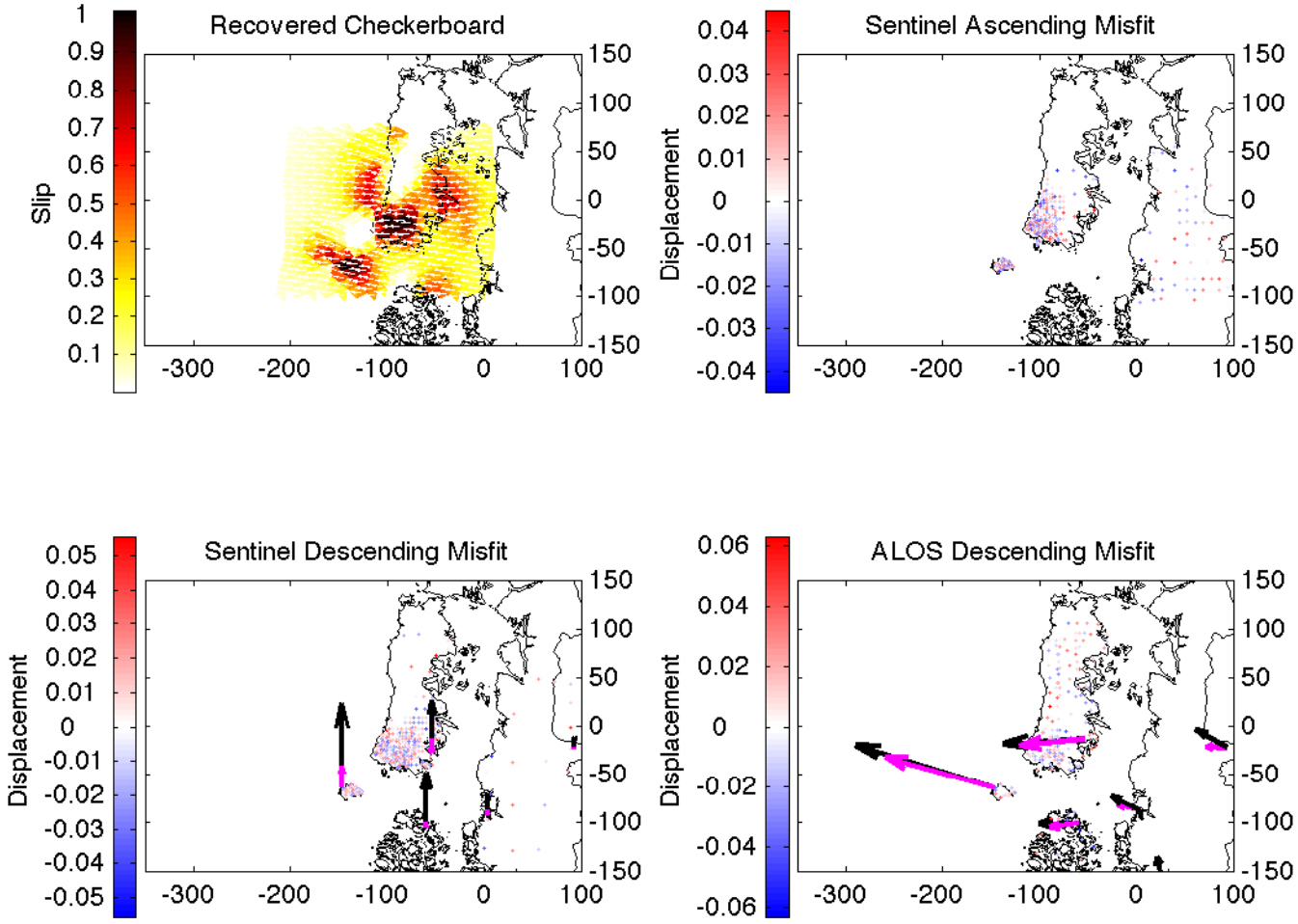
Recovered Checkerboard
Slip
1
0.9
0.8
0.7
0.6
0.5
0.4
0.3
0.2
0.1
-300
-200
-100
0
100
150
100
50
0
-50
-100
-150
Sentinel Ascending Misfit
Displacement
0.04
0.03
0.02
0.01
0
-0.01
-0.02
-0.03
-0.04
Sentinel Descending Misfit
0.05
0.04
0.03
0.02
0.01
0
-0.01
-0.02
-0.03
-0.04
-0.05
ALOS Descending Misfit
0.06
0.04
0.02
0
-0.02
-0.04
-0.06

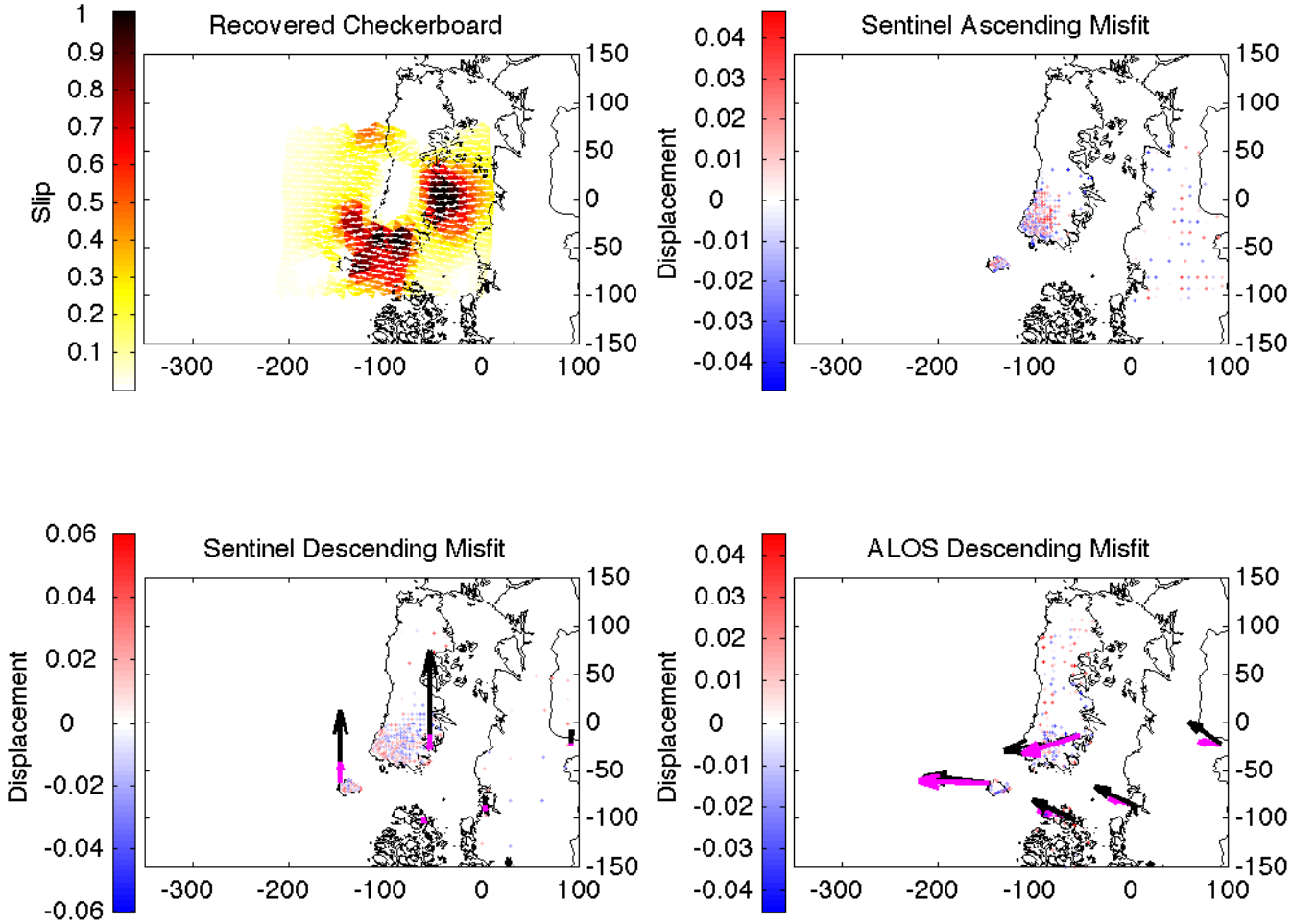
Recovered Checkerboard
Slip
1
0.9
0.8
0.7
0.6
0.5
0.4
0.3
0.2
0.1
-300
-200
-100
0
100
150
100
50
0
-50
-100
-150
Sentinel Ascending Misfit
Displacement
0.04
0.03
0.02
0.01
0
-0.01
-0.02
-0.03
-0.04
Sentinel Descending Misfit
0.06
0.04
0.02
0
-0.02
-0.04
-0.06
ALOS Descending Misfit

Figure S6. Histogram showing the number of aftershocks versus days after the earthquake.

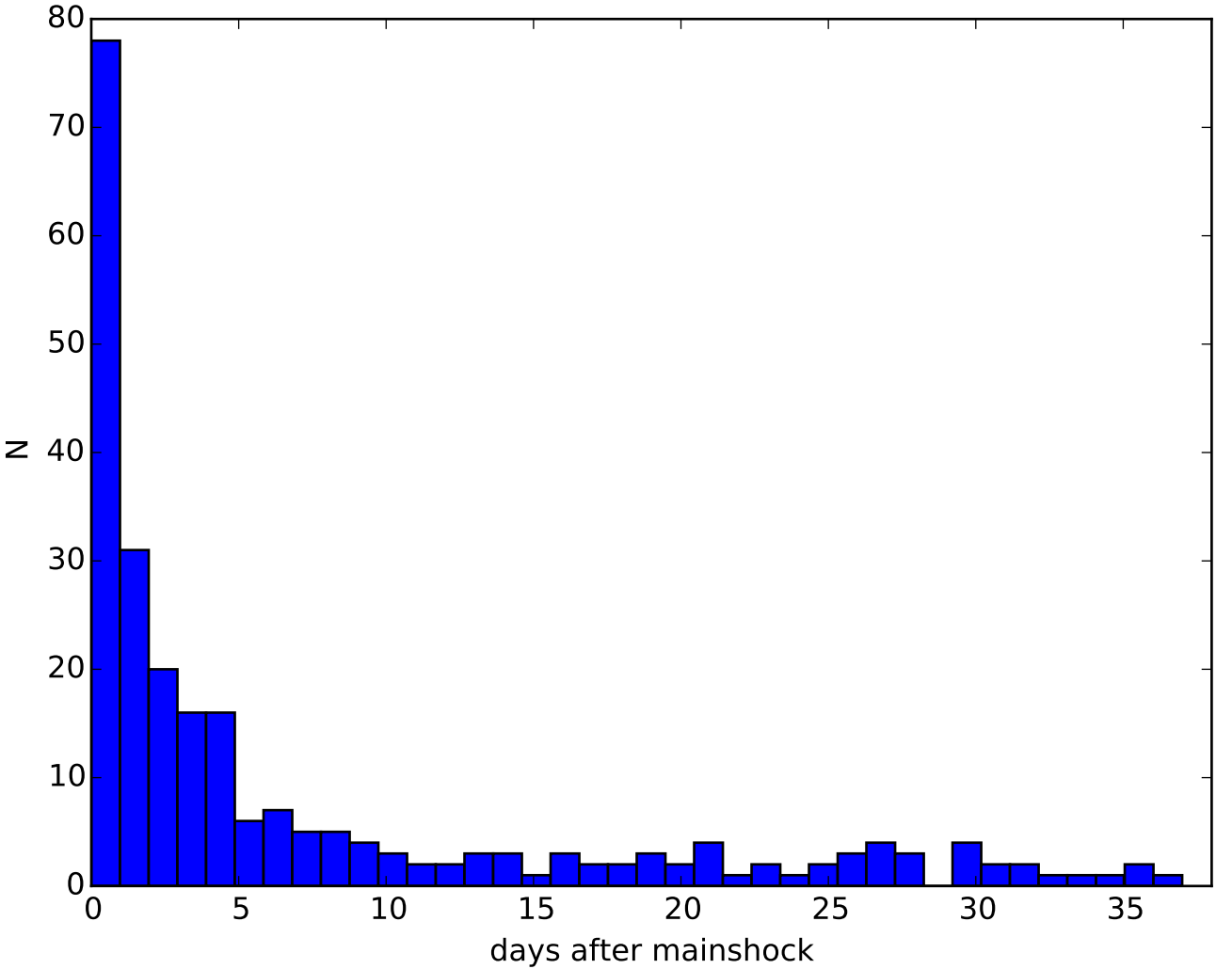
80
70
60
50
40
30
20
10
0
N
0
5
10
15
20
25
30
35
days after mainshock

Figure S7. a. Post-stack time migration of the trench, deformation front, continental slope and shelf across seismic profile XY (Figure 3 in the main text). The blue curve denotes the location of the seafloor, whereas the red curve corresponds to the top of the oceanic and continental basement seawards and landwards of the deformation, respectively. The red curve along the continental slope denotes the base of the sediment apron. b. Seismic reflectors converted from two way travel time to depth using a linear velocity-depth distribution with constant vertical velocity gradient.

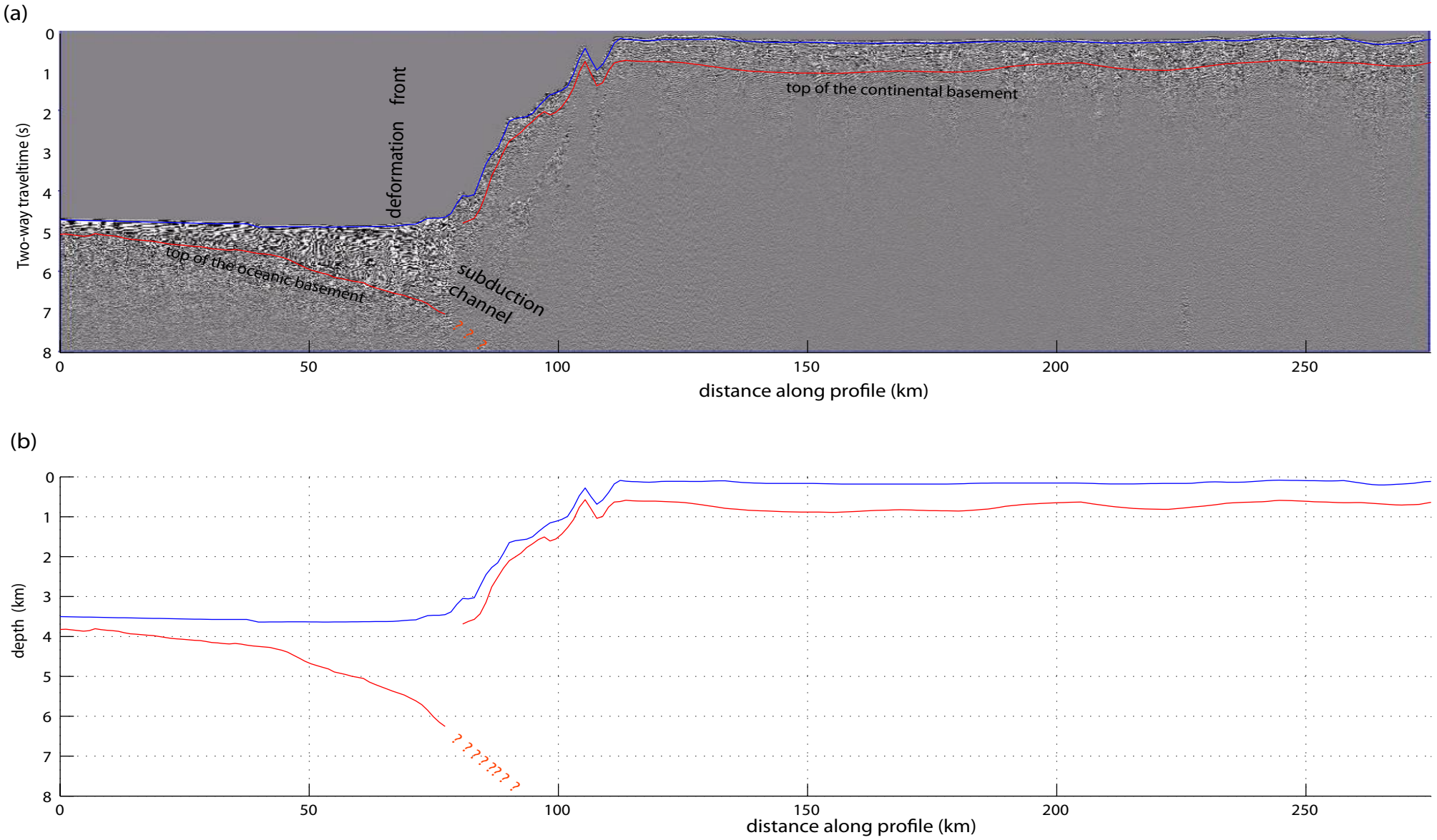
(a)
Two-way traveltime (s)
0
1
2
3
4
5
6
7
8
deformation front
top of the continental basement
top of the oceanic basement
subduction channel
? ? ?
0
50
100
150
200
250
distance along profile (km)
(b)
depth (km)
0
1
2
3
4
5
6
7
8
? ? ? ? ? ? ? ?
0
50
100
150
200
250
distance along profile (km)

Figure S8. Modelling set up. Schematic plot of the FEM model structure and fault boundary conditions.

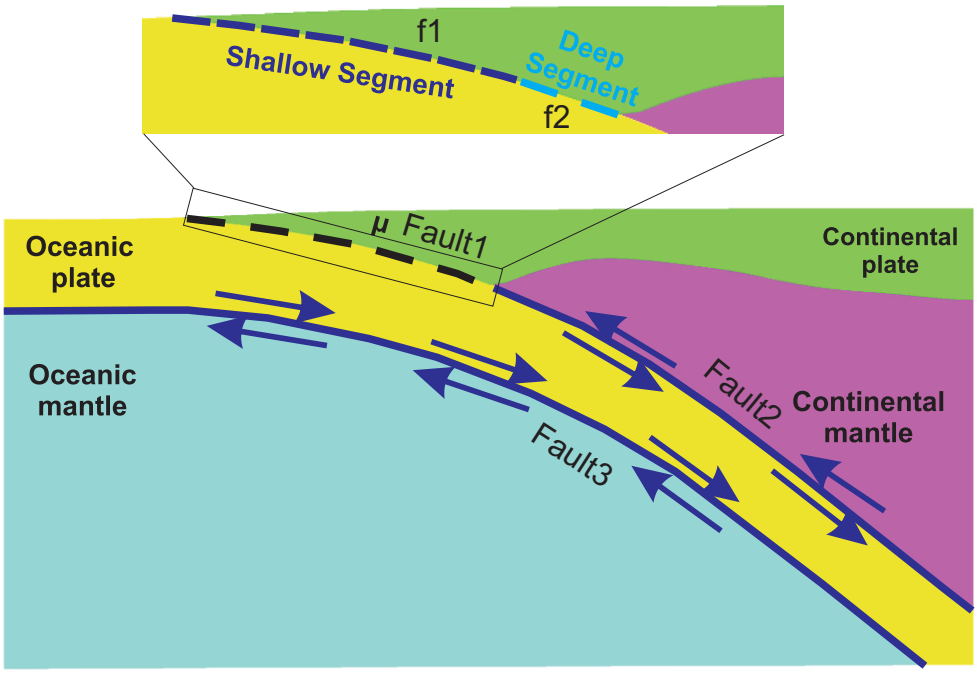
f1
Shallow Segment
Deep Segment
f2
μ Fault1
Oceanic plate
Continental plate
Oceanic mantle
Fault2
Continental mantle
Fault3

Figure S9. Series of figures showing of shear traction and coupling after 50, 100, and 150 years of loading for asperities of different size. The locking degree distribution is used to define the limits of the asperity. We show the results of clamping the fault inside the locking contours of 0.95, 0.90 and 0.80. A high effective coefficient of friction (0.04) is applied inside these regions, while low friction coefficient (0.004) is applied outside the selected regions. This configuration facilitates the clamping of the asperity and allows the surrounding interface to slip. Stress build-up concentrates in the downdip part of the coupled asperity. The size of the coupled asperity controls both the pattern of stress energy concentration and the uncoupling of the fault.

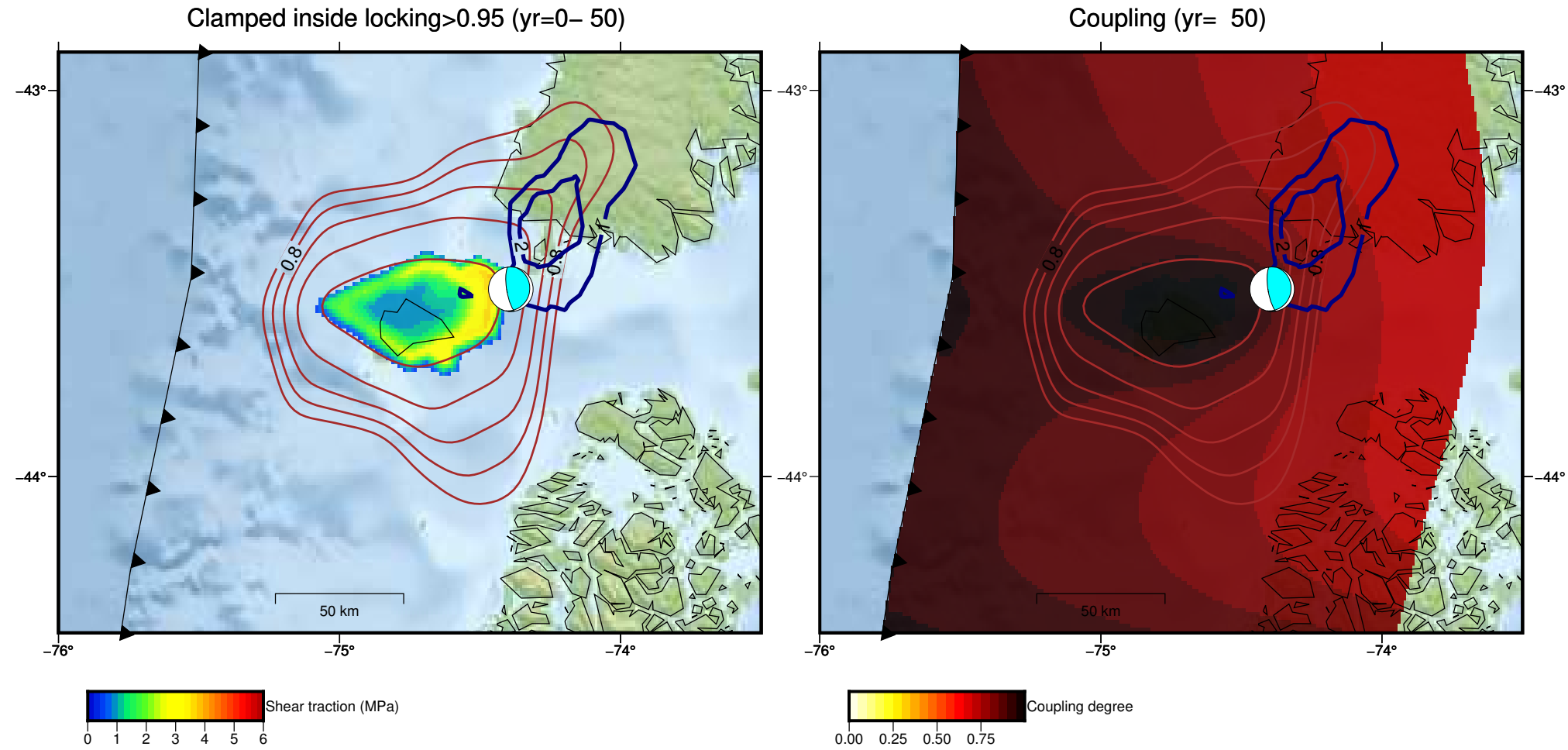
Clamped inside locking>0.95 (yr=0– 50)
Coupling (yr= 50)
–43°
–44°
–76°
–75°
–74°
0.8
2
50 km
Shear traction (MPa)
0 1 2 3 4 5 6
Coupling degree
0.00 0.25 0.50 0.75

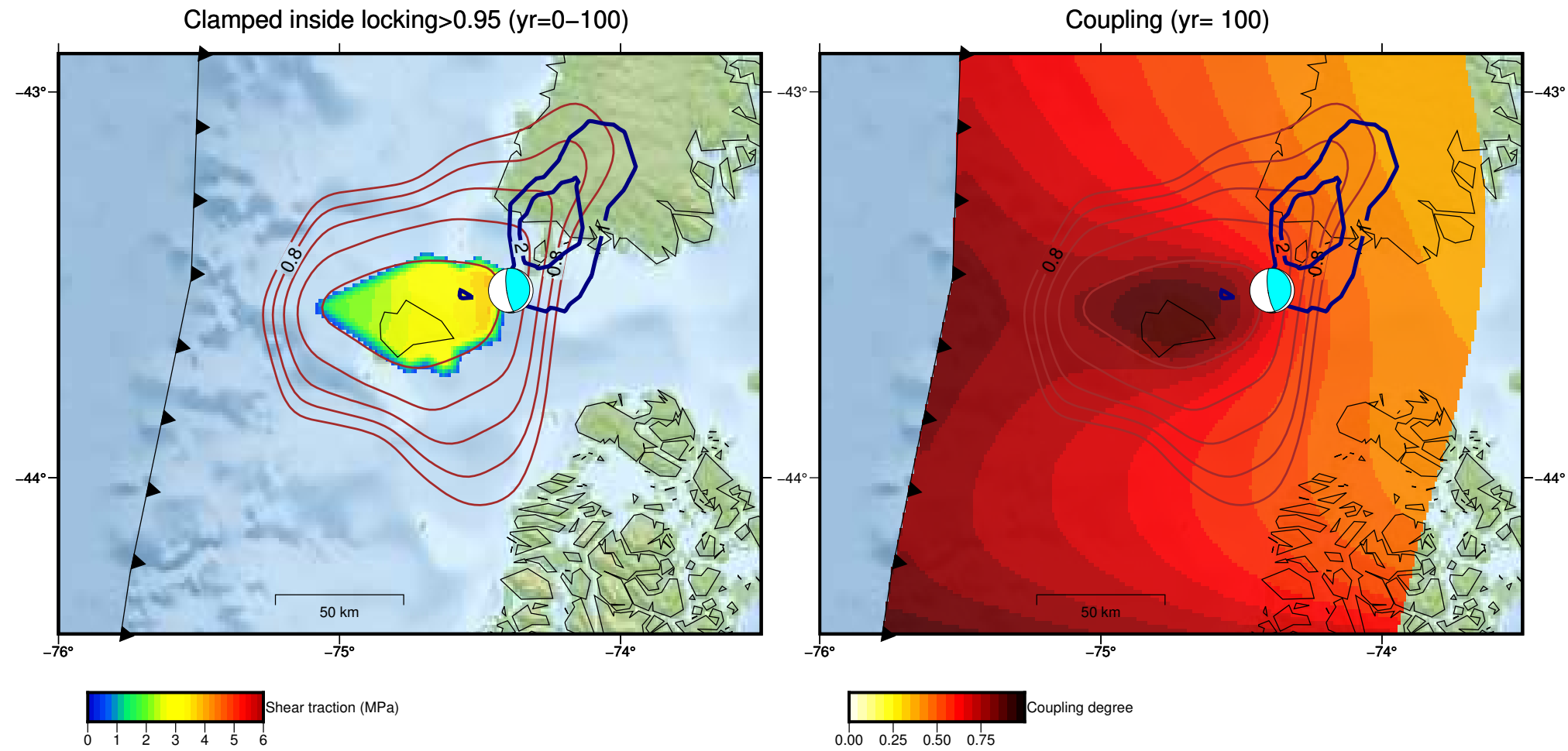
Clamped inside locking>0.95 (yr=0–100)
Coupling (yr= 100)
–43°
–44°
–76°
–75°
–74°
0.8
2
4
50 km
Shear traction (MPa)
0 1 2 3 4 5 6
Coupling degree
0.00 0.25 0.50 0.75

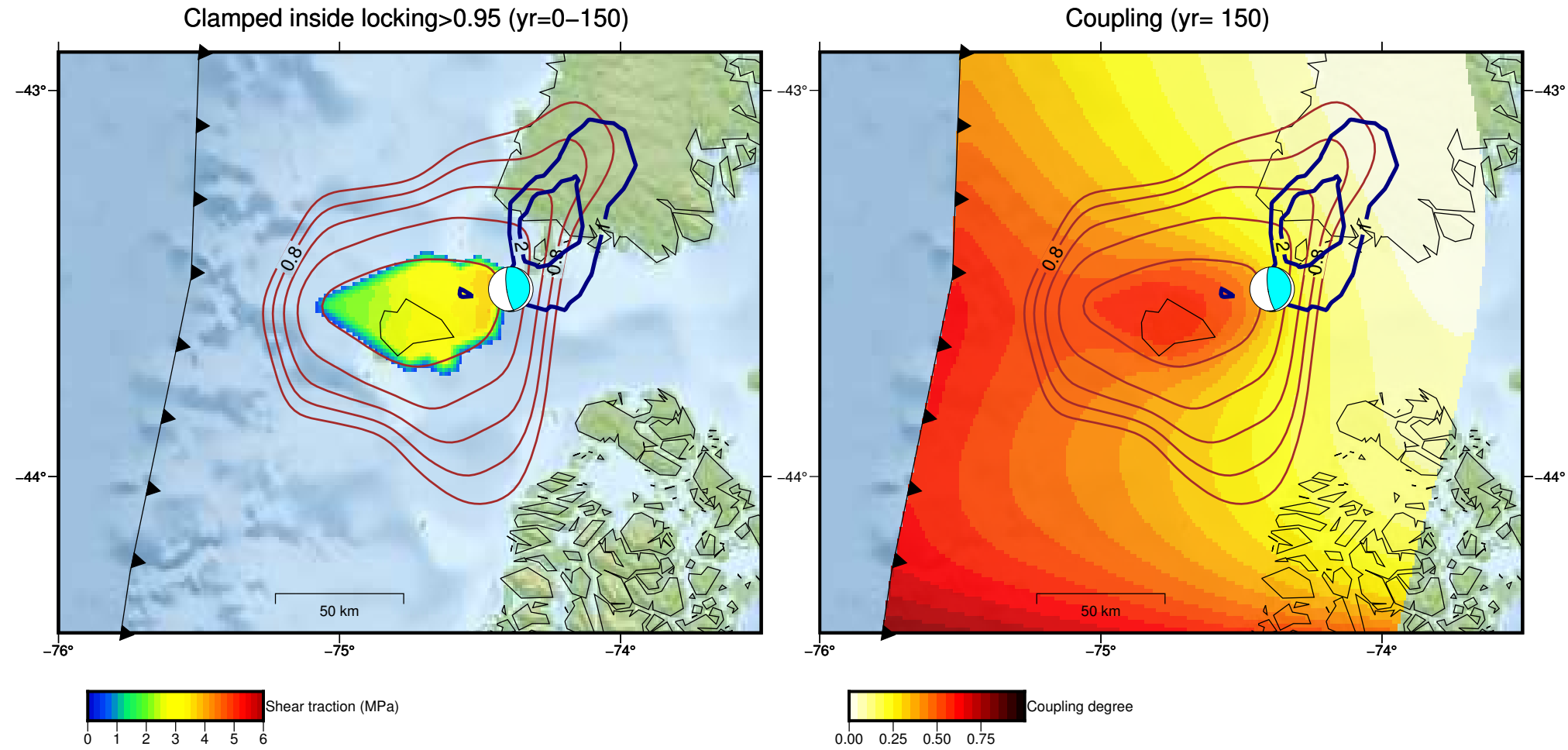
Clamped inside locking>0.95 (yr=0–150)
Coupling (yr= 150)
–43°
–44°
–76°
–75°
–74°
0.8
2
4
50 km
Shear traction (MPa)
0 1 2 3 4 5 6
Coupling degree
0.00 0.25 0.50 0.75

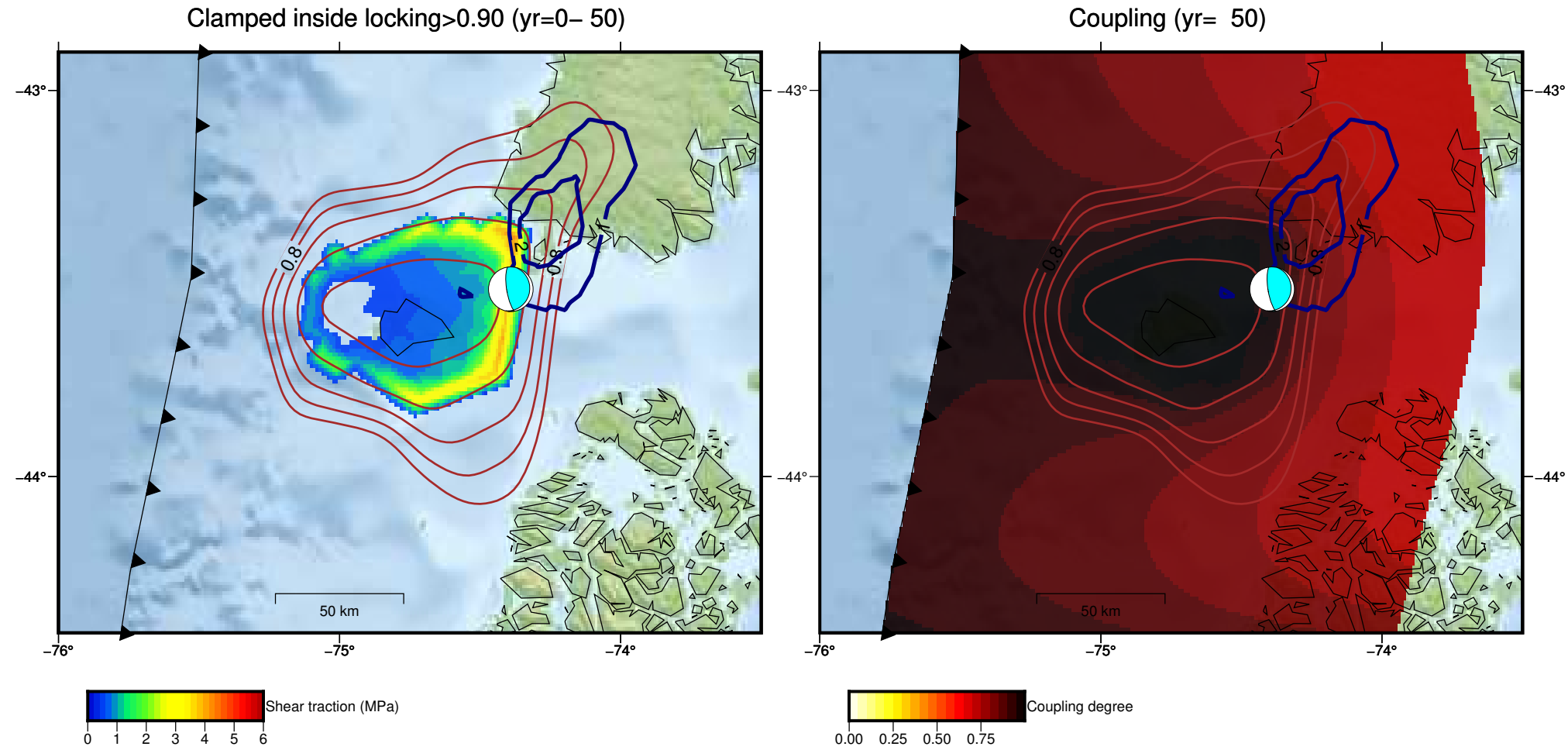
Clamped inside locking>0.90 (yr=0– 50)
Coupling (yr= 50)
–43°
–44°
–76°
–75°
–74°
0.8
2
4
50 km
Shear traction (MPa)
0 1 2 3 4 5 6
Coupling degree
0.00 0.25 0.50 0.75

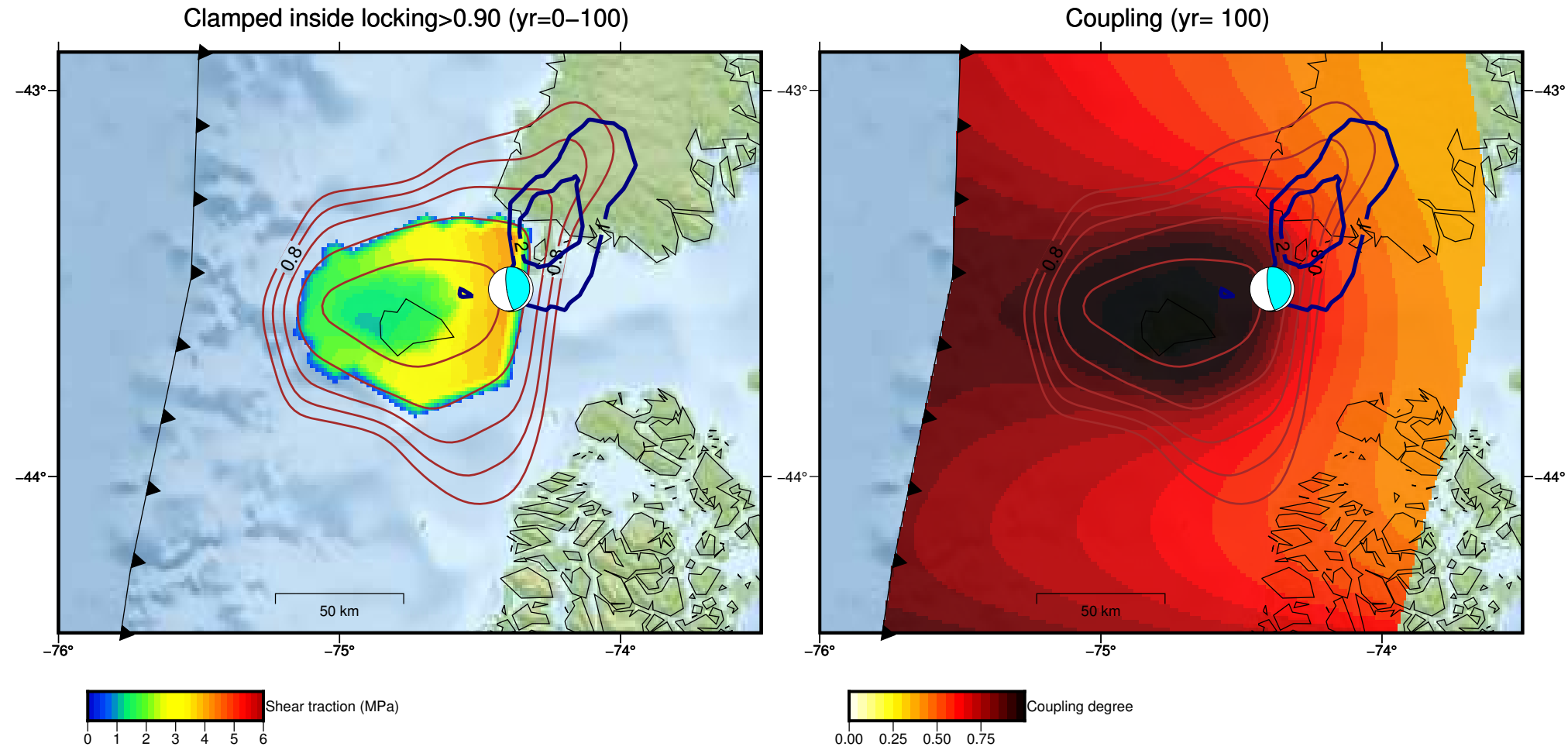
Clamped inside locking>0.90 (yr=0–100)
Coupling (yr= 100)
–43°
–44°
–76°
–75°
–74°
0.8
2
50 km
Shear traction (MPa)
0 1 2 3 4 5 6
Coupling degree
0.00 0.25 0.50 0.75

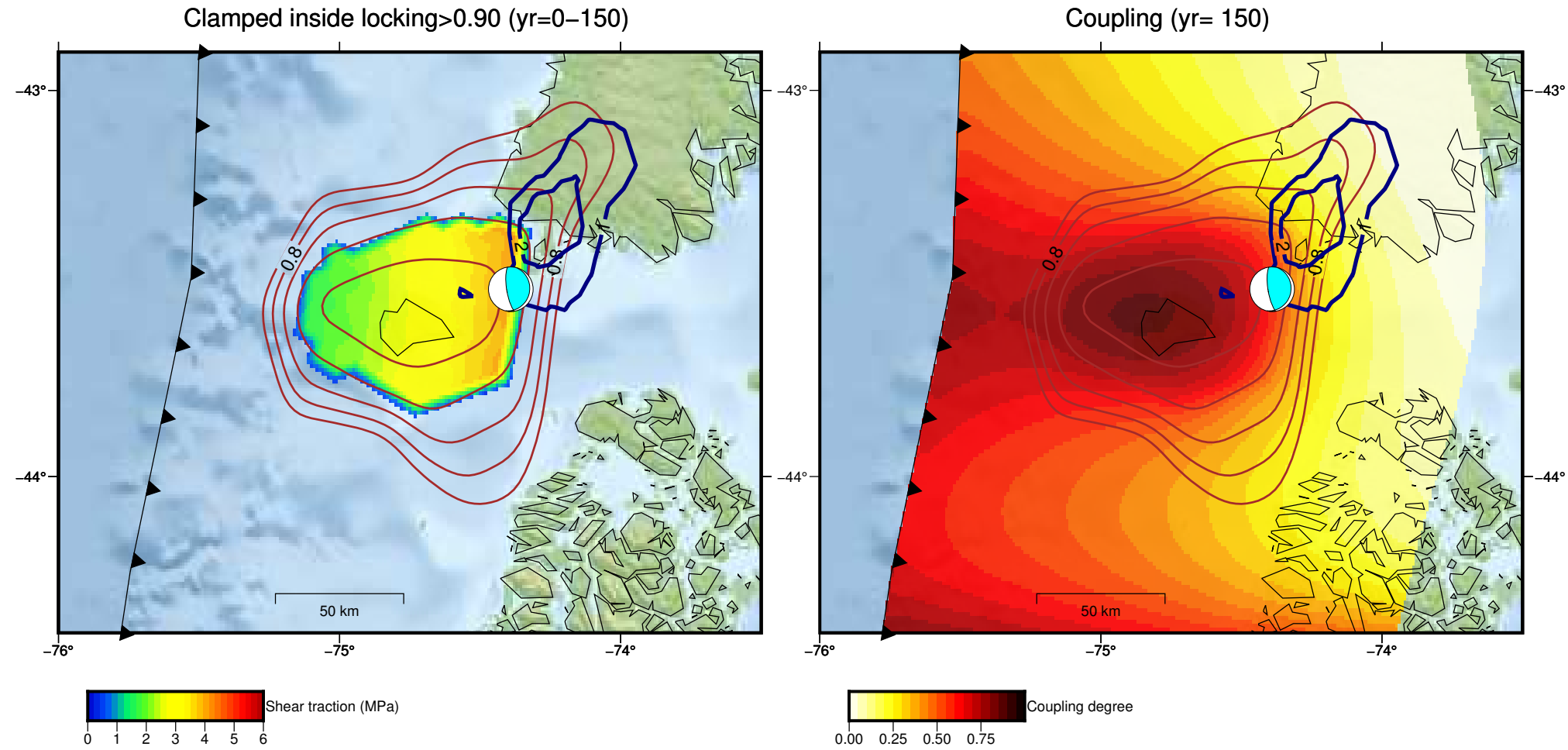
Clamped inside locking>0.90 (yr=0–150)
Coupling (yr= 150)
–43°
–44°
–76°
–75°
–74°
0.8
2
50 km
Shear traction (MPa)
0 1 2 3 4 5 6
Coupling degree
0.00 0.25 0.50 0.75

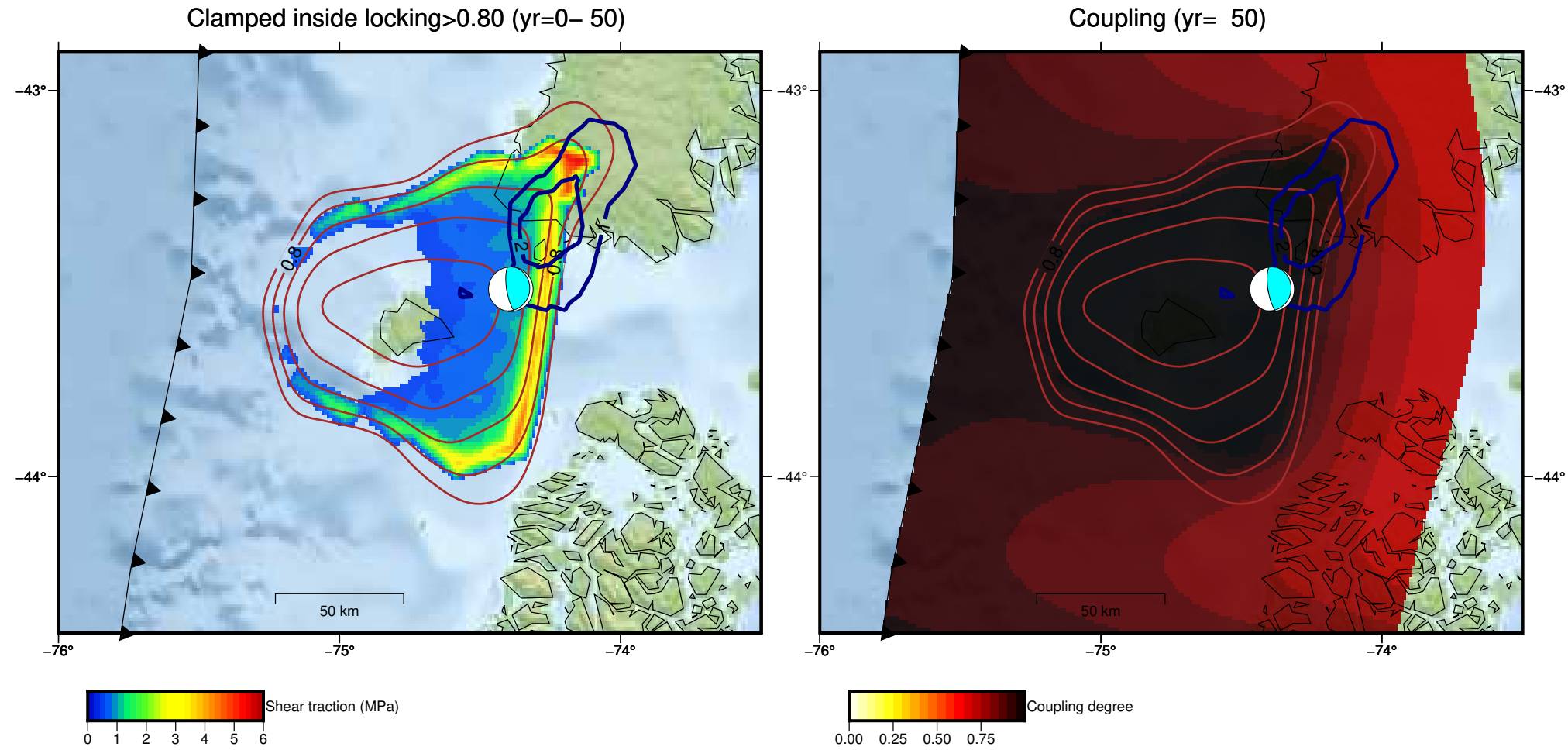
Clamped inside locking>0.80 (yr=0– 50)
Coupling (yr= 50)
–43°
–44°
–76°
–75°
–74°
0.8
2
4
50 km
Shear traction (MPa)
0 1 2 3 4 5 6
Coupling degree
0.00 0.25 0.50 0.75

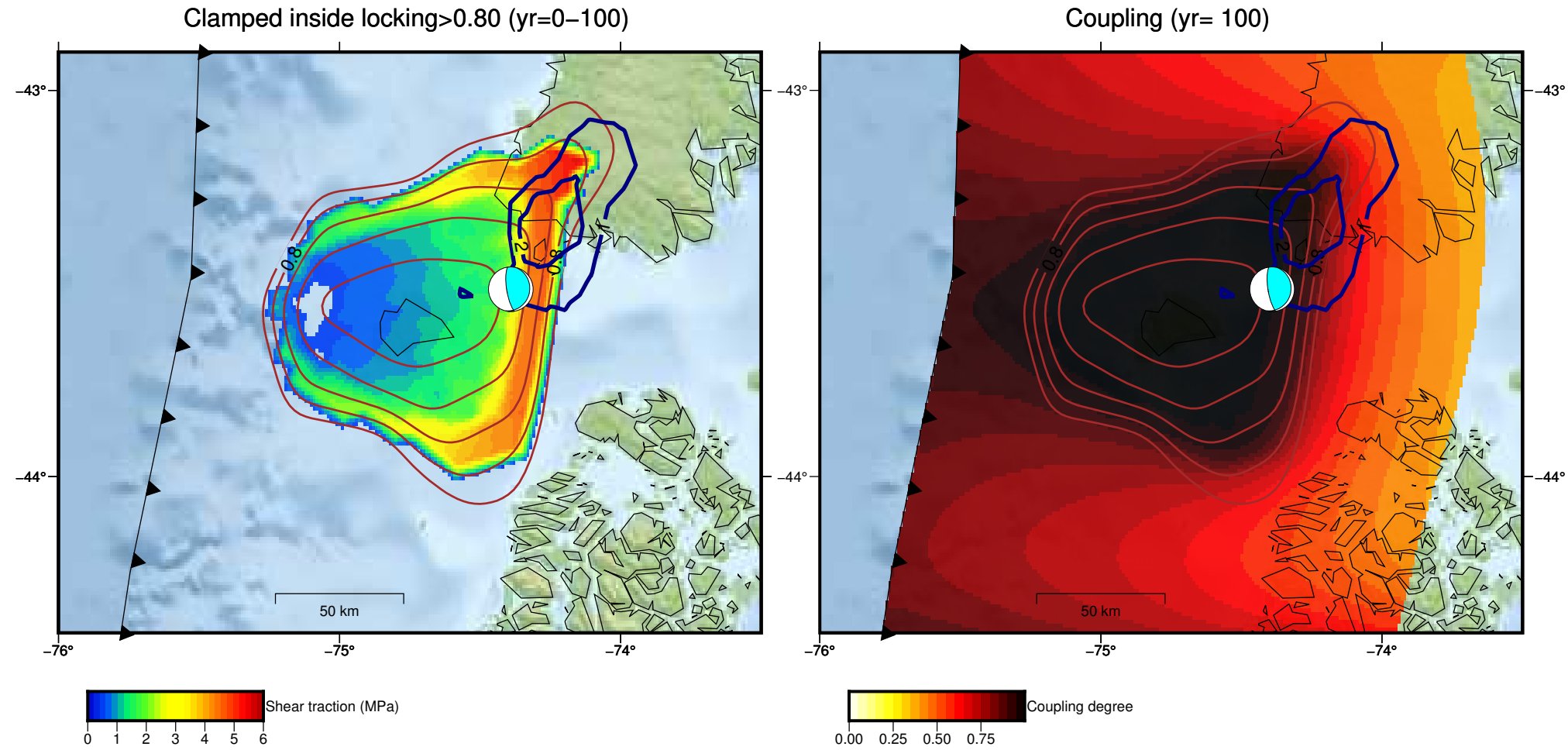
Clamped inside locking>0.80 (yr=0–100)
Coupling (yr= 100)
–43°
–44°
–76°
–75°
–74°
0.8
2
4
50 km
Shear traction (MPa)
0 1 2 3 4 5 6
Coupling degree
0.00 0.25 0.50 0.75

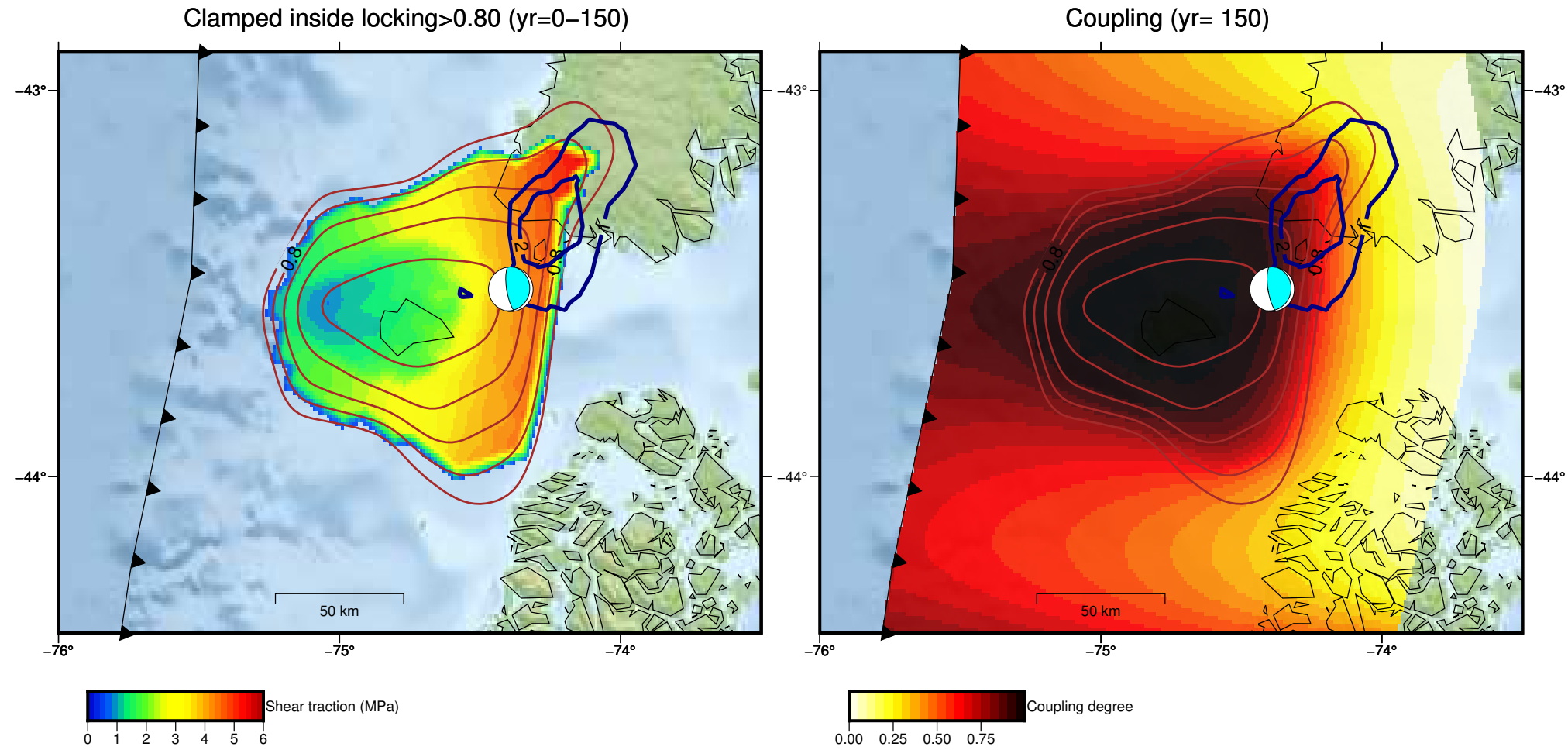
Clamped inside locking>0.80 (yr=0–150)
Coupling (yr= 150)
–43°
–44°
–76°
–75°
–74°
0.8
2
4
50 km
Shear traction (MPa)
0 1 2 3 4 5 6
Coupling degree
0.00 0.25 0.50 0.75

Figure S10. Combinations of effective friction coefficient of the shallow and deep segments coloured by the time when the deep (left side figure) and shallow (right side figure) segments rupture. Black circles indicate combinations of frictions that allow the deeper segment to rupture after 60 years of accumulation of stress (lag time of the 2016 event).

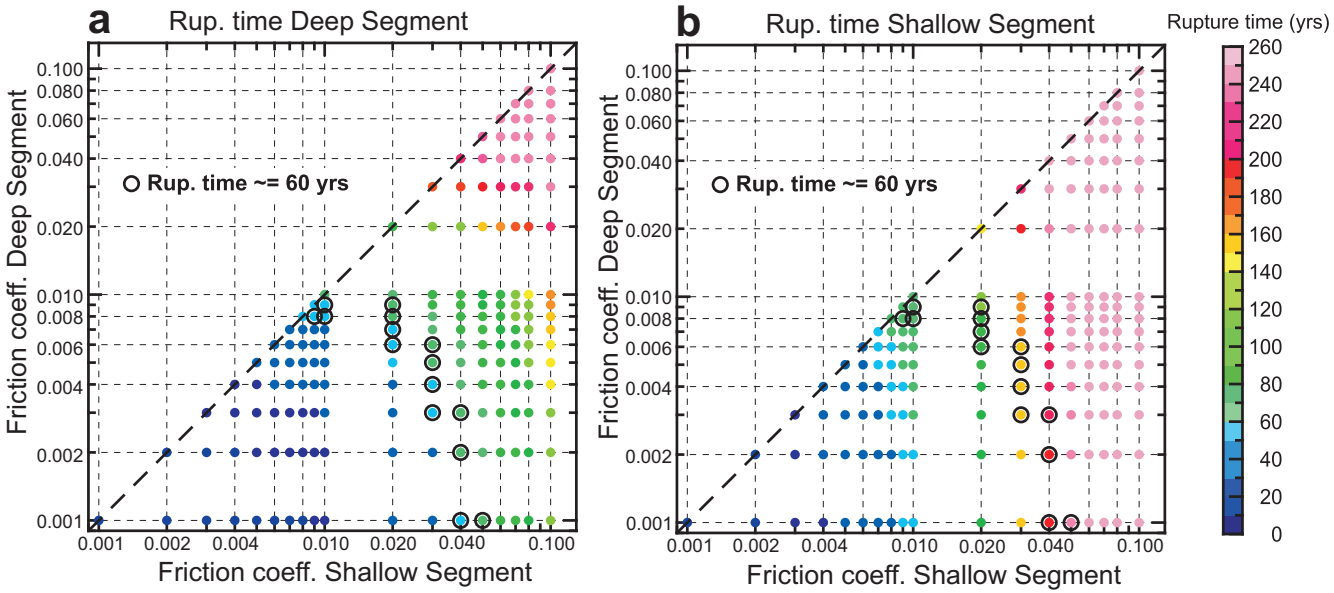
a
Rup. time Deep Segment
Rup. time ~= 60 yrs
Friction coeff. Deep Segment
Friction coeff. Shallow Segment
0.100
0.080
0.060
0.040
0.020
0.010
0.008
0.006
0.004
0.002
0.001
0.001
0.002
0.004
0.010
0.020
0.040
0.100
b
Rup. time Shallow Segment
Rupture time (yrs)
260
240
220
200
180
160
140
120
100
80
60
40
20
0

Figure S11. Series of figures showing of shear traction and coupling after 60 years of loading for different effective friction contrasts between the deep and shallow segments. f1 and f2 are the effective friction values of the shallow and deep segments, respectively.

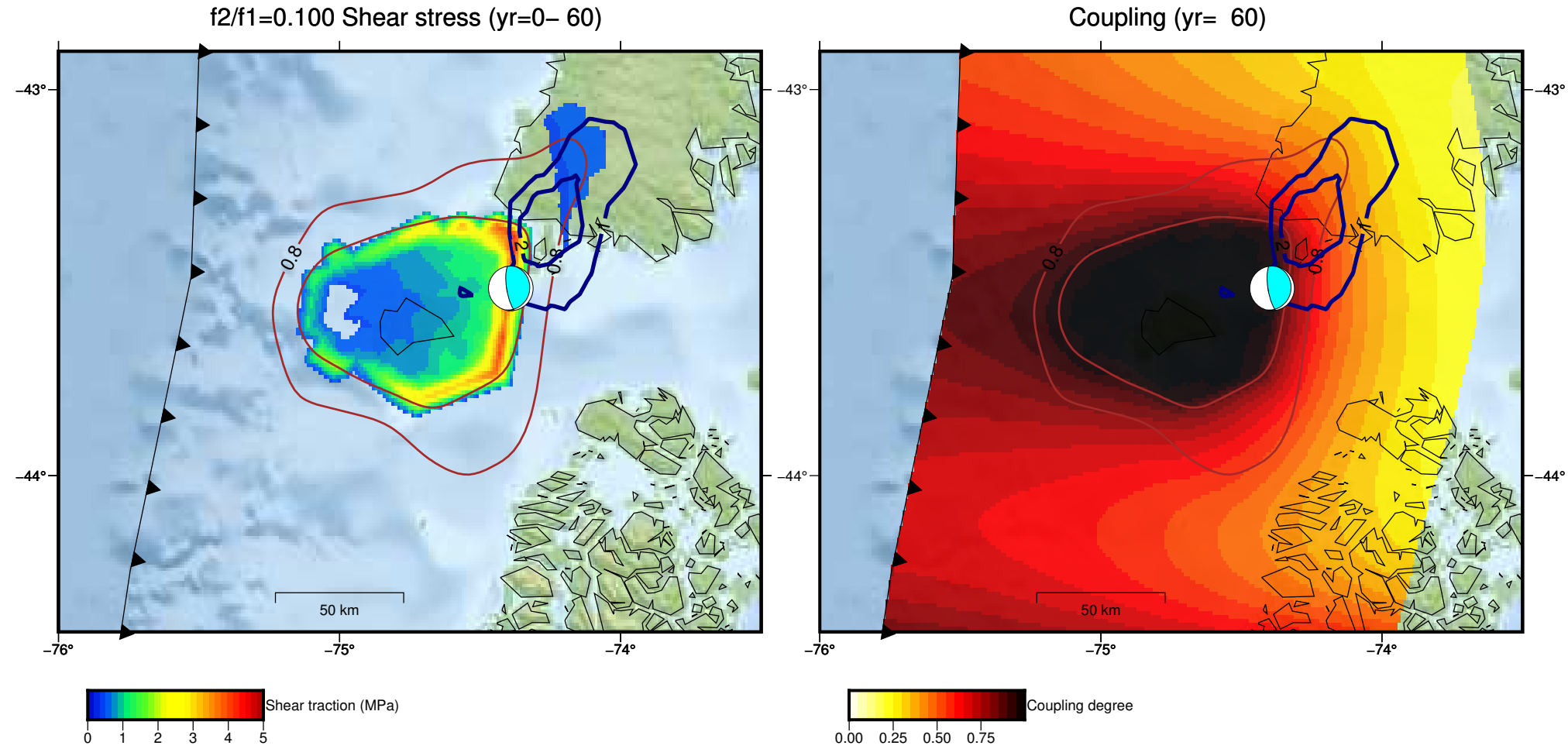
f2/f1=0.100 Shear stress (yr=0– 60)
Coupling (yr= 60)
–43°
–44°
–76°
–75°
–74°
0.8
2
50 km
Shear traction (MPa)
0 1 2 3 4 5
Coupling degree
0.00 0.25 0.50 0.75

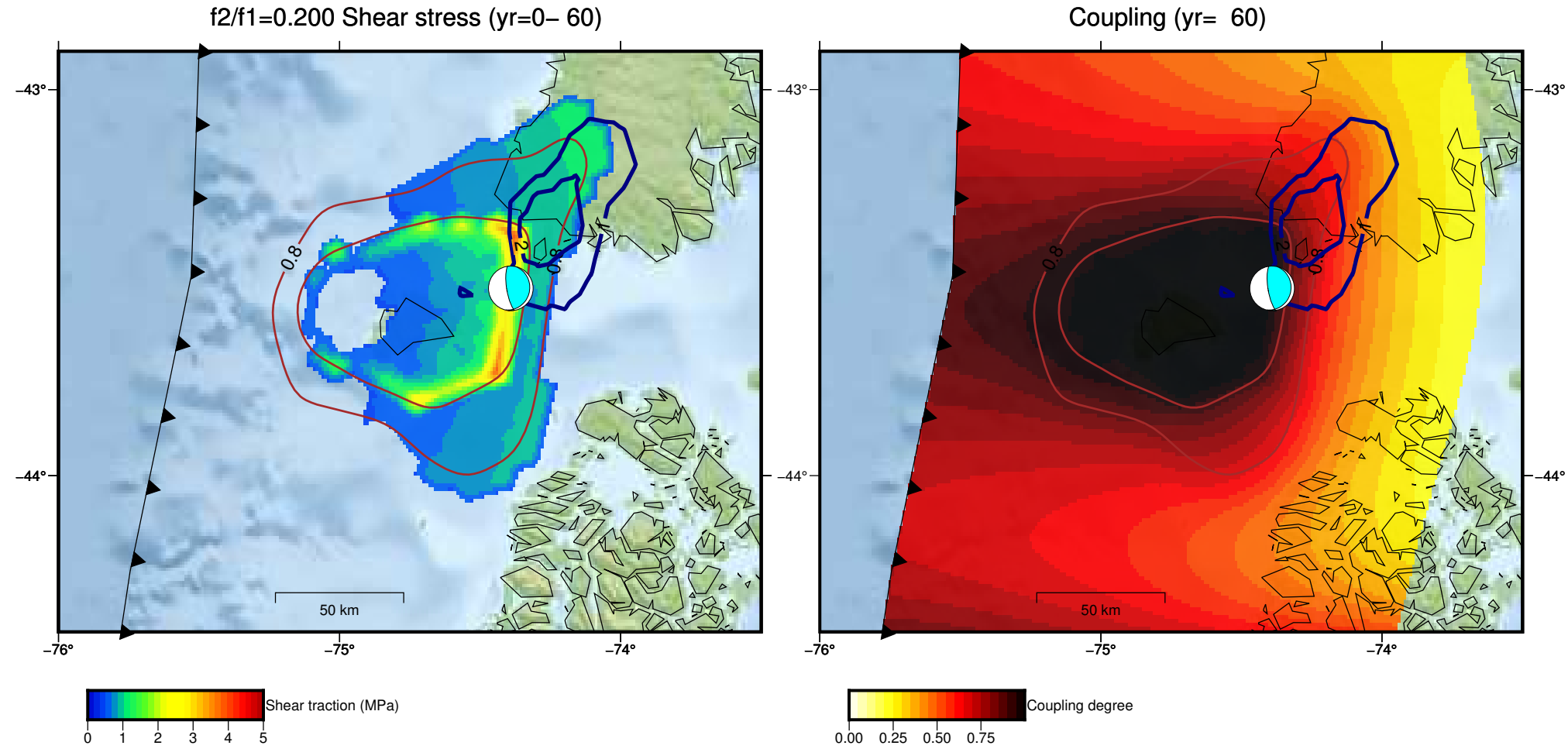
f2/f1=0.200 Shear stress (yr=0– 60)
Coupling (yr= 60)
–43°
–44°
–76°
–75°
–74°
0.8
2.2
50 km
Shear traction (MPa)
0 1 2 3 4 5
Coupling degree
0.00 0.25 0.50 0.75

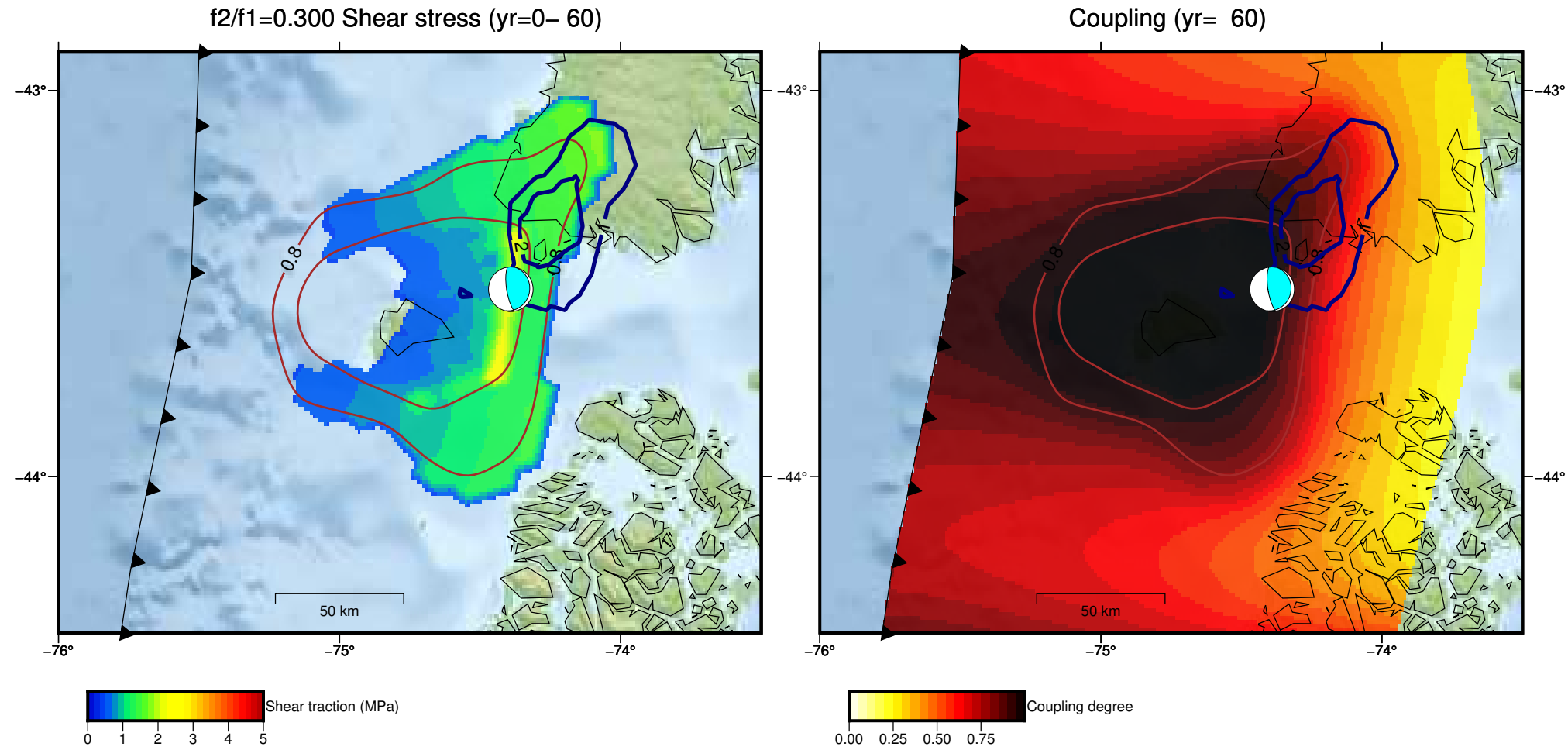
f2/f1=0.300 Shear stress (yr=0– 60)
Coupling (yr= 60)
–43°
–44°
–76°
–75°
–74°
0.8
2
0.8
1
50 km
Shear traction (MPa)
0 1 2 3 4 5
Coupling degree
0.00 0.25 0.50 0.75

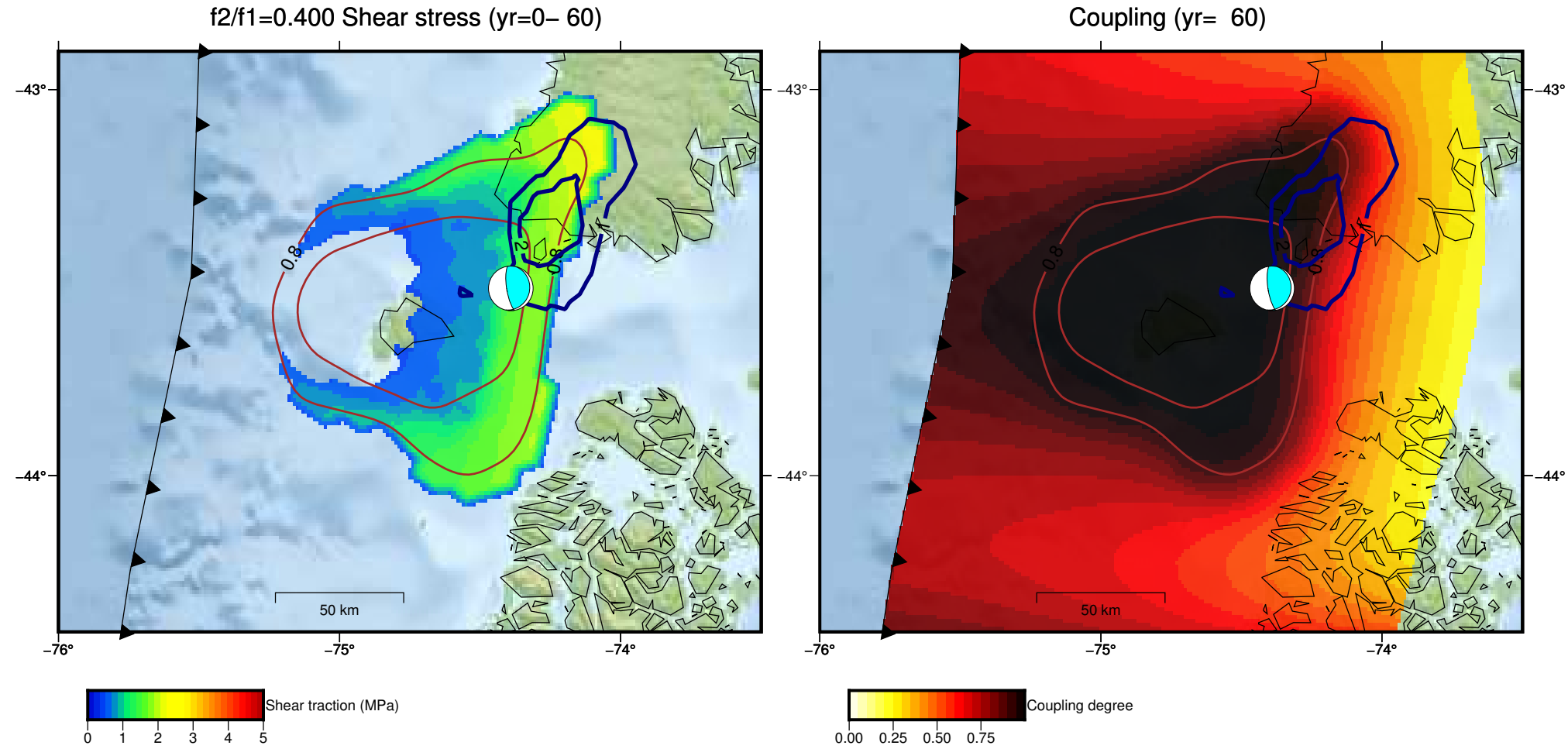
f2/f1=0.400 Shear stress (yr=0– 60)
Coupling (yr= 60)
–43°
–44°
–76°
–75°
–74°
0.8
2
4
50 km
Shear traction (MPa)
0 1 2 3 4 5
Coupling degree
0.00 0.25 0.50 0.75

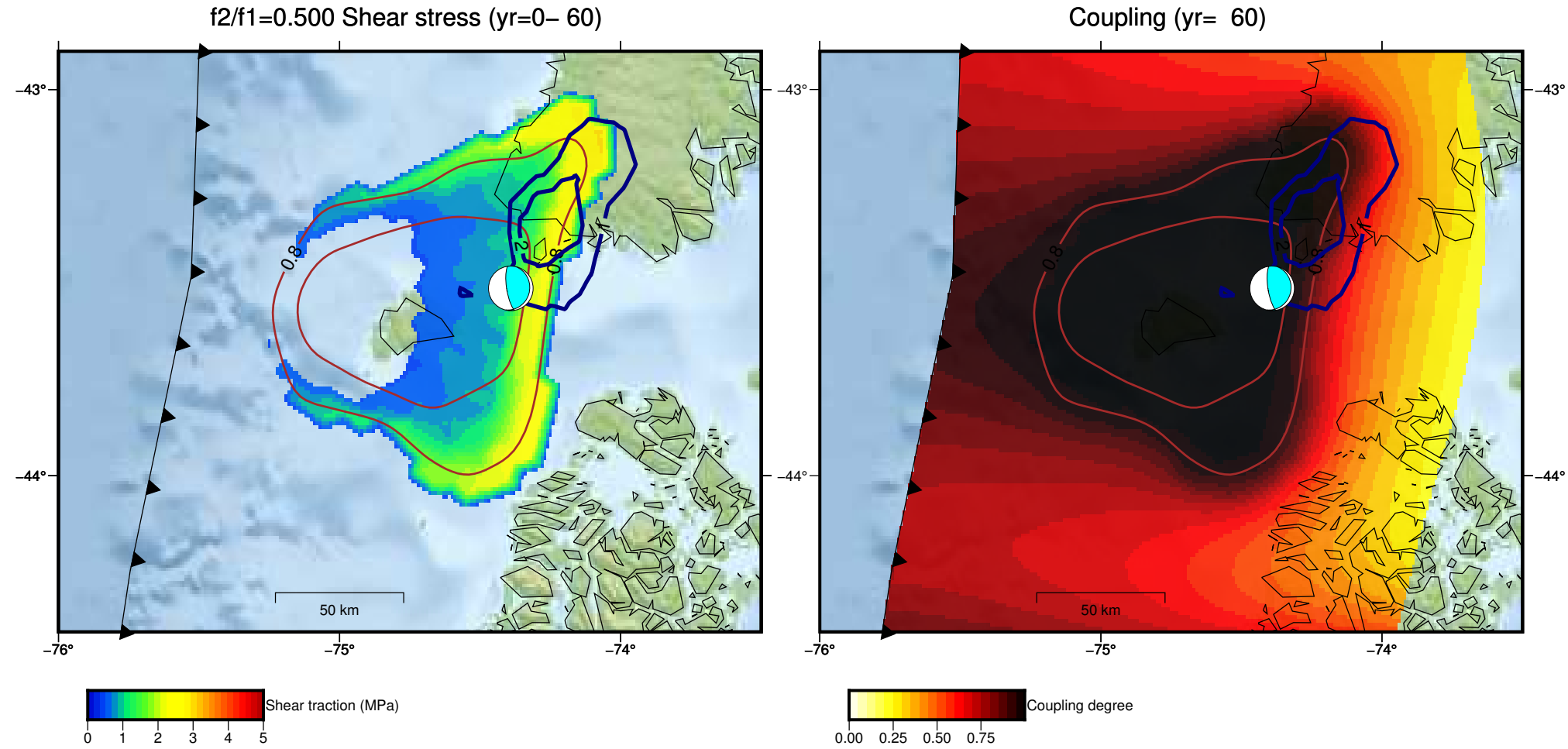
f2/f1=0.500 Shear stress (yr=0– 60)
Coupling (yr= 60)
–43°
–44°
–76°
–75°
–74°
0.8
2
4
50 km
Shear traction (MPa)
0 1 2 3 4 5
Coupling degree
0.00 0.25 0.50 0.75

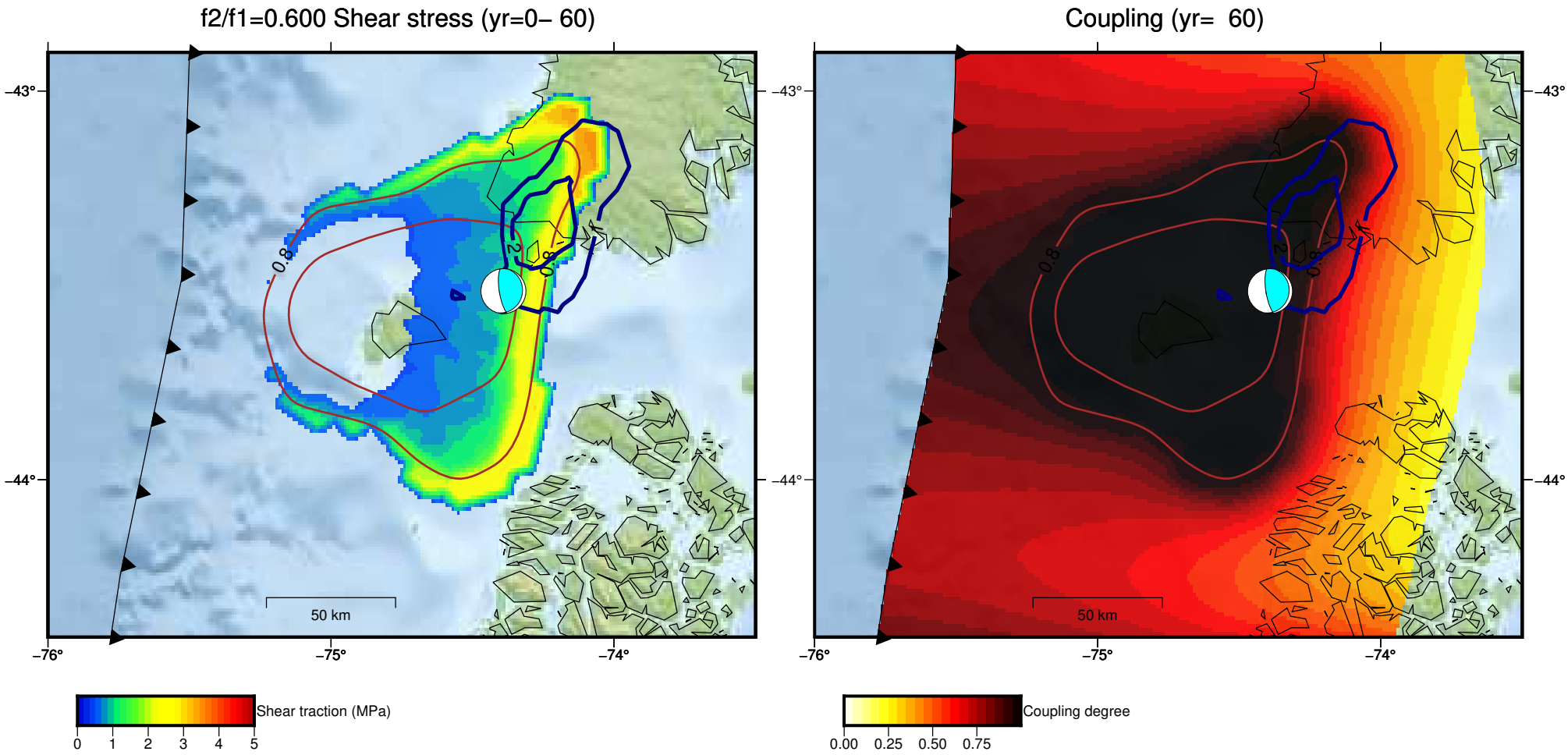
f2/f1=0.600 Shear stress (yr=0– 60)
Coupling (yr= 60)
–43°
–44°
–76°
–75°
–74°
0.8
2
4
50 km
Shear traction (MPa)
0 1 2 3 4 5
Coupling degree
0.00 0.25 0.50 0.75

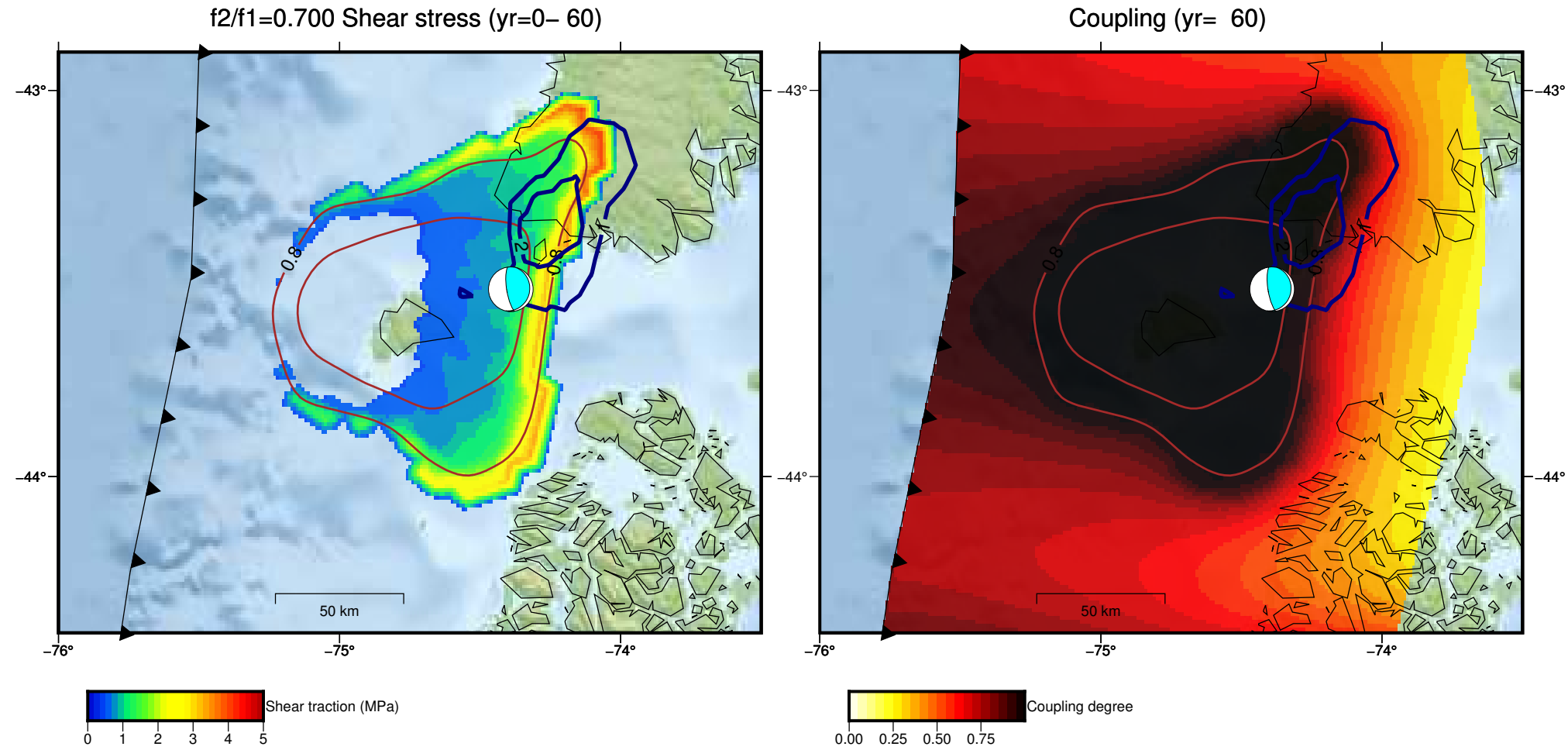
f2/f1=0.700 Shear stress (yr=0– 60)
Coupling (yr= 60)
–43°
–44°
–76°
–75°
–74°
0.8
0.2
50 km
Shear traction (MPa)
0 1 2 3 4 5
Coupling degree
0.00 0.25 0.50 0.75

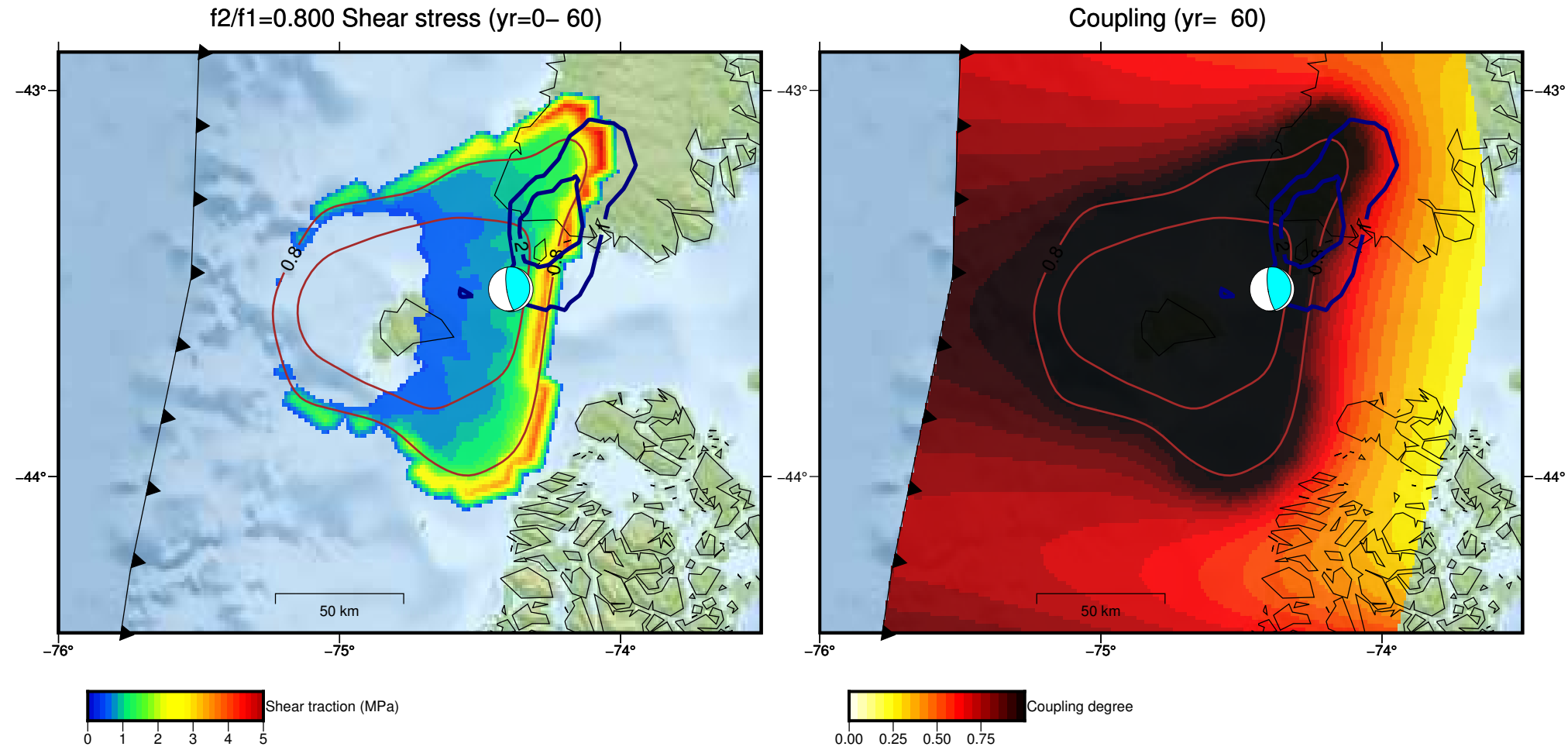
f2/f1=0.800 Shear stress (yr=0– 60)
Coupling (yr= 60)
–43°
–44°
–76°
–75°
–74°
0.8
0.8
50 km
50 km
Shear traction (MPa)
0 1 2 3 4 5
Coupling degree
0.00 0.25 0.50 0.75

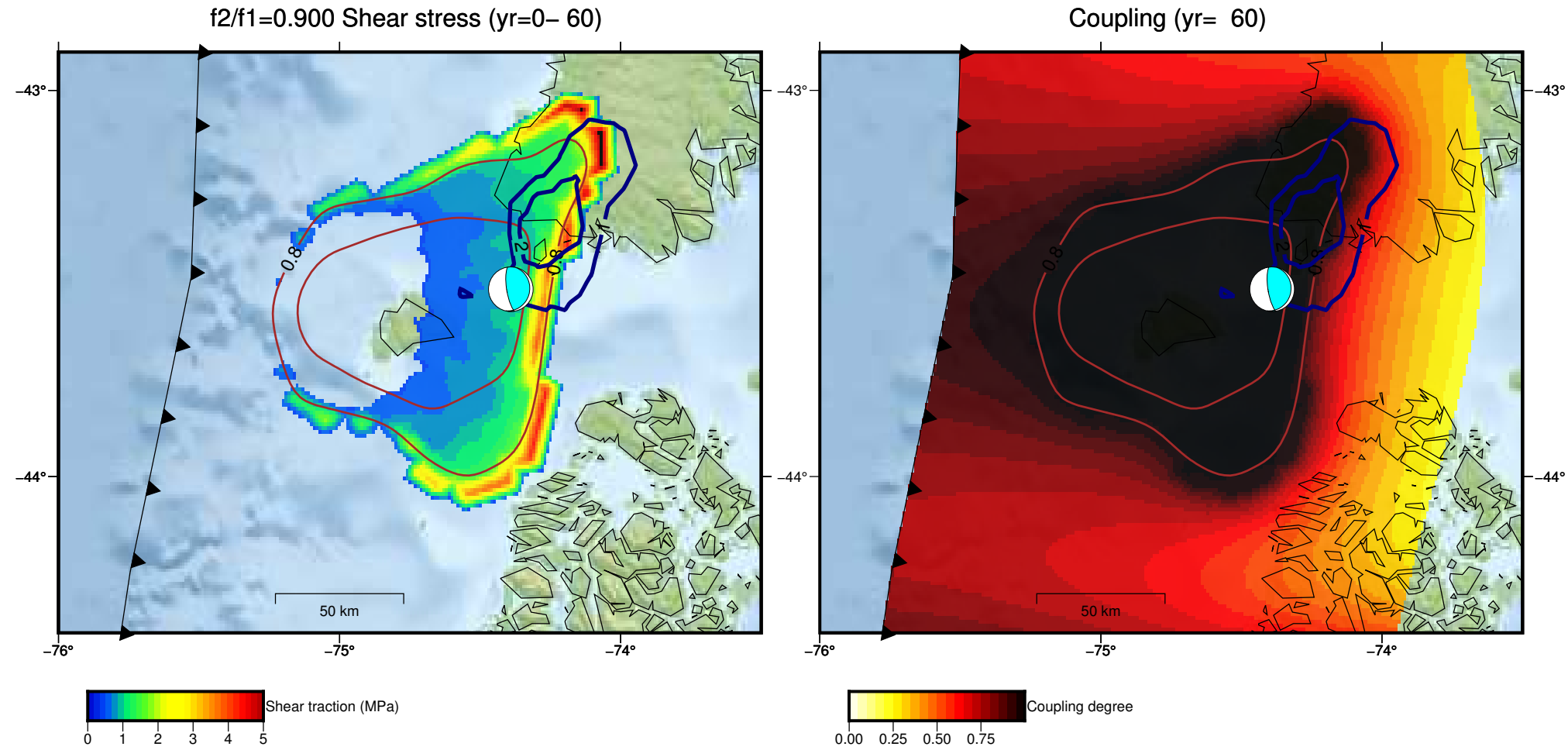
f2/f1=0.900 Shear stress (yr=0– 60)
Coupling (yr= 60)
–43°
–44°
–76°
–75°
–74°
0.8
1
2
50 km
Shear traction (MPa)
0 1 2 3 4 5
Coupling degree
0.00 0.25 0.50 0.75

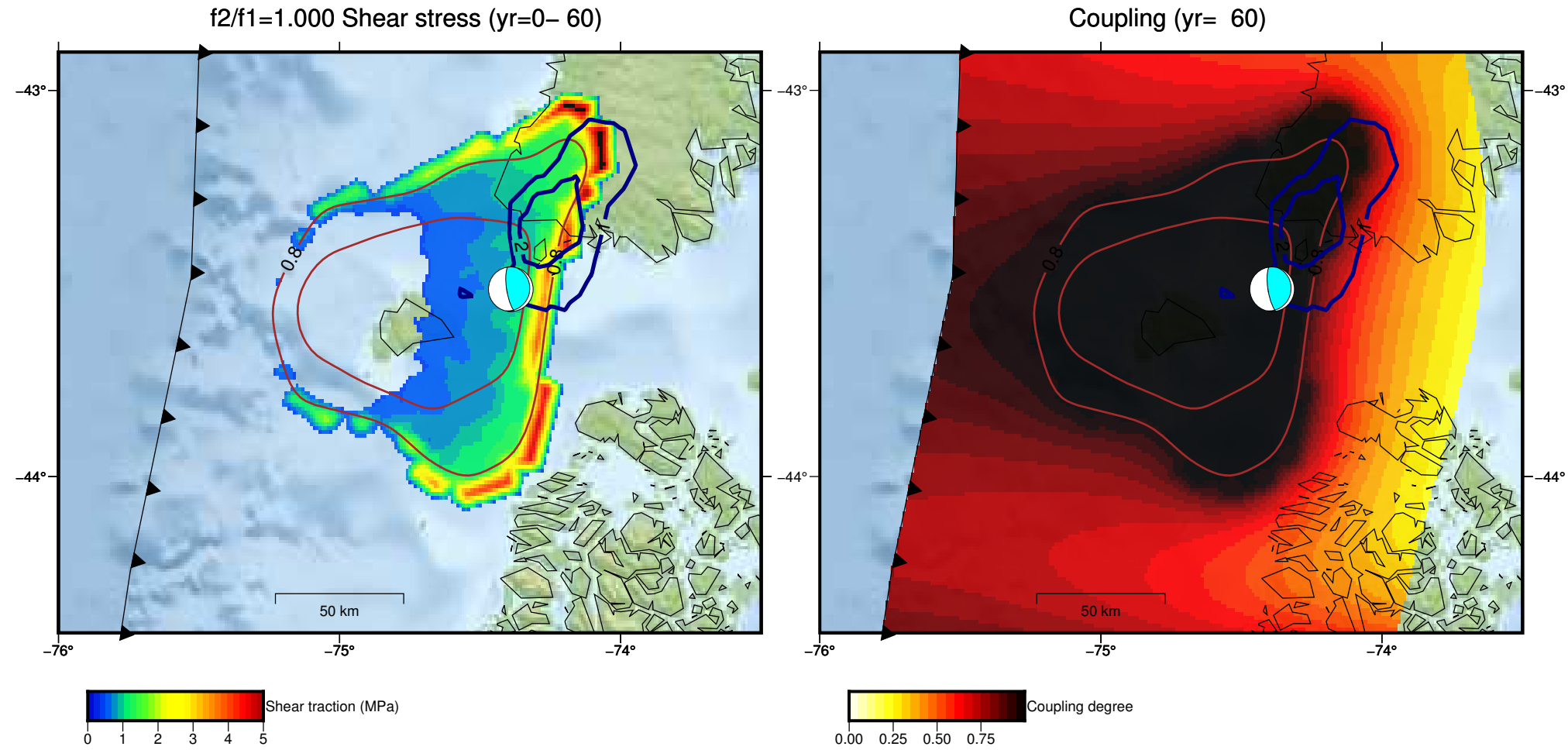
f2/f1=1.000 Shear stress (yr=0– 60)
Coupling (yr= 60)
–43°
–44°
–76°
–75°
–74°
0.8
1
2
50 km
Shear traction (MPa)
0 1 2 3 4 5
Coupling degree
0.00 0.25 0.50 0.75

Figure S12. Coulomb stress changes computed from the slip distribution.

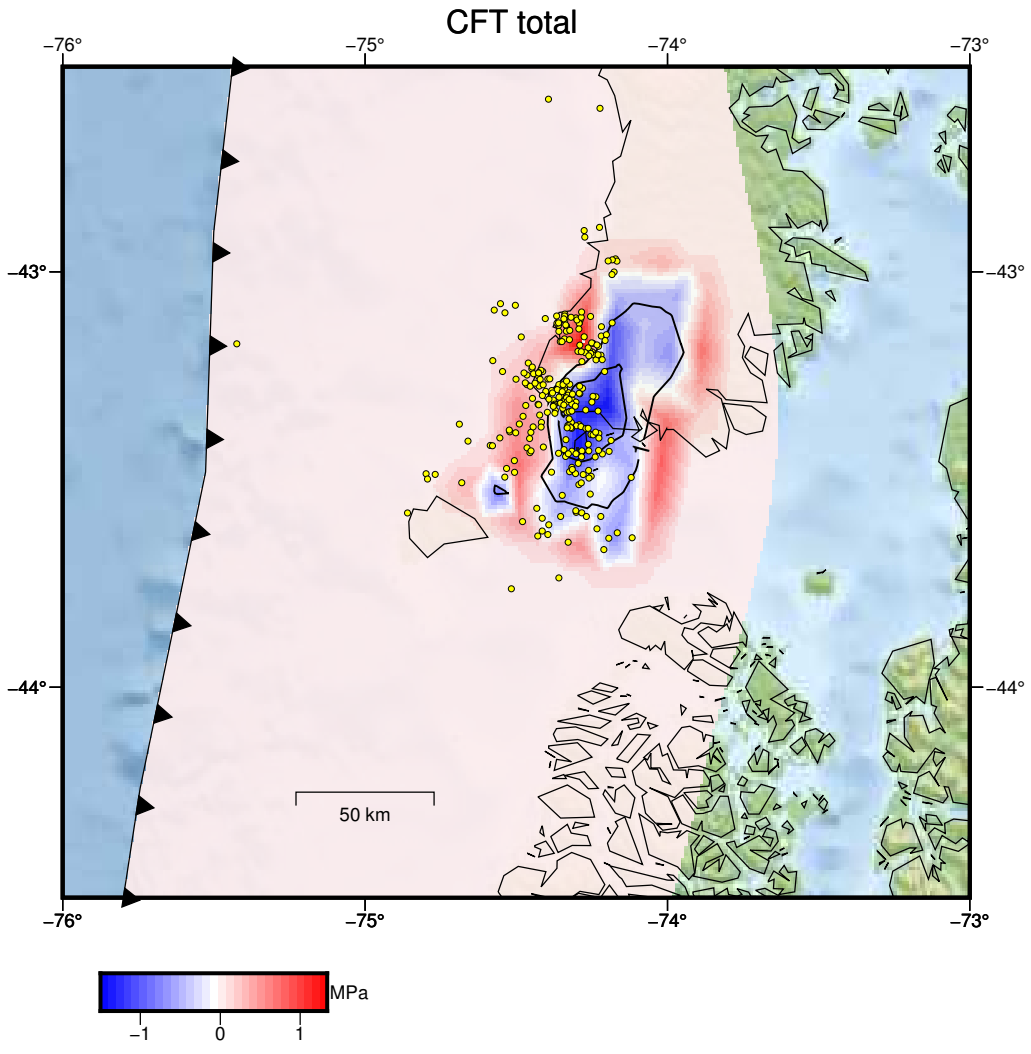
CFT total
−76°
−75°
−74°
−73°
−43°
−44°
50 km
MPa
−1
0
1

Figure S13. Series of figures showing the evolution of shear traction and coupling within 60 years of loading. This model incorporates an effective friction coefficient of the deep segment 0.35 times smaller than the value of the shallow segment. This model produces a shear traction accumulation similar in magnitude with the stress drop of the 2016 earthquake.

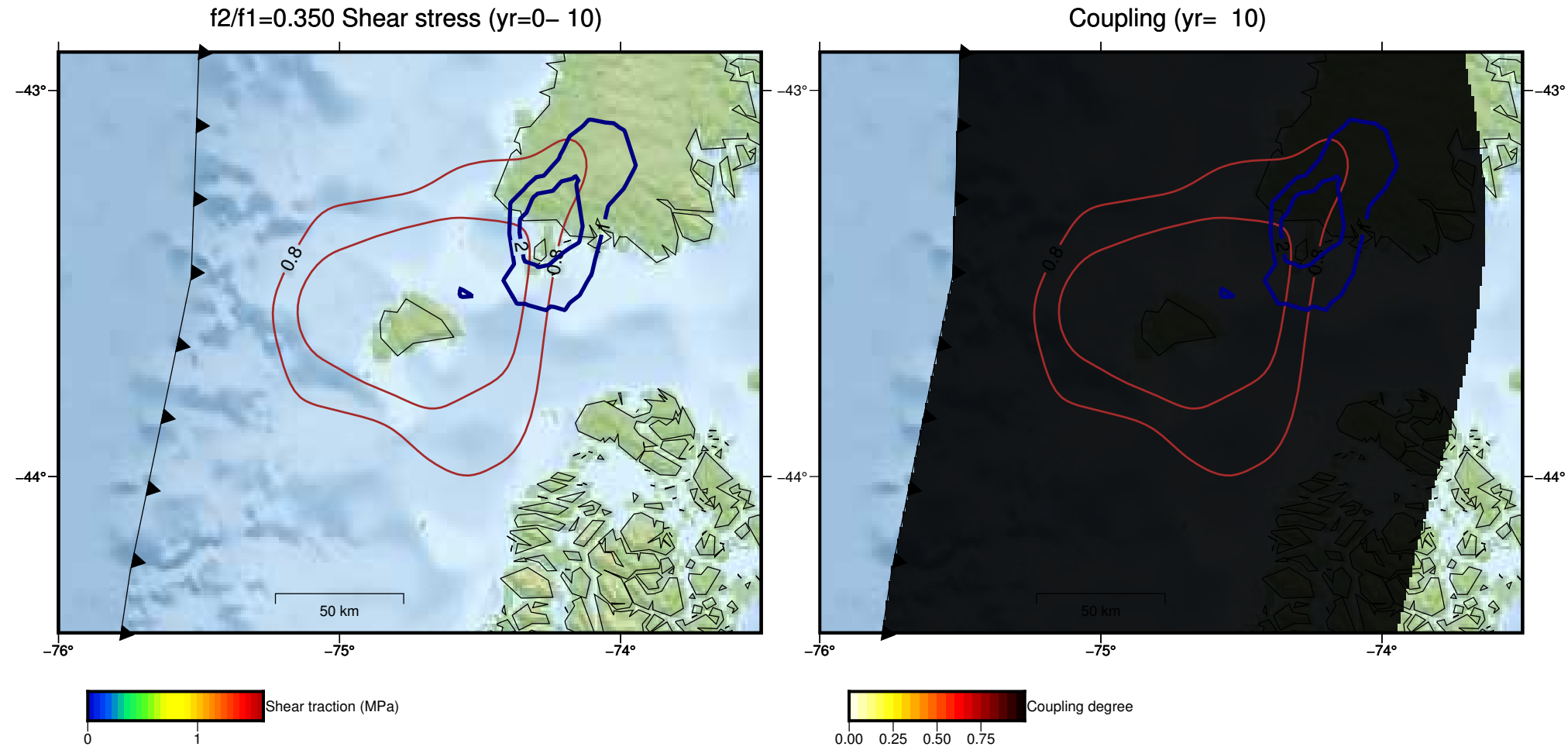
f2/f1=0.350 Shear stress (yr=0– 10)
Coupling (yr= 10)
–43°
–44°
–76°
–75°
–74°
0.8
0.8
50 km
50 km
Shear traction (MPa)
0
1
Coupling degree
0.00
0.25
0.50
0.75

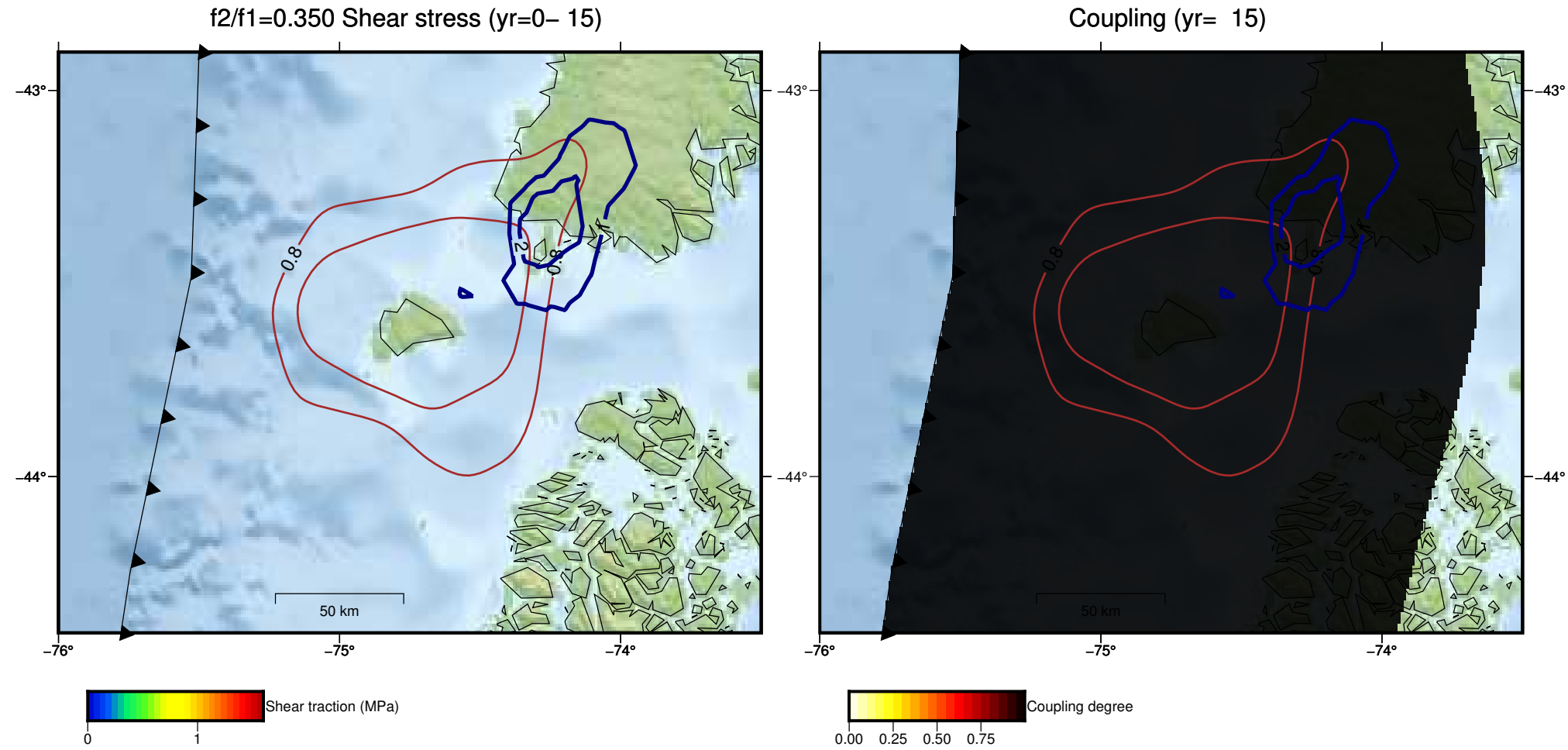
f2/f1=0.350 Shear stress (yr=0– 15)
Coupling (yr= 15)
–43°
–44°
–76°
–75°
–74°
0.8
0.8
50 km
50 km
Shear traction (MPa)
0
1
Coupling degree
0.00
0.25
0.50
0.75

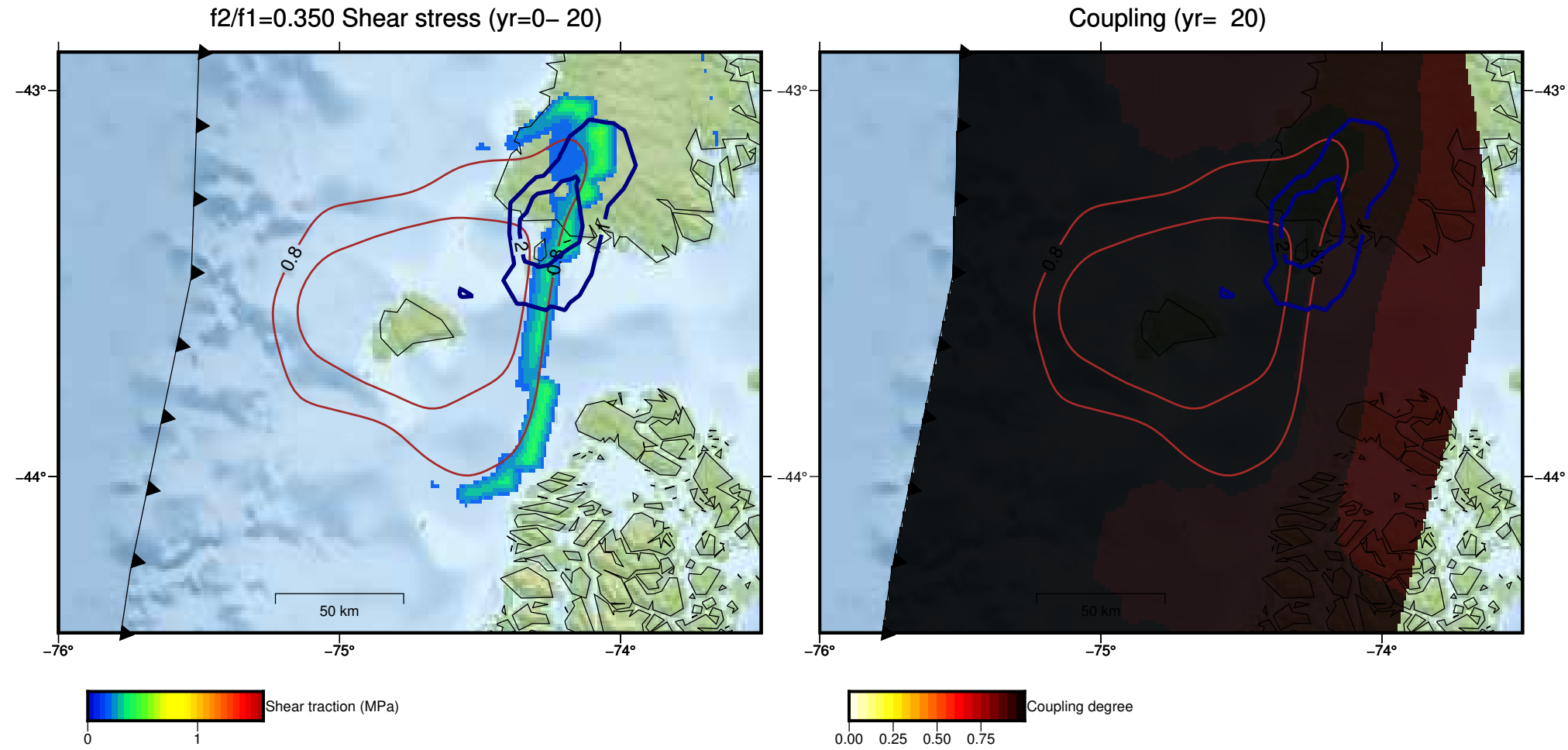
f2/f1=0.350 Shear stress (yr=0– 20)
Coupling (yr= 20)
–43°
–44°
–76°
–75°
–74°
0.8
2
0.8
50 km
Shear traction (MPa)
0
1
Coupling degree
0.00
0.25
0.50
0.75

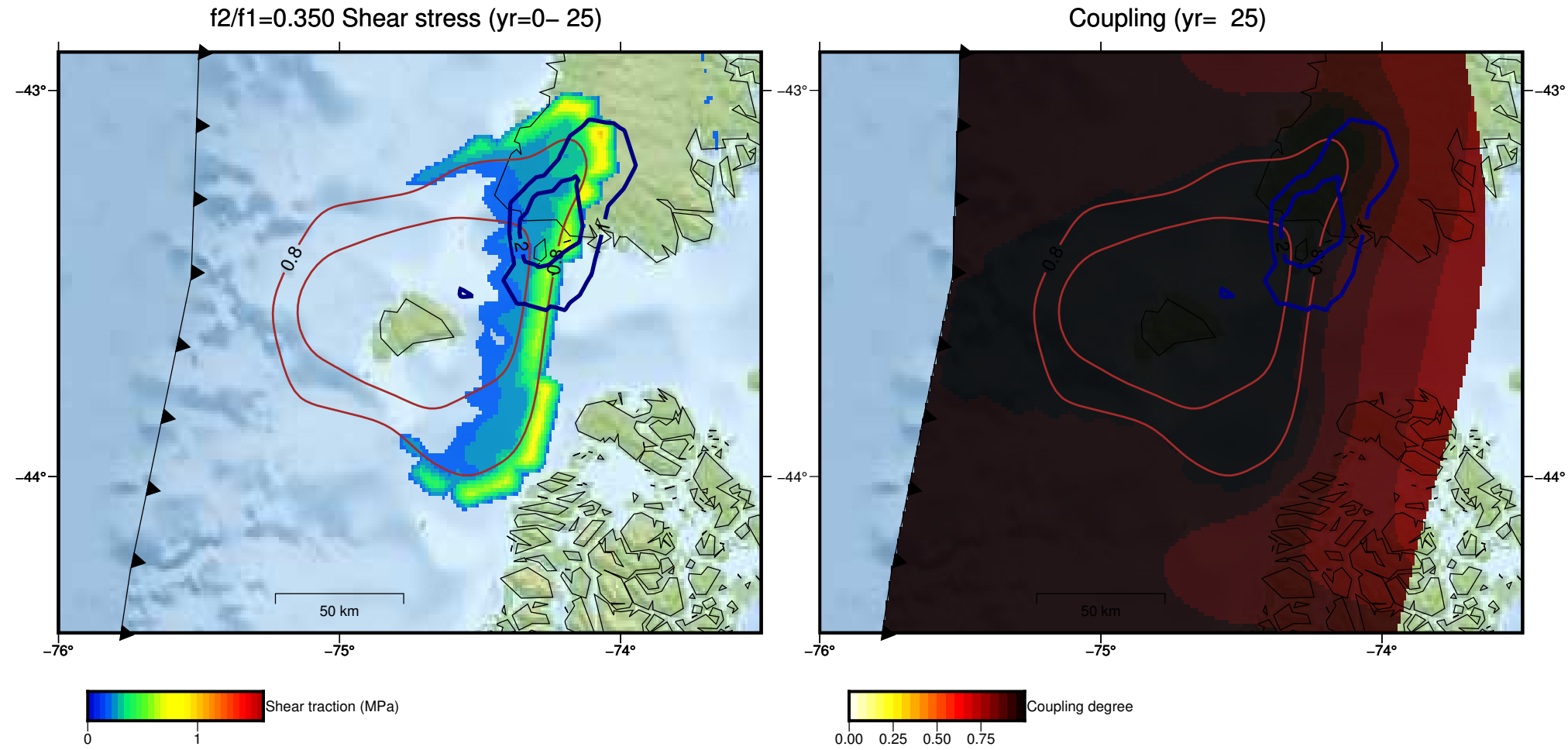
f2/f1=0.350 Shear stress (yr=0– 25)
Coupling (yr= 25)
–43°
–44°
–76°
–75°
–74°
0.8
2
50 km
Shear traction (MPa)
0
1
Coupling degree
0.00
0.25
0.50
0.75

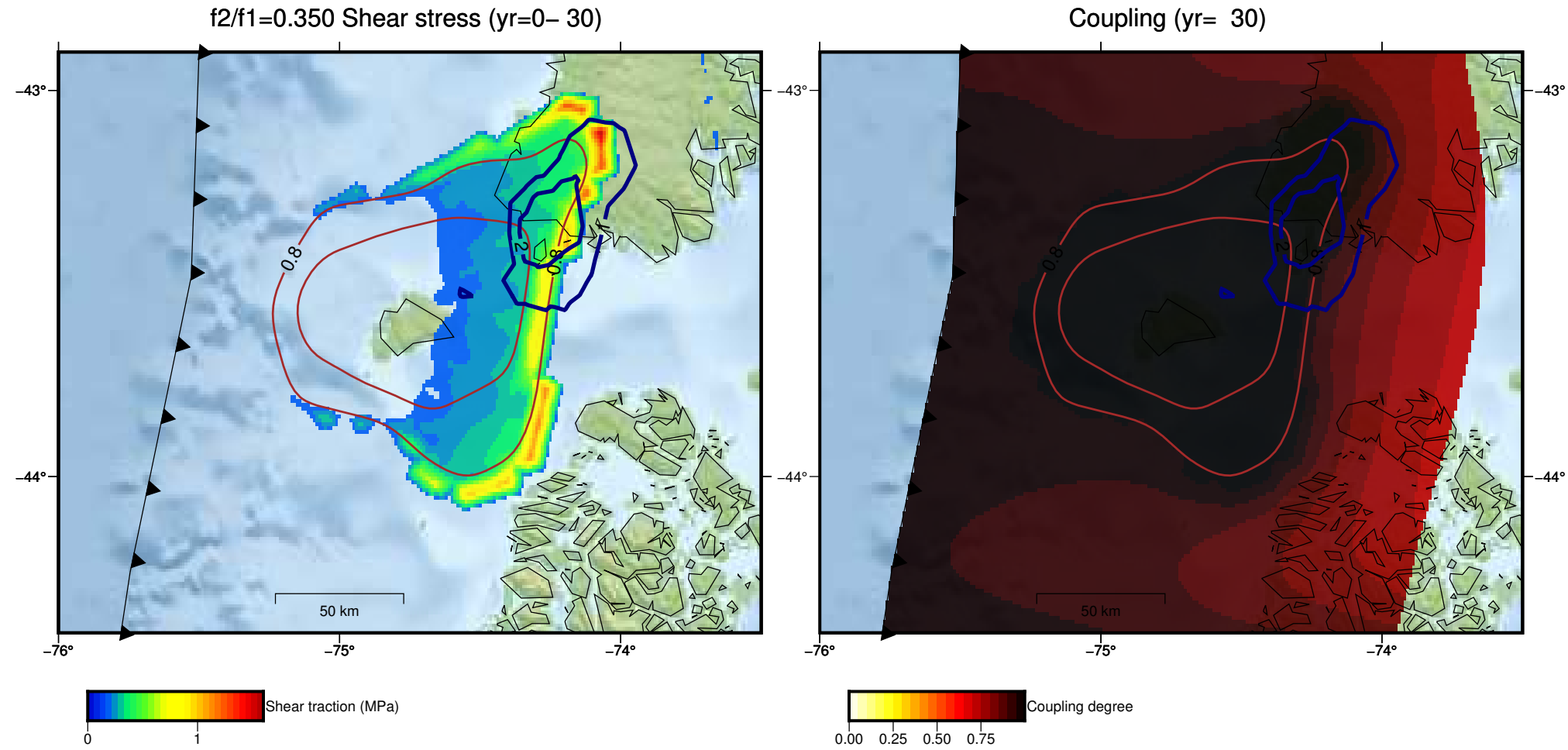
f2/f1=0.350 Shear stress (yr=0– 30)
Coupling (yr= 30)
–43°
–44°
–76°
–75°
–74°
0.8
0.8
50 km
50 km
Shear traction (MPa)
0
1
Coupling degree
0.00
0.25
0.50
0.75

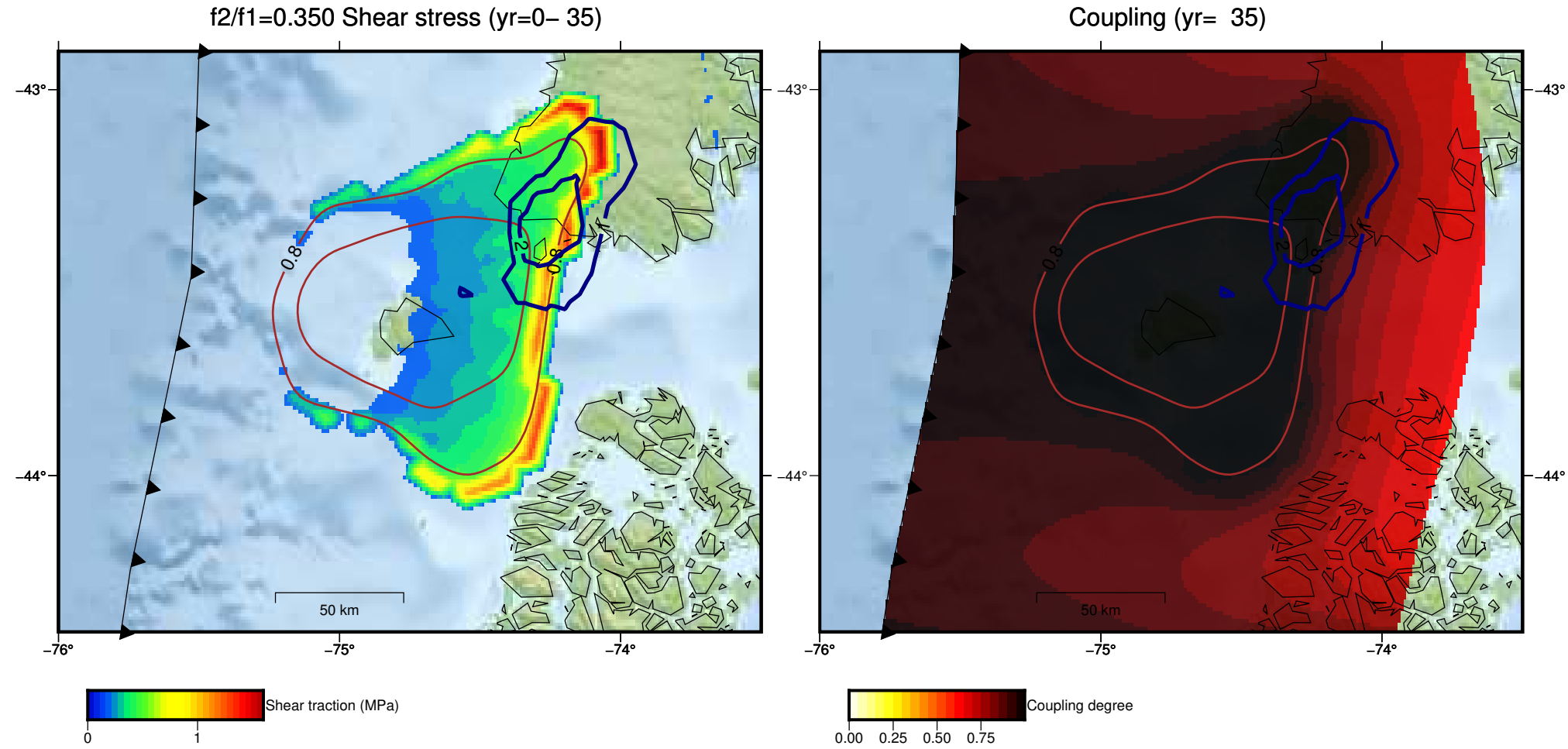
f2/f1=0.350 Shear stress (yr=0– 35)
Coupling (yr= 35)
–43°
–44°
–76°
–75°
–74°
0.8
1.2
50 km
Shear traction (MPa)
0
1
Coupling degree
0.00
0.25
0.50
0.75

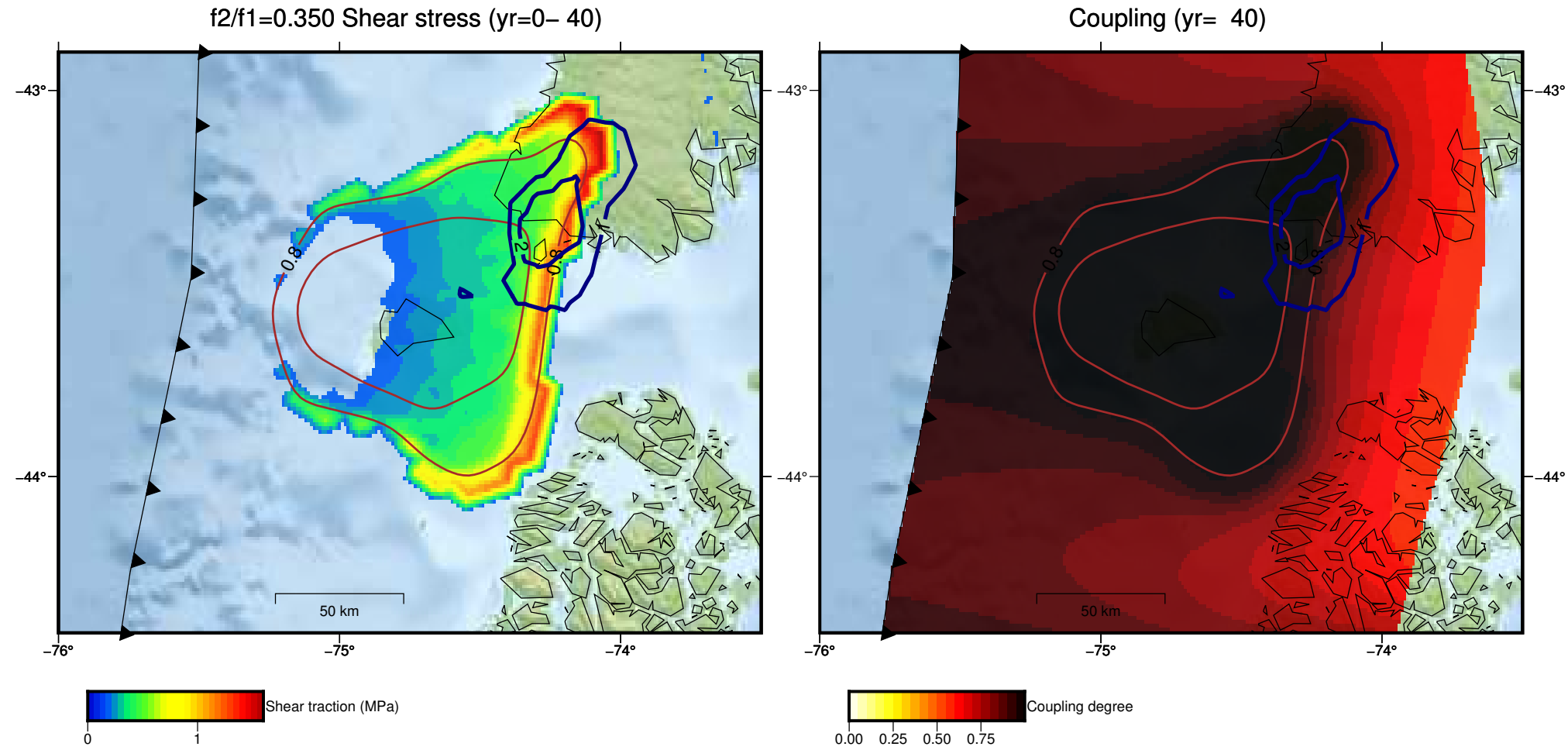
f2/f1=0.350 Shear stress (yr=0– 40)
Coupling (yr= 40)
–43°
–44°
–76°
–75°
–74°
0.8
2
50 km
Shear traction (MPa)
0
1
Coupling degree
0.00
0.25
0.50
0.75

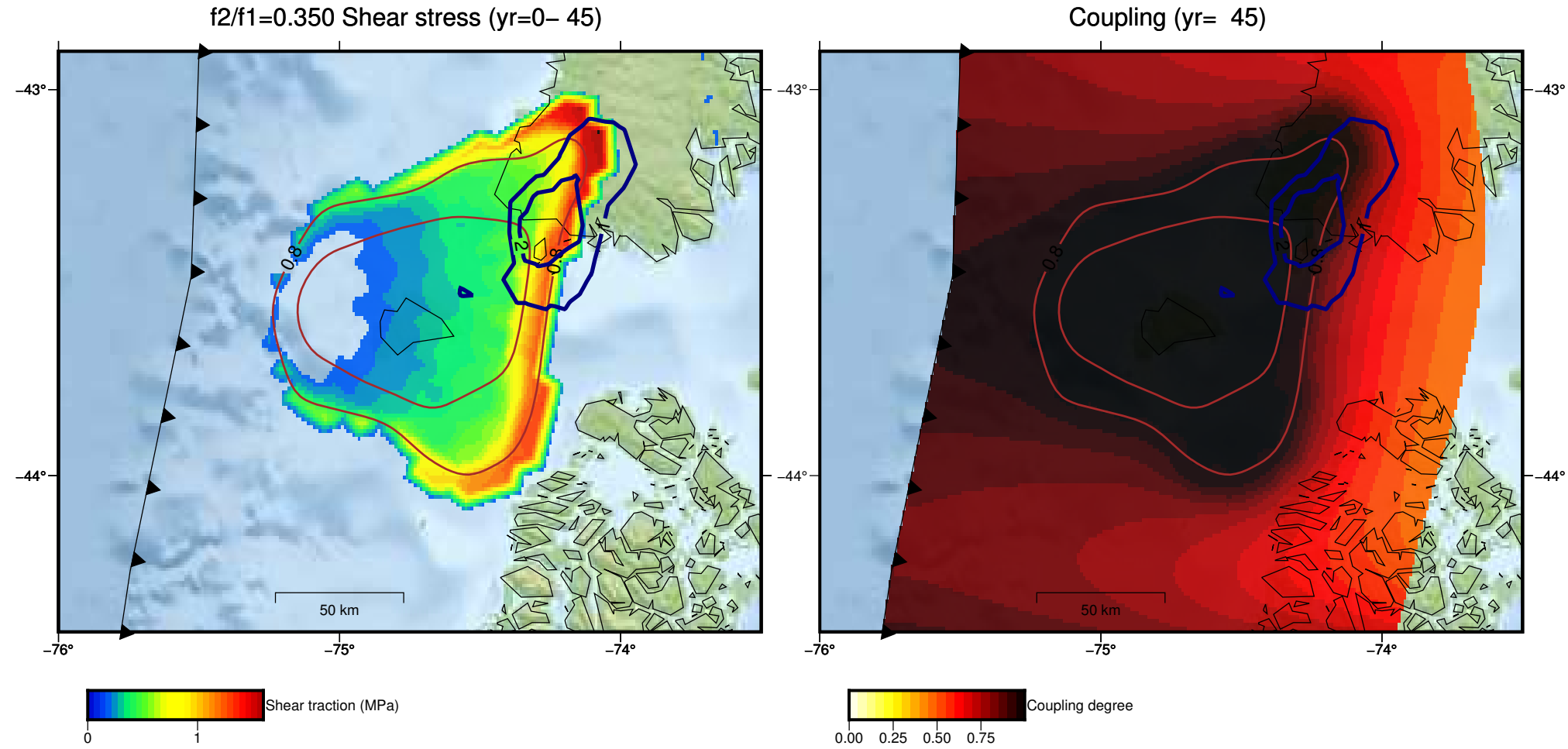
f2/f1=0.350 Shear stress (yr=0– 45)
Coupling (yr= 45)
–43°
–44°
–76°
–75°
–74°
0.8
2
50 km
Shear traction (MPa)
0
1
Coupling degree
0.00
0.25
0.50
0.75

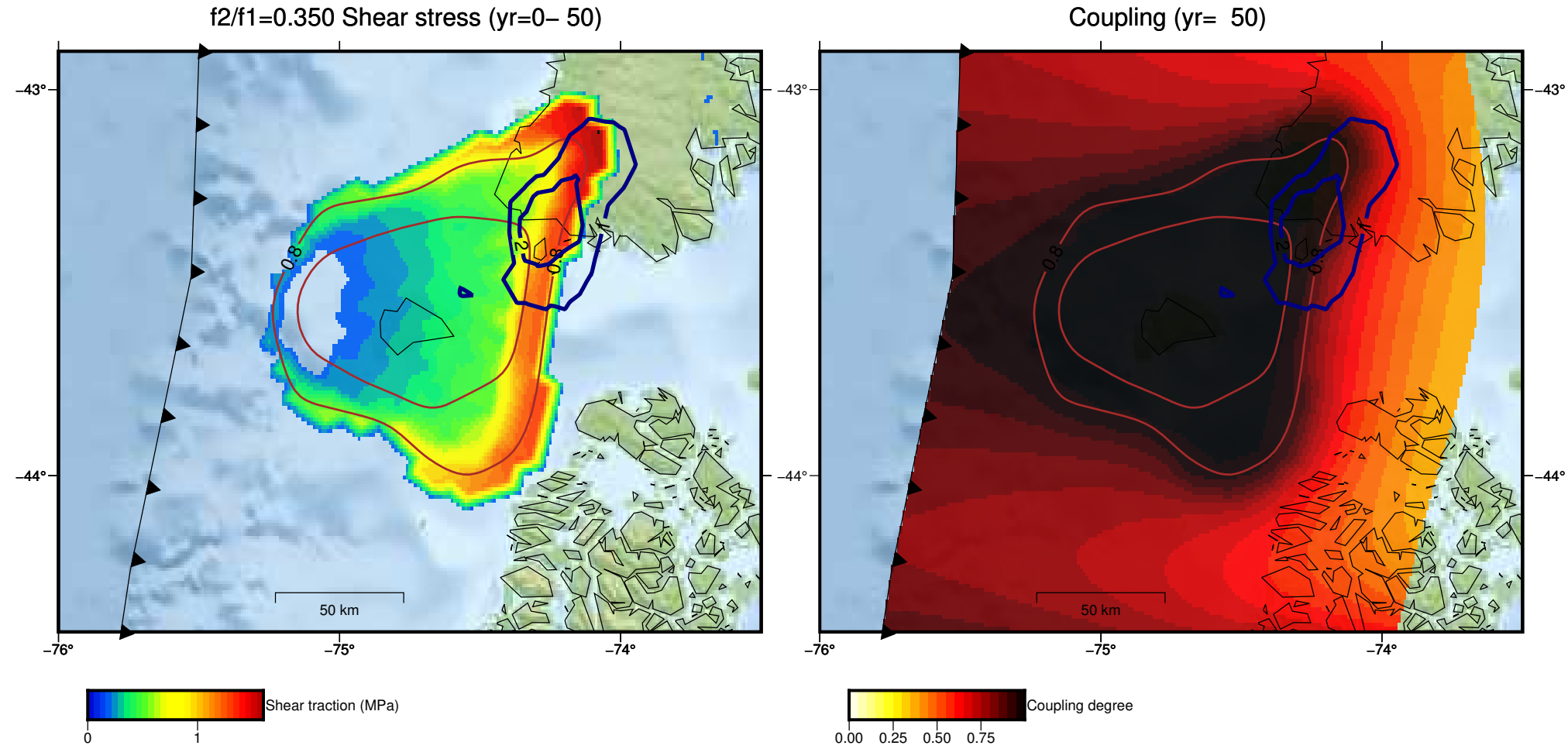
f2/f1=0.350 Shear stress (yr=0– 50)
Coupling (yr= 50)
–43°
–44°
–76°
–75°
–74°
0.8
1.2
50 km
Shear traction (MPa)
0
1
Coupling degree
0.00
0.25
0.50
0.75

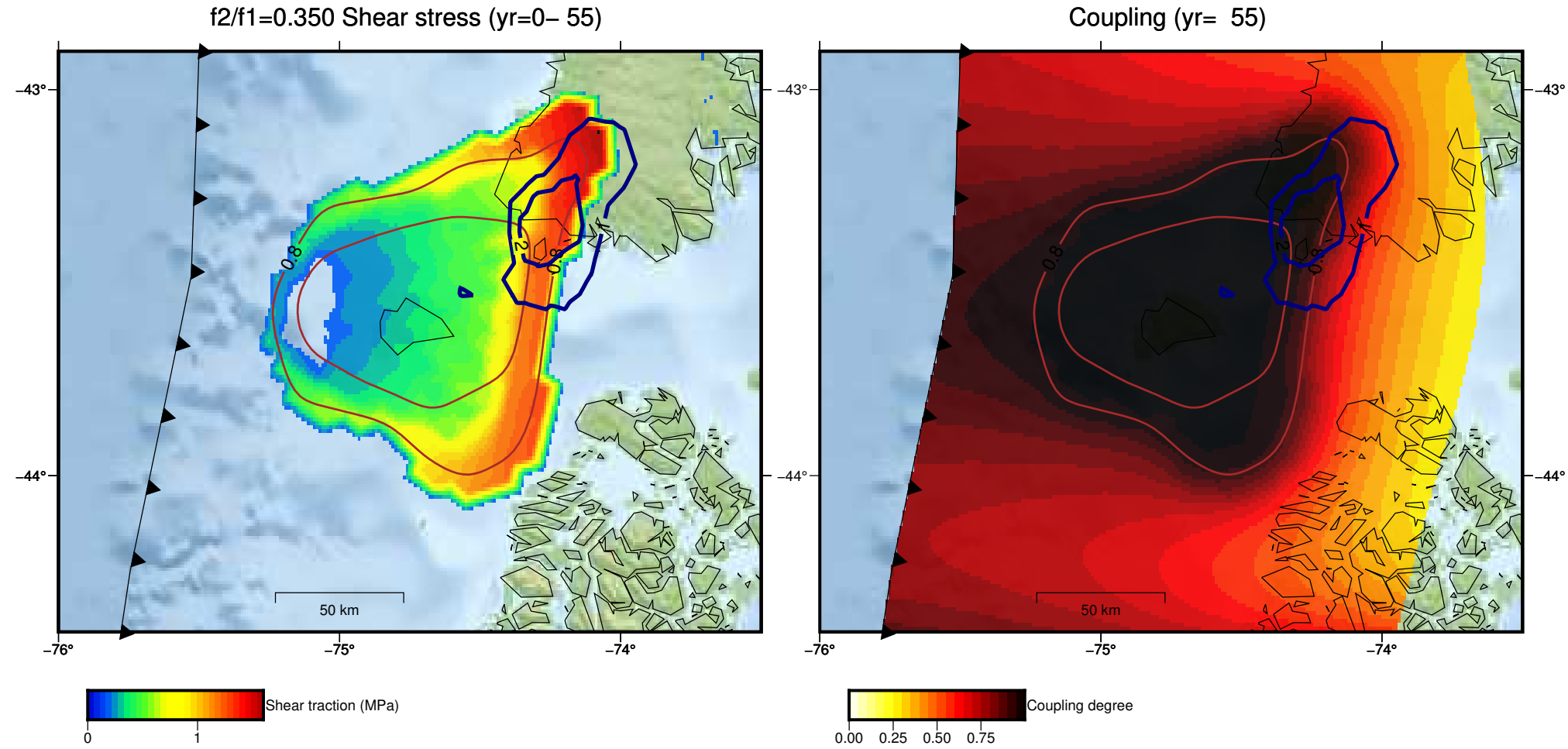
f2/f1=0.350 Shear stress (yr=0– 55)
Coupling (yr= 55)
–43°
–44°
–76°
–75°
–74°
0.8
0.8
50 km
50 km
Shear traction (MPa)
0
1
Coupling degree
0.00
0.25
0.50
0.75

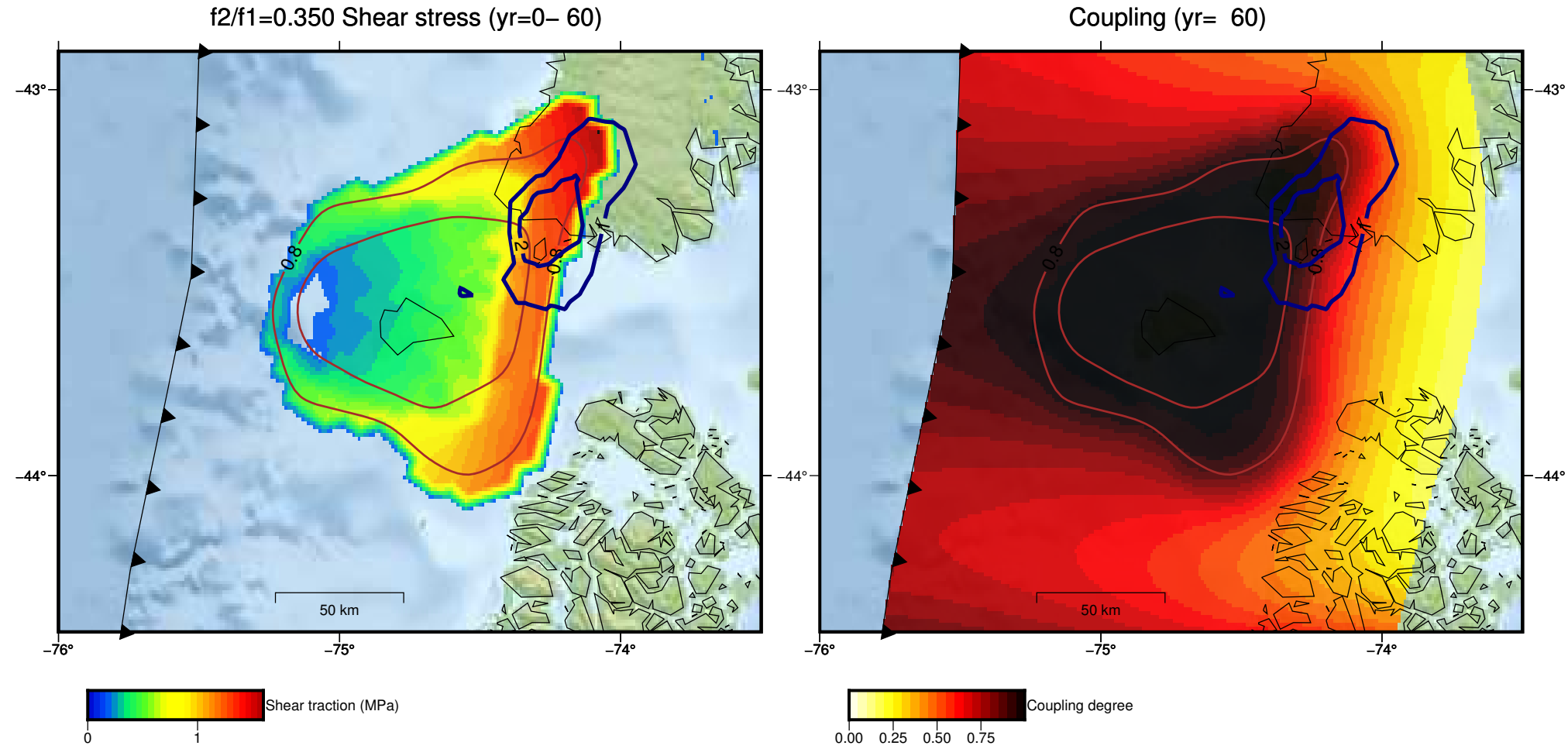
f2/f1=0.350 Shear stress (yr=0– 60)
Coupling (yr= 60)
–43°
–44°
–76°
–75°
–74°
0.8
1.2
50 km
Shear traction (MPa)
0
1
Coupling degree
0.00
0.25
0.50
0.75

Figure S14. Normal stress anomaly on the subducting plate interface. White dashed contours show the rupture zone of the 1960 earthquake. The projected location of vertical sections of the underlying 3D density model are given as grey dashed lines.

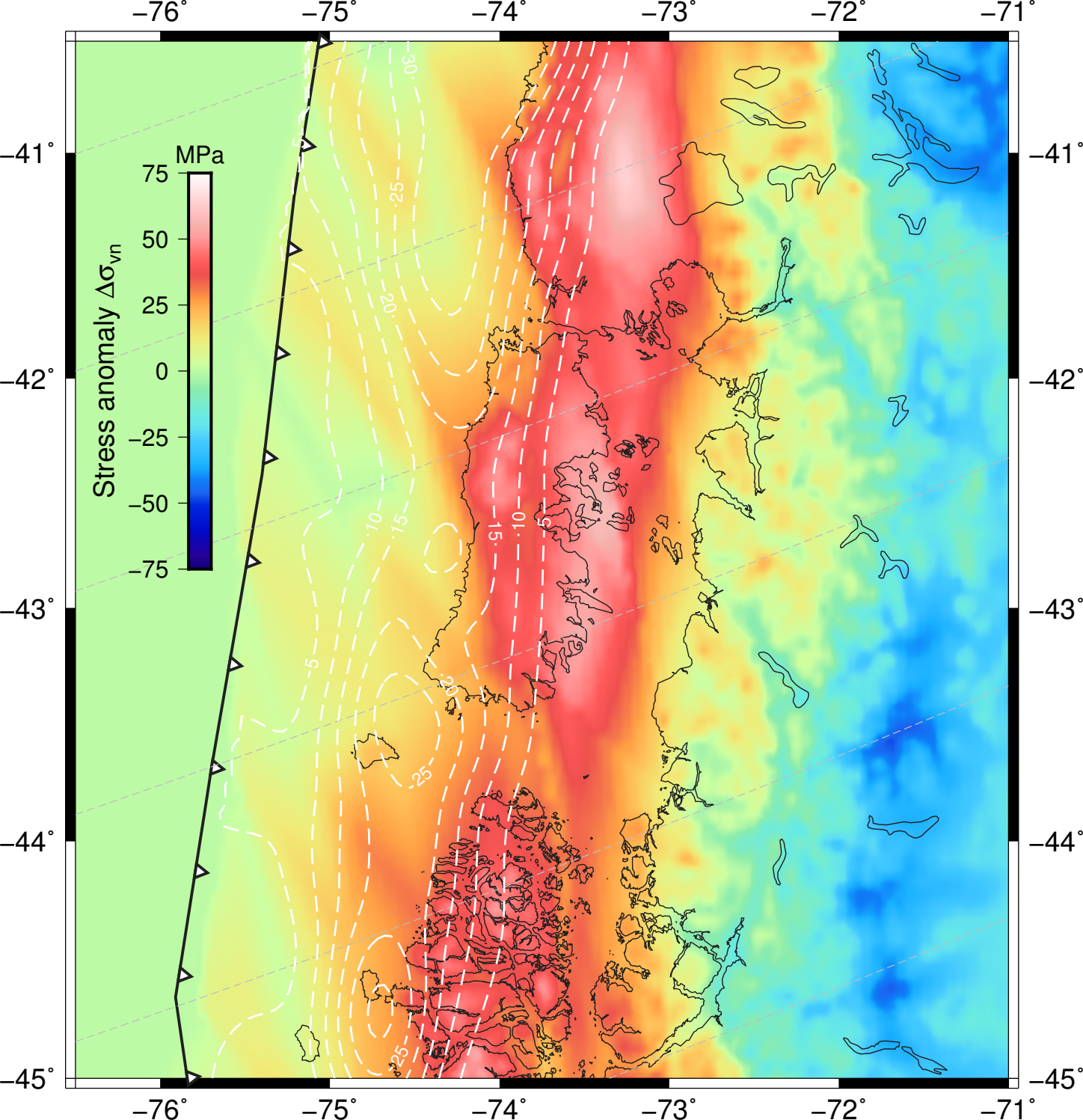
−76°
−75°
−74°
−73°
−72°
−71°
−41°
−42°
−43°
−44°
−45°
MPa
75
50
25
0
−25
−50
−75
Stress anomaly Δσvn
30
25
20
15
10
5
−5
−10
−15
−20
−25

Figure S15. Series of figures showing the evolution of shear traction and coupling evolutions after 20, 40 and 60 years of loading. This model incorporates the normal stress anomaly estimated from the density model of the forearc, and incorporates a constant value for the effective friction coefficient. Only by including the vertical stress anomaly we cannot reproduce the clamp of an asperity.

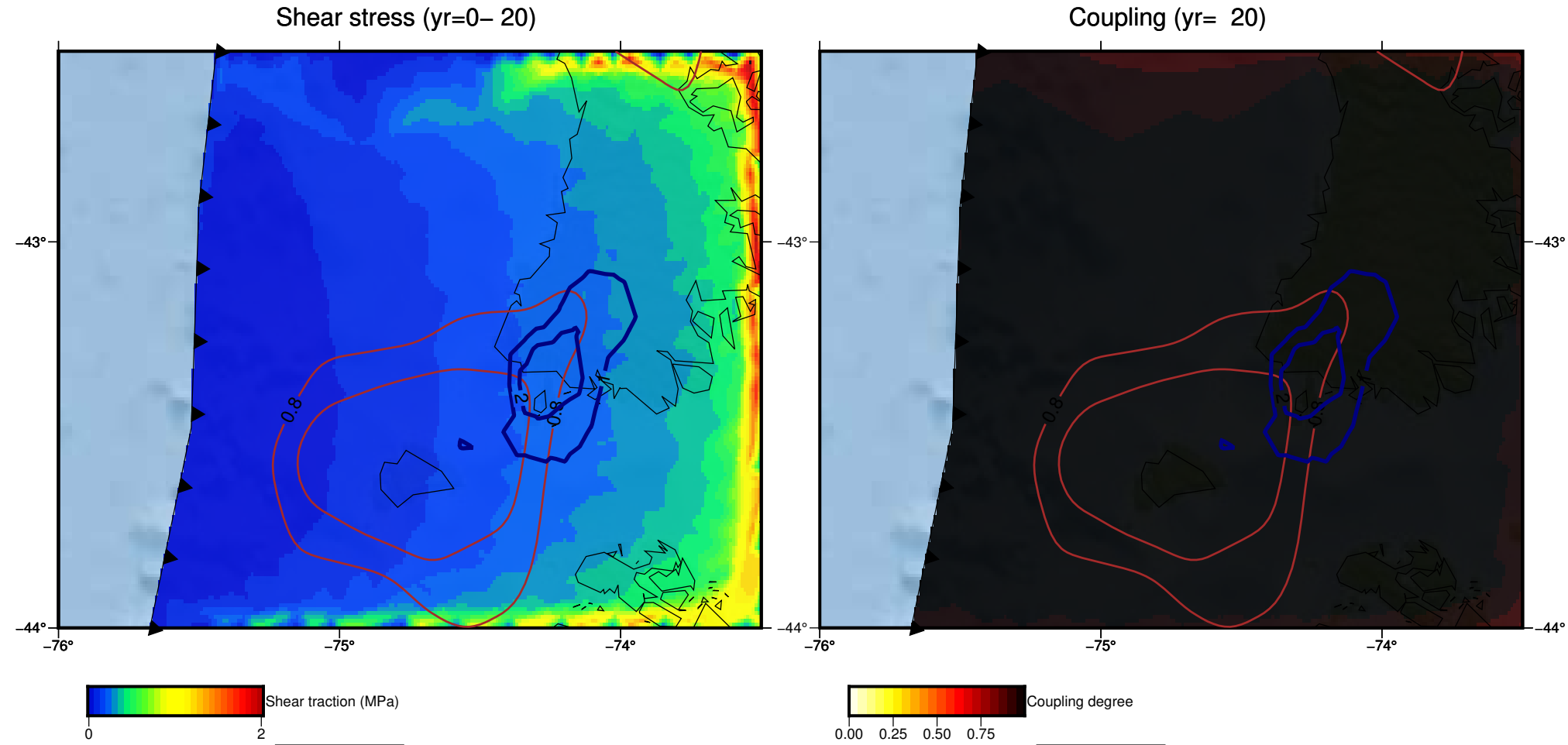
Shear stress (yr=0– 20)
Coupling (yr= 20)
–43°
–44°
–76°
–75°
–74°
0.8
2.0
Shear traction (MPa)
0
2
Coupling degree
0.00
0.25
0.50
0.75

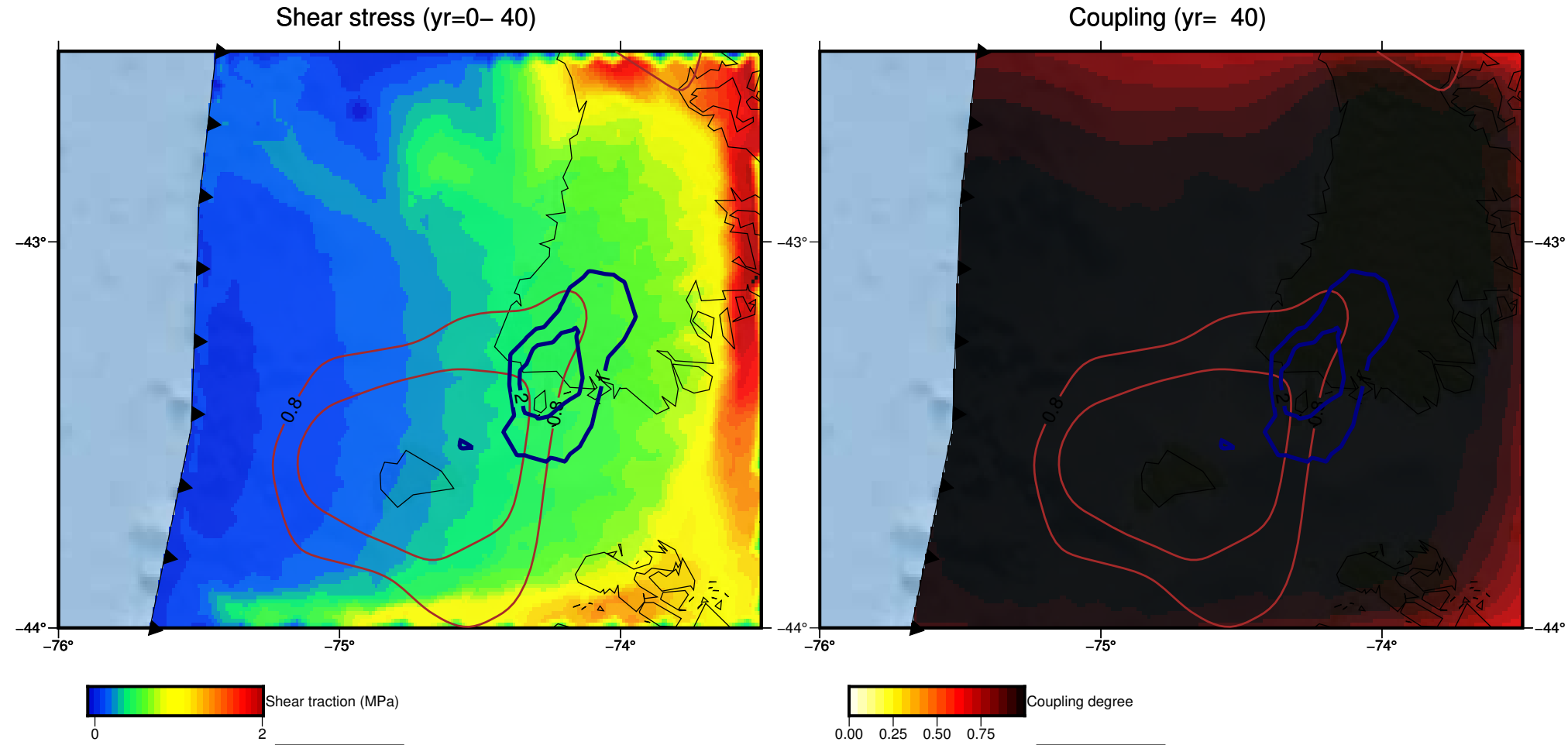
Shear stress (yr=0– 40)
Coupling (yr= 40)
–43°
–44°
–76°
–75°
–74°
0.8
2.0
Shear traction (MPa)
0
2
Coupling degree
0.00
0.25
0.50
0.75

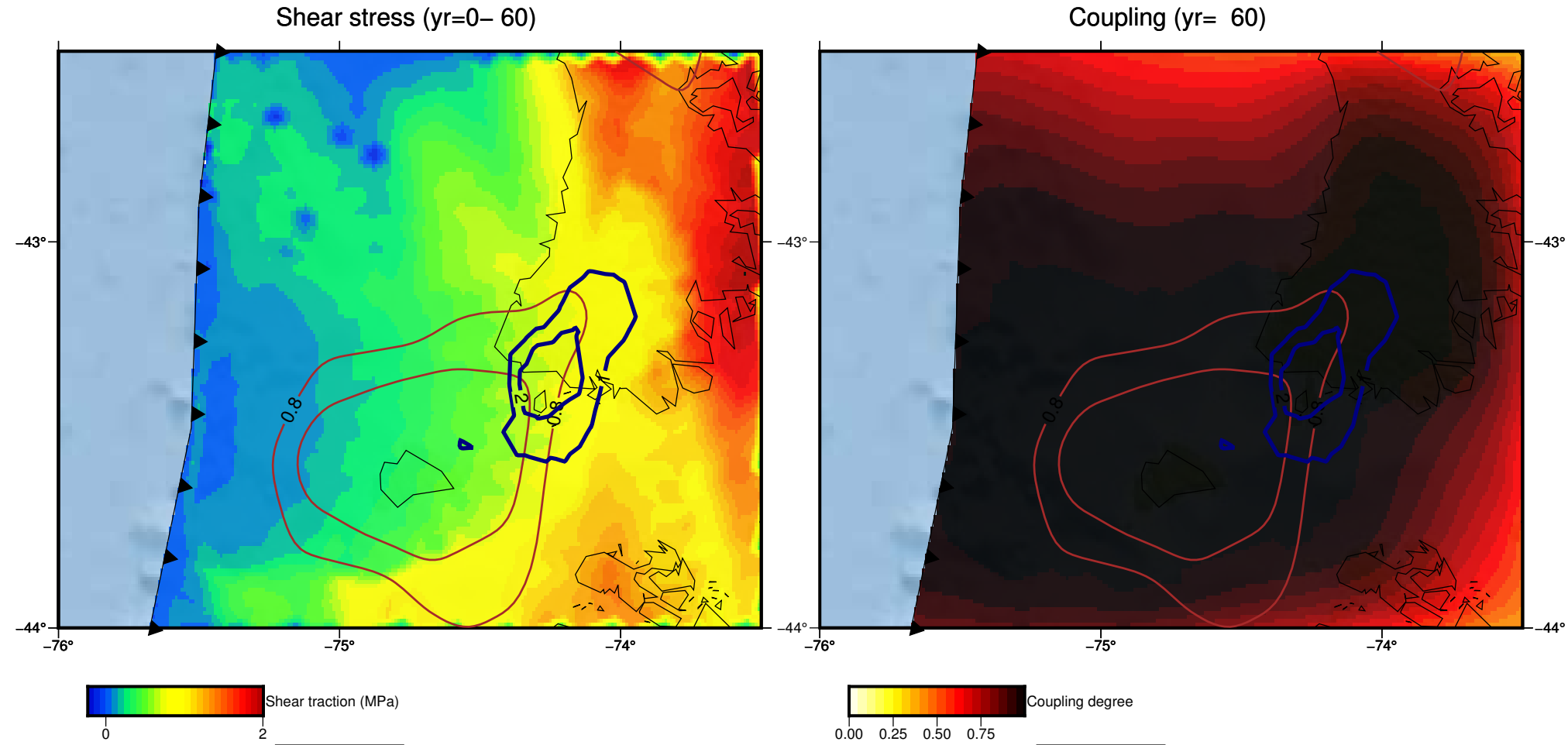
Shear stress (yr=0– 60)
Coupling (yr= 60)
–43°
–44°
–76°
–75°
–74°
0.8
2.0
Shear traction (MPa)
0
2
Coupling degree
0.00
0.25
0.50
0.75